Reflection and transmission problems for high-frequency waves at a randomly perturbed interface: generalized Snell's laws

Christophe Gomez, Knut Sølna

Reflection and transmission problems for high-frequency waves at a randomly perturbed interface: generalized Snell's laws

Christophe Gomez[1] and Knut Sølna[2]

[1]Aix Marseille Univ, CNRS, I2M, Marseille, France
[2]Department of Mathematics, University of California, Irvine

December 1, 2023

Abstract

In this paper we consider the problem of reflexion and transmission of a high-frequency pulse at a rapidly oscillating rough interface with general mixing properties. Using an asymptotic analysis based on a separation of scale technique, corresponding to the paraxial (parabolic) scaling, the specular and speckle (diffusive) components of the reflected and transmitted signals are precisely characterized. A *critically scaled* interface is considered, in the sense that the amplitudes of the interface fluctuations and the central wavelength are of the same order. If the correlation length of the interface fluctuations and the beam width are of the same order, random specular components are observed for the reflected and transmitted wave, but no speckle component. That is, the reflected and transmitted fields are to leading order confined essentially to the specular cones and these fields exhibit relatively small random intensity fluctuations. The situation with a correlation length smaller than the beam width leads to a specular homogenization situation so that the rough interface can be approximated by an effective flat interface providing deterministic specular reflected and transmitted paraxial wave cones. However, in this situation, there are now relatively broad cones (containing the specular cones) where the wavefields form speckle patterns whose total energy is leading order and we give the two-points correlation functions for these speckle patterns. We also present a central limit theorem type result for the speckle patterns and show that they can be modeled as Gaussian random fields. These descriptions allow the derivation of generalized Snell's laws of refraction and transmission depending on an effective scattering operator at the interface.

Keywords: wave propagation, random surface, wave scattering, generalized Snell's laws, Gaussian speckle pattern.

Introduction

Wave scattering by rough surfaces is at the heart of several branches of physics and engineering, and the understanding of these phenomena is crucial for a wide array of disciplines including optics, solid state physics, remote sensing, radar technology, environmental monitoring, communications, and non-destructive testing [4, 8, 19, 24, 26]. The interaction between waves and rough surfaces gives rise to a complex interplay of reflection, transmission, and diffraction. When waves impinge upon a rough surface, they undergo scattering events due to the irregularities in the surface profile. These scattering events lead to changes in the wave's direction, amplitude, and phase. Consequently, the study of wave scattering phenomena by rough surfaces involves unraveling the intricate details of these interactions to predict and analyze the behavior of waves in practical scenarios. For radar system for instance, electromagnetic wave scattering theory from rough surface is crucial to describe the effects of the roughness of the land or the sea surface. In optics a similar theory can be deployed. For acoustic waves, one can refer to applications in ocean acoustic tomography or thermometry, where the sea bed and sea surface roughness play a critical role, but also in non-destructive testing using ultrasonic waves.

Despite the huge importance of this problem and the wide range of applications, there is a limited number of rigorous results that characterize the wavefield either transmitted through or reflected from a rough interface [1, 3, 18, 25]. A number of works in the physical literature consider a random interface problem in a perturbative situation when the effect of small interface variations in the medium gives rise to relatively small corrections in the transmitted and reflected wavefield. In this work we model the interface fluctuations as a random field, enabling us to describe the transmitted and reflected field even though these are modified to leading order due

to the presence of the random interface. The case of beam propagation with reflection from or transmission through a rough boundary requires specialized techniques somewhat different from those associated with bulk propagation. From the analytic viewpoint we here approach the problem from the point of view of separation of scales in complex media. The basic configuration we consider is illustrated in Figure 1: a beam like wavefield

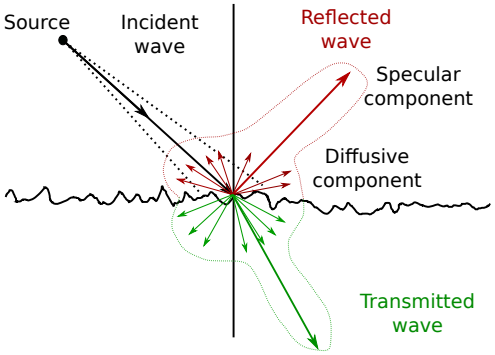

Figure 1: Illustration of the basic physical setup. A source illuminates a rough surface producing a reflected (in red) and transmitted waves (in green). Both of these waves exhibit in general specular and diffusive components. The diffusive components, the speckle, correspond to scattering of the incident wave by the rough interface.

(under the paraxial/parabolic scaling) illuminates a rough surface with the medium parameters being constant, but different above and below the interface. The incident wave is then in general decomposed into a reflected wave and a transmitted wave. We decompose these wavefields into two main components: the specular component and the speckle, also called incoherent or diffuse component, generated by scattering. Some central questions are then: i) how is the specular component modified by the presence of the fluctuations in the interface, ii) how can we describe the speckle component of the wavefield and what governs its relative magnitude and support. It turns out the the central scaling ratio that distinguishes various canonical scattering situations is the correlation range or characteristic scale of variations for the interface relative to the beam width. Indeed this is the situation in the critical scaling scenario considered here with the amplitude of the interface fluctuations being of the order of the wavelength. In this paper we show in particular that if the interface spatial fluctuations happen on the scale of the width of the probing cone, then the reflected and transmitted specular cones exhibit random arrival time properties, but their main wave energy are confined to the specular cones as the interface fluctuations does not generate strong coupling in between modes with different lateral wave number magnitude (traveling in relative oblique direction). On the other hand if the interface spatial fluctuations happen on a scale small relative to the width of the probing cone then such a coupling takes place generating homogenized specular reflected and transmitted cones with frequency-depend attenuations related the interface elevation statistics. The missing energy from these effective specular cones have been converted into wide speckle cones that carries energy of relative order one total magnitude. In our situation the roughness of the interface is not strong enough to generate the enhanced backscattering effects [20], the scattering operator we obtained is similar as the one obtained in [28] under the Born (single scattering) approximation.

There is a quite large literature on the important rough surface or interface scattering problem. Most of the literature deal with physically motivated expansions such as perturbative approaches or a Kirchhoff type approximations giving strong conditions on the scaling regime that can be considered [2, 8, 22, 14, 24, 11, 32]. There are also much work related to integral equations formulations [10, 23, 31] in particular to describe near field scattering [27]. Sophisticated numerical methods have been developed [6, 29] to understand wave scattering from complicated geometries, here we are interested in the case when we only describe such geometries in a statistical way. Note that homogenization techniques have been used to derive effective interface conditions [13, 25] for random interfaces, while here our focus is additionally on the statistical description of the diffuse components of the scattered field with the energy carried by the diffusive or speckle component may be of the order of the energy carried by the specular component.

In the high frequency situation we consider family of characteristic scaling regimes depending on the magnitude of the beam width relative to the correlation radius of the interface fluctuations. A main technical challenge then is that the standard theory for studying stochastic partial differential equations (SPDEs) [7] may not be used since we assume stationarity of the interface height fluctuations and then the noise cannot provide an Hilbert-Schmidt covariance operator. From this point of view the situation is then similar to that considered in [9] where well-posedness of the white-noise paraxial (Ito-Schrödinger) equation was considered. However, in

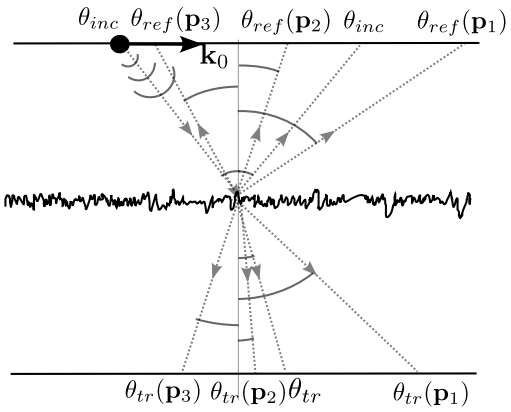

Figure 2: Illustration of the generalized Snell's laws of refraction and transmission.

our situation the randomness is carried by the interface fluctuations rather than being bulk fluctuations and we start with a description with finite scales and then take a scaling limit rather than taking as starting point a white noise type of model. A second technical challenge in our context is that we also want to describe the reflected wave, in addition to the transmitted wavefield. This is accomplished via an embedding type description parameterizing the wavefield in terms of a family of up- and down-propagating wave components. A third technical challenge here is that the random interface depends on the 'lateral' variable, but not the 'propagation' variable so that the classic framework of diffusion approximation does not apply [12].

Our main focus here is to develop a novel framework that allows us to characterize precisely the statistics of the diffusively scattered wave from rough interfaces in term of a Gaussian random field, both in transmission and (radar) backscattering. We remark that such analytic frameworks can be used in remote sensing type imaging problems: (i) imaging of the parameters of the rough (random) interface, (ii) imaging of an object hidden behind the interface based on computing the empirical spectrum of the reflected speckle [16, 17, 21, 30]. The analysis can furthermore be generalized to Synthetic Aperture Radar (SAR) probing scenarios where the source cone is moving and in the typical case mounted on an aircraft. In general imaging contexts one may aim to exploit the memory effect which means that the speckle pattern illuminating a hidden object is not completely changed, but rather shifted a specific amount when the source incoming angle is shifted. One may further exploit weak localization effects which means that the speckle in the direction of the illuminating wave cone is relatively high. We further remark that in the context of polarimetric imaging schemes it is important to capture the coupling of different polarization modes at the interface and how this depends on the interface statistics. Generalization to such imaging configuration, the case with general hyperbolic systems [15] and the strongly fluctuating case with the spatial scale of the interface fluctuations being large relative to the wavelength will be considered elsewhere.

The proposed analytic frameworks allow to derive from first principle of physics generalized Snell's laws of refraction and transmission illustrated in Figure 2. For an impinging wave with frequency ω, 2D slowness vector $\mathbf{k}_0$ and incident angle $\theta_{inc} > 0$, the refraction angle θ_{ref} is given through the relation

$$\frac{\tan(\theta_{ref}(\mathbf{p}))}{\tan(\theta_{inc})} = \sqrt{\Big(1 + \xi \frac{\mathbf{p}\cdot\mathbf{k}_0}{\cos^2(\theta_{inc})}\Big)^2 + \xi^2(\mathbf{p}\cdot\mathbf{k}_0^{\perp})^2}, \qquad \text{with} \qquad \xi = \frac{\lambda}{l_c}\frac{c_0^2}{\pi \sin^2(\theta_{inc})}, \tag{1}$$

$\mathbf{k}_0^{\perp} = (-\mathbf{k}_{0,2}, \mathbf{k}_{0,1})^T$, and where λ corresponds to the central wavelength of the source and l_c to the characteristic scale of variations for the interface. In this formula, the scattered slowness vector $\mathbf{p}$ is distributed according to the effective scattering operator

$$\mathcal{A}(v, \omega, \mathbf{p}) := \int \mathbb{E}\big[e^{i\omega v(V(\mathbf{y})-V(0))}\big] e^{-i\omega \mathbf{p}\cdot\mathbf{y}} d\mathbf{y}, \qquad \text{with} \qquad v = \frac{2\cos(\theta_{inc})}{c_0},$$

involving the stationary random interface elevation V through the characteristic function of the relative elevation $V(\mathbf{y}) - V(0)$. This effective scattering operator has already been derived in [28] to describe the mean intensity of the diffusive reflected wavefield. Regrading the transmission angle, with θ_{inc} smaller than the critical angle, the Snell's law reads

$$\frac{\sin(\theta_{tr}(\mathbf{p}))}{c_1} = \frac{\sin(\theta_{inc})}{c_0} \sqrt{\frac{\Xi}{1 + \sin^2(\theta_{tr})\Big(\Xi - 1\Big)}} \qquad \text{with} \qquad \Xi = \Big(1 + \xi \frac{\mathbf{p}\cdot\mathbf{k}_0}{\cos^2(\theta_{tr})}\Big)^2 + \xi^2(\mathbf{p}\cdot\mathbf{k}_0^{\perp})^2, \tag{2}$$

where θ_{tr} corresponds to the specular transmission angle for a flat interface and given by the standard Snell's law $\sin(\theta_{tr})/c_1 = \sin(\theta_{inc})/c_0$. The scattered slowness vector $\mathbf{p}$ is distributed according to the effective scattering operator $\mathcal{A}(v, \omega, \mathbf{p})$ but this time for $v = \cos(\theta_{inc})/c_0 - \cos(\theta_{tr})/c_1$. The key parameter in both relations (1) and (2) is the ratio λ/l_c charactering how rough the surface is for the incident wave and the cone size of the diffusive component. A surface is considered rough if $\lambda \sim l_c$, and for a relatively smooth surface $\lambda/l_c \ll 1$, the Snell's relations read

$$\theta_{ref}(\mathbf{p}) \simeq \theta_{inc} + \xi \tan(\theta_{inc})\mathbf{p} \cdot \mathbf{k}_0 \qquad \text{and} \qquad \theta_{tr}(\mathbf{p})) \simeq \theta_{tr} + \xi \frac{\tan(\theta_{tr})}{\cos^2(\theta_{tr})}\mathbf{p} \cdot \mathbf{k}_0.$$

providing small deviations from the specular refraction and transmission angles of order λ/l_c. Finally, for a null incident angle $\theta_{inc} = 0$, the above relations simply turn to

$$\theta_{ref}(\mathbf{p}) = \arctan\Big(\frac{\lambda c_0 |\mathbf{p}|}{\pi l_c}\Big) \qquad \text{and} \qquad \theta_{tr}(\mathbf{p}) = \arctan\Big(\frac{\lambda c_1 |\mathbf{p}|}{\pi l_c}\Big).$$

The outline of the paper is as follows. In Section 1 we describe the wave propagation scenario and the scaling regime that we consider. In this section we moreover discuss mixing aspects in the statistical modeling of the interface fluctuations. In Section 2 we discuss the basic wavefield decomposition in lateral Fourier (wave number) modes and in up- and down- propagating components. We introduce this decomposition in the context of a flat interface. This decomposition allow us moreover to identify refection and transmission conditions at the (flat) interface which couple up- and down-propagating wave modes for each lateral wave number. In the next Section 3 we generalize this description to the case with a random interface. This then entails the identification of a (random) scattering operator at the interface which captures the coupling of the up- and down-propagating wave modes at the interface at different lateral wave numbers that is caused by the random interface fluctuations. In Section 4 we dicuss the case when the interface fluctuations decorrelate at a scale corresponding to the width of the probing cone, this is the regime when the specular cones carry essentially all energy. In Sections 5-7 we present the case when the interface fluctuations decorrelate on a scale small relative to the width of the probing cone, but large relative to the wavelength. In this case the interface generates both specular cones and additionally wide speckle cones. Finally, in Sections 8 and 9, as well as Appendices A and B, present detailed proofs.

1 The physical model

The wave equation. In this paper we consider three-dimensional linear wave propagation modeled by the scalar wave equation:

$$\Delta u - \frac{1}{c^2(\mathbf{x}, z)}\partial_{tt}^2 u = \nabla \cdot F(t, \mathbf{x}, z) \qquad (t, \mathbf{x}, z) \in \mathbb{R} \times \mathbb{R}^2 \times \mathbb{R}, \tag{3}$$

equipped with zero initial conditions

$$u(t = 0, \mathbf{x}, z) = \partial_t u(t = 0, \mathbf{x}, z) = 0 \qquad (\mathbf{x}, z) \in \mathbb{R}^2 \times \mathbb{R},$$

and continuity conditions at the interface that will be specified below. The coordinate z represents the main propagation axis while $\mathbf{x}$ represents the transverse directions and F is the source. Here, the Laplacian operator $\Delta = \Delta_\perp + \partial_{zz}^2$ acts on all spatial variables $\mathbf{x}$ and z. The propagation medium consists of two homogeneous subdomains delimited by a randomly perturbed interface around $z = z_{int}$:

$$\mathcal{D}^0 := \{(\mathbf{x}, z) \in \mathbb{R}^2 \times \mathbb{R} \quad \text{s.t.} \quad z < z_{int} + \sigma V(\mathbf{x}/l_c)\} \tag{4}$$

and

$$\mathcal{D}^1 := \{(\mathbf{x}, z) \in \mathbb{R}^2 \times \mathbb{R} \quad \text{s.t.} \quad z > z_{int} + \sigma V(\mathbf{x}/l_c)\}. \tag{5}$$

We refer to Figure 3 for an illustration of the physical setup. The term V corresponds to a mean-zero random field, with second order derivatives, modeling the variations of the interface and characterizing its roughness. Away from the interface the velocity field is given by:

$$c(\mathbf{x}, z) := \begin{cases} c_0 & \text{if} \quad (\mathbf{x}, z) \in \mathcal{D}^0, \\ c_1 & \text{if} \quad (\mathbf{x}, z) \in \mathcal{D}^1. \end{cases} \tag{6}$$

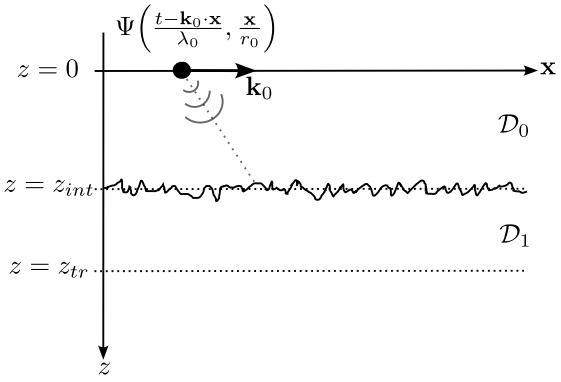

Figure 3: Illustration of the physical setup. The plan $z = 0$ contains the source location, while $z = z_{int}$ is the plan around which the rough interface between $\mathcal{D}_0$ and $\mathcal{D}_1$ takes place. The reflected wave will be observed at $z = 0$, while the transmitted wave will be observed at $z = z_{tr}$.

The forcing term

$$F(t, \mathbf{x}, z) := \Psi\Big(\frac{t - \mathbf{k}_0 \cdot \mathbf{x}}{T_0}, \frac{\mathbf{x}}{r_0}\Big)\delta(z)\mathbf{e}_z, \tag{7}$$

where $\mathbf{e}_z$ denotes the unit vector pointing in the z-direction, models a source located in the plane $z = 0$ and emitting a quasi plan wave Ψ in the spatial direction $(\mathbf{k}_0, \sqrt{c_0^{-2} - |\mathbf{k}_0|^2})$ towards the random interface (requirering $|\mathbf{k}_0| < c_0^{-1}$). The divergence form of the source term in (3) is standard in linear acoustics where u represents the pressure wave, see [12] for instance. This divergence form is considered here for mathematical convenience, and other type of source term could be handled in a similar manner. Also, T_0 represents the pulse width and r_0 the spatial beam width of the source term.

The wave equation (3) is naturally equipped with the two following continuity relations across the randomly perturbed interface:

$$u(z = z_{int}(\mathbf{x})^+) = u(z = z_{int}(\mathbf{x})^-) \qquad \text{and} \qquad \partial_z u(z = z_{int}(\mathbf{x})^+) = \partial_z u(z = z_{int}(\mathbf{x})^-), \tag{8}$$

where

$$z_{int}(\mathbf{x}) := z_{int} + \sigma V(\mathbf{x}/l_c).$$

The derivation of these two relations is provided in Appendix A. Finally, no wave is assumed to come from above the source location nor below the interface. The only waves propagating into the system are produced by the source term.

The parameter scaling. The approach considered in this paper is based on a separation of scale technique for which the scales of interest are the following: the central wavelength λ (related to the pulse width through the relation $\lambda = c_0 T_0$), the spatial radius r_0 of the source, the correlation length l_c and the amplitude σ of the fluctuations V, and finally the typical propagation distance that we denote L. We denote the distance from the source to the interface by z_{int} and the distance from the source to the plane where the transmitted wave is recorded by z_{tr}. Let L be a typical propagation distance with z_{int}/L and z_{tr}/L of order one and introduce the dimensionless parameter

$$\varepsilon := \frac{\lambda}{L} = \frac{c_0 T_0}{L} \ll 1.$$

We will consider a high-frequency regime with $\varepsilon \ll 1$ and, moreover, a paraxial (or parabolic) scaling by enforcing

$$\frac{\pi r_0^2}{\lambda} \sim L,$$

which corresponds to a Rayleigh length of order the typical propagation distance. In the homogeneous case the Rayleigh length $L_R = \pi r_0^2/\lambda$ corresponds to the distance from the beam waist to the place where the area of its cross-section is doubled. The interface fluctuations are *critically scaled* so that the magnitude of the interface fluctuations and the central wavelength are of the same order

$$\sigma \sim \lambda.$$

Finally, let l_c be the correlation radius of the homogeneous and isotropic interface fluctuations, we consider then situations where this radius ranges from the central wavelength to the beam width so that

$$\lambda \lesssim l_c \lesssim r_0.$$

We remark that if $r_0 \ll l_c$ the situation is trivial and corresponds essentially to a planar interface. The ratio λ/l_c characterizes how rough the surface is for the incident wave, and will describe the cone radius for the reflected and transmitted speckle components. A surface is considered rough if $\lambda \sim l_c$, and for a relatively smooth surface $\lambda/l_c \ll 1$. The situation with $l_c \ll \lambda$ gives a homogenization situation with an effective planar interface and initial conditions, but no leading order random effects.

In what follows, for simplicity, we consider a dimensionless situation and set

$$L = L_R \sim 1, \qquad T_0 = \varepsilon, \qquad r_0 = \sqrt{\varepsilon}, \qquad \sigma = \varepsilon, \qquad \text{and} \qquad l_c = \varepsilon^\gamma, \tag{9}$$

with

$$\gamma \in [1/2, 1].$$

In the forthcoming analysis, a distinction will be made for $\gamma = 1/2$ (that is $l_c \sim r_0$) and $1/2 < \gamma \leq 1$ (corresponding to $\lambda \lesssim l_c \ll r_0$). These two cases give different behaviors for the reflected and transmitted signals. While the former produces only random specular components, the latter, due to fast oscillations of the interface compared to the beam radius ($l_c \ll r_0$), produces a homogenization effect for the specularly reflected and the transmitted wave components, as well as random speckles over cones larger than the ones covered by the specular and transmitted components.

Random fluctuations. In (4) and (5), the random fluctuations of the interface delimiting the two subspaces are defined by the mean-zero stationary random field V. These random fluctuations are assumed to satisfy *mixing* properties describing the loss of statistical dependency for V over the interface. In our context, the basic idea of *mixing* is the following. For a given set of locations $\mathbf{x}_1, \ldots, \mathbf{x}_n \in \mathbb{R}^2$, the corresponding values of the field $V(\mathbf{x}_1), \ldots, V(\mathbf{x}_n)$ become independent as these locations are far enough from each other:

$$\mathbb{P}(V(\mathbf{x}_1) \in A_1, \ldots, V(\mathbf{x}_n) \in A_n) \to \mathbb{P}(V(\mathbf{x}_1) \in A_1) \cdots \mathbb{P}(V(\mathbf{x}_n) \in A_n), \tag{10}$$

for any Borel set $A_1, \ldots, A_n \subset \mathbb{R}$, as

$$\min_{j,l \in \{1,\ldots,n\}} |\mathbf{x}_j - \mathbf{x}_l| \to \infty.$$

This property is readily satisfied if V is a Gaussian random field with correlation function

$$R(\mathbf{x}) = \mathbb{E}[V(\mathbf{x}+\mathbf{y})V(\mathbf{y})],$$

that decays to 0 as $\mathbf{x} \to \infty$. For more general random fields (non-necessarily Gaussian), the property (10) can be formalized through the notion of α-mixing as follows. Introducing

$$\alpha(r) := \sup_{\substack{S,S' \subset \mathbb{R}^2 \\ d(S,S') > r}} \sup_{\substack{A \in \sigma(V(\mathbf{x}),\, \mathbf{x} \in S) \\ B \in \sigma(V(\mathbf{x}),\, \mathbf{x} \in S')}} |\mathbb{P}(A \cap B) - \mathbb{P}(A)\mathbb{P}(B)|,$$

where

$$d(S, S') = \inf_{\substack{s \in S \\ s' \in S'}} |s - s'|$$

is the distance between two nonempty subsets S and S', and $\sigma(V(\mathbf{x}), \mathbf{x} \in S)$ is the σ-field generated by the family $V_{|S} := (V(\mathbf{x}))_{\mathbf{x} \in S}$. Roughly speaking, the value $\alpha(r)$ quantifies the degree of statistical dependence for the random field V over the pair of regions at distance at least r. The α-mixing situation corresponds to assuming

$$\alpha(r) \to 0 \qquad \text{as} \qquad r \to \infty, \tag{11}$$

giving a vanishing of statistical dependency between $V_{|S}$ and $V_{|S'}$ as the distance between S and S' tends to infinity. This notion of mixing is convenient to exhibit the homogenization phenomenon for the specular components, the self-averaging property of two-point empirical correlation functions of the speckle components, as well as the Gaussianity of the speckle patterns themselves.

To articulate quantitatively the effect of mixing for physical quantities and their covariation it will also be convenient to introduce a related measure, ρ-mixing, capturing coherence, or lack thereof, and which is defined through

$$\rho(r) := \sup_{\substack{S,S'\subset\mathbb{R}^2\\ d(S,S')>r}} \sup_{\substack{V\in\mathcal{L}^2(\sigma(V(\mathbf{x}),\mathbf{x}\in S))\\ W\in\mathcal{L}^2(\sigma(V(\mathbf{x}),\mathbf{x}\in S'))}} |Corr(V,W)| \qquad \text{with} \qquad \rho(r)\to 0 \qquad \text{as} \qquad r\to\infty, \tag{12}$$

Here, $\mathcal{L}^2(\mathcal{A})$ stands for the set of $\mathcal{A}$-measurable random variables with a finite second-order moment, and $Corr$ denotes the correlation coefficient between V and W:

$$Corr(V,W) = \frac{Cov(V,W)}{\sqrt{Var(V)Var(W)}}.$$

According to [5, Theorem 1][1], it turns out that

$$\alpha(r) \le \rho(r) \le 2\pi\,\alpha(r) \qquad r>0, \tag{13}$$

so that the notions of α- and ρ-mixing are equivalent. From the ρ-mixing property, the following lemma translates the idea of (10) in a way that will be used in the forthcoming asymptotic analysis.

Lemma 1.1 *Let $n\ge 1$ and V be ρ-mixing, we then have:*

1. *For n bounded functions $f_1,\dots,f_n$: $\mathbb{R}\to\mathbb{C}$, and distinct $\mathbf{x}_1,\cdots,\mathbf{x}_n\in\mathbb{R}^2$*

$$\lim_{\eta\to 0}\mathbb{E}\Big[\prod_{j=1}^n f_j\Big(V\Big(\frac{\mathbf{x}_j}{\eta}\Big)\Big)\Big] = \lim_{\eta\to 0}\prod_{j=1}^n \mathbb{E}\Big[f_j\Big(V\Big(\frac{\mathbf{x}_j}{\eta}\Big)\Big)\Big] = \prod_{j=1}^n \mathbb{E}\Big[f_j\big(V(0)\big)\Big];$$

2. *For n bounded functions $g_1,\dots,g_n$: $\mathbb{R}^2\to\mathbb{C}$, $\mathbf{y}_1,\cdots,\mathbf{y}_n\in\mathbb{R}^2$, and distinct $\mathbf{x}_1,\cdots,\mathbf{x}_n\in\mathbb{R}^2$,*

$$\begin{aligned}\lim_{\eta\to 0}\mathbb{E}\Big[\prod_{j=1}^n g_j\Big(V\Big(\frac{\mathbf{x}_j}{\eta}+\frac{\mathbf{y}_j}{2}\Big),V\Big(\frac{\mathbf{x}_j}{\eta}-\frac{\mathbf{y}_j}{2}\Big)\Big)\Big] &= \lim_{\eta\to 0}\prod_{j=1}^n \mathbb{E}\Big[g_j\Big(V\Big(\frac{\mathbf{x}_j}{\eta}+\frac{\mathbf{y}_j}{2}\Big),V\Big(\frac{\mathbf{x}_j}{\eta}-\frac{\mathbf{y}_j}{2}\Big)\Big)\Big]\\ &= \prod_{j=1}^n \mathbb{E}\Big[g_j\Big(V\Big(\frac{\mathbf{y}_j}{2}\Big),V\Big(-\frac{\mathbf{y}_j}{2}\Big)\Big)\Big].\end{aligned}$$

The detailed proof of this lemma is presented in Appendix B.

2 Reflection and transmission for an unperturbed interface

Before going into the analysis of the wave scattering at the random interface we describe in this section the reflection and transmission mechanisms for an *unperturbed interface*. This serves in particular to introduce central wave quantities and associated terminology in a simple setting, and then we will see below how this generalizes in the random setting. This section is split into four parts dealing respectively with the incident wave at the interface, the transmission and reflection conditions at the unperturbed interface, and then the descriptions of the reflected and transmitted wave cones.

For the study of the reflection and transmission of the incident wave, we introduce the following specific Fourier transform,

$$\hat{f}^\varepsilon(\omega,\mathbf{k}) := \iint f(t,\mathbf{x})e^{i\omega(t/\varepsilon-\mathbf{k}\cdot\mathbf{x}/\sqrt{\varepsilon})}dtd\mathbf{x}, \qquad \text{and} \qquad f(t,\mathbf{x}) = \frac{1}{(2\pi)^3\varepsilon^2}\iint \hat{f}_\varepsilon(\omega,\mathbf{k})e^{-i\omega(t/\varepsilon-\mathbf{k}\cdot\mathbf{x}/\sqrt{\varepsilon})}\omega^2 d\omega d\mathbf{k}, \tag{14}$$

which is scaled according to the source profile (see (7) and (9)). In the Fourier domain, the wave equation (3), with $z\in(-\infty,z_{int})$, turns into the following Helmholtz equation

$$\partial_z^2\hat{u}^\varepsilon_\omega(\mathbf{k},z) + \frac{\omega^2}{\varepsilon^2 c_0^2}\Big(1-\varepsilon c_0^2|\mathbf{k}|^2\Big)\hat{u}^\varepsilon_\omega(\mathbf{k},z) = \varepsilon^2\hat{\Psi}\Big(\omega,\mathbf{k}-\frac{\mathbf{k}_0}{\sqrt{\varepsilon}}\Big)\delta(z), \tag{15}$$

[1]The functions α and ρ in this present paper correspond to α^* and ρ^* in [5]

where

$$\hat{\Psi}(\omega,\mathbf{k}) := \iint \Psi(t,\mathbf{x}) e^{i\omega(t-\mathbf{k}\cdot\mathbf{x})} dt d\mathbf{x}$$

corresponds to the unscaled Fourier transform of the source profile Ψ. In what follows, $\mathbf{k}$-modes satisfying $\sqrt{\varepsilon}\, c_0|\mathbf{k}| < 1$ are referred to *propagating modes*, and those satisfying $\sqrt{\varepsilon}\, c_0|\mathbf{k}| > 1$ are referred to *evanescent modes*. To avoid unnecessary treatments of the evanescent modes during transmission at the interface, we assume for convenience that

$$c_1 < c_0.$$

This assumption is only used for sake of simplicity of presentation. After some minor adaptations the results presented in this paper hold true also for $c_0 < c_1$ and any $\mathbf{k}_0$ satisfying $|\mathbf{k}_0| < c_1^{-1}$ to avoid the critical transmission angle. Under proper assumptions on the source profile $\hat{\Psi}$ (compactly supported in both variables and bounded away from 0 with respect to ω), the source term only generates propagating modes into the medium for ε small enough. In fact, setting

$$\mathbf{k} = \mathbf{q} + \frac{\mathbf{k}_0}{\sqrt{\varepsilon}}, \tag{16}$$

so that $\mathbf{q}$ lies in the support of $\hat{\Psi}$, we have

$$\sqrt{\varepsilon}\, c_0|\mathbf{k}| \le \sqrt{\varepsilon}\, c_0|\mathbf{q}| + c_0|\mathbf{k}_0| < 1, \tag{17}$$

for ε small enough and depending only on the support of $\hat{\Psi}$.

For $z \in (z_{int}, z_{tr})$, the wave equation (3) in the Fourier domain turns into the following Helmholtz equation

$$\partial_z^2 \hat{u}_\omega^\varepsilon(\mathbf{k},z) + \frac{\omega^2}{\varepsilon^2 c_1^2}\Big(1 - \varepsilon c_1^2|\mathbf{k}|^2\Big)\hat{u}_\omega^\varepsilon(\mathbf{k},z) = 0. \tag{18}$$

Throughout this paper, we denote with a slight abuse of notation

$$\lambda_j^\varepsilon(\mathbf{k}) := \frac{1}{c_j}\sqrt{1-\varepsilon c_j^2|\mathbf{k}|^2}, \qquad \text{for} \qquad \sqrt{\varepsilon}\, c_j|\mathbf{k}| < 1, \quad j = 0,1, \tag{19}$$

the vertical lowness associated with (15) and (18). Note that the condition on $\mathbf{k}$ in (19) is readily satisfied thanks to (17) and the assumption $c_1 < c_0$. In the forthcoming analysis, the following expansion will be used

$$\frac{1}{\varepsilon}\lambda_j^\varepsilon(\mathbf{q} + \mathbf{k}_0/\sqrt{\varepsilon}) = \frac{\lambda_j}{\varepsilon} - \frac{\mathbf{k}_0\cdot\mathbf{q}}{\sqrt{\varepsilon}\,\lambda_j} - c_j \mathbf{q}^T A_j \mathbf{q} + \mathcal{O}(\sqrt{\varepsilon}) \qquad j = 0,1, \tag{20}$$

where $\mathbf{q}^T$ stands for the transposition of $\mathbf{q}$, and

$$A_j := \frac{1}{2(1-c_j^2|\mathbf{k}_0|^2)^{3/2}}\begin{pmatrix} 1-c_j^2\mathbf{k}_{0,2}^2 & c_j^2\mathbf{k}_{0,1}\mathbf{k}_{0,2} \\ c_j^2\mathbf{k}_{0,1}\mathbf{k}_{0,2} & 1-c_j^2\mathbf{k}_{0,1}^2 \end{pmatrix} = \frac{1}{2c_j^3\lambda_j^3}\big(\mathbf{I}_2 - c_j^2\,\mathbf{k}_0^\perp(\mathbf{k}_0^\perp)^T\big). \tag{21}$$

Here, $\mathcal{O}$ holds uniformly with respect to $\mathbf{q}$ in the support of $\hat{\Psi}$, and

$$\lambda_j := \frac{\sqrt{1-c_j^2|\mathbf{k}_0|^2}}{c_j} \qquad j = 0,1. \tag{22}$$

Moreover, $\mathbf{I}_2$ stands for the 2×2 identity matrix, and $\mathbf{k}_0^\perp := (-\mathbf{k}_{0,2}, \mathbf{k}_{0,1})^T$.

2.1 The incident wavefield at the interface

Introducing the up- and down-going mode decomposition with respect to the z-direction, and remembering that no wave is assumed to come from above the source location nor below the rough interface, the wavefield reads

$$\begin{aligned}
\hat{u}_\omega^\varepsilon(\mathbf{k},z) = {} & \frac{\hat{b}_{0,\omega}^\varepsilon(\mathbf{k})}{\sqrt{\omega\lambda_0^\varepsilon(\mathbf{k})}} e^{-i\omega\lambda_0^\varepsilon(\mathbf{k})z/\varepsilon}\,\mathbf{1}_{(-\infty,0)}(z) \\
& + \Big(\frac{\hat{a}_{0,\omega}^\varepsilon(\mathbf{k})}{\sqrt{\omega\lambda_0^\varepsilon(\mathbf{k})}} e^{i\omega\lambda_0^\varepsilon(\mathbf{k})(z-z_{int})/\varepsilon} + \frac{\hat{b}_\omega^{\varepsilon,ref}(\mathbf{k})}{\sqrt{\omega\lambda_0^\varepsilon(\mathbf{k})}} e^{-i\omega\lambda_0^\varepsilon(\mathbf{k})(z-z_{int})/\varepsilon}\Big)\mathbf{1}_{(0,z_{int})}(z) \\
& + \frac{\hat{a}_\omega^{\varepsilon,tr}(\mathbf{k})}{\sqrt{\omega\lambda_1^\varepsilon(\mathbf{k})}} e^{i\omega\lambda_1^\varepsilon(\mathbf{k})(z-z_{int})/\varepsilon}\mathbf{1}_{(z_{int},\infty)}(z),
\end{aligned}$$

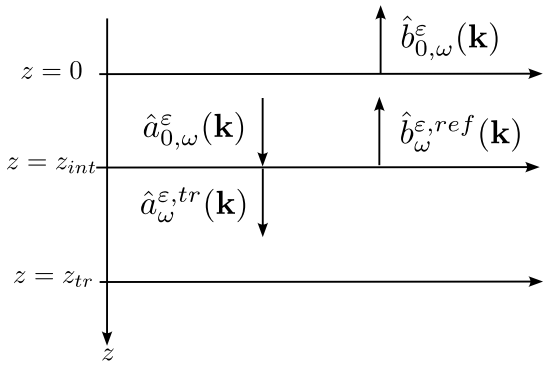

Figure 4: Illustration of the up- and down-going mode amplitudes.

where $\hat{b}^{\varepsilon}_{0,\omega}(\mathbf{k})$ corresponds to the amplitude of the up-going modes for $z < 0$, $\hat{a}^{\varepsilon}_{0,\omega}$ to the amplitude of the down-going incident modes toward the interface, $\hat{b}^{\varepsilon,ref}_{\omega}(\mathbf{k})$ to the amplitude of the reflected modes at the interface, and $\hat{a}^{\varepsilon,tr}_{\omega}(\mathbf{k})$ to the amplitude to those transmitted at the interface (see Figure 4 for an illustration).

The amplitudes of the incident modes toward the interface are determined through the following jump conditions across the plane $z = 0$. These conditions are produced by the source term in (15) and derived from (82) in Appendix A:

$$\begin{aligned}\hat{u}^{\varepsilon}_{\omega}(\mathbf{k}, z = 0^+) - \hat{u}^{\varepsilon}_{\omega}(\mathbf{k}, z = 0^-) &= \varepsilon^2 \hat{\Psi}\Big(\omega, \mathbf{k} - \frac{\mathbf{k}_0}{\sqrt{\varepsilon}}\Big)\\ \partial_z \hat{u}^{\varepsilon}_{\omega}(\mathbf{k}, z = 0^+) - \partial_z \hat{u}^{\varepsilon}_{\omega}(\mathbf{k}, z = 0^-) &= 0,\end{aligned}$$

yielding

$$\hat{a}^{\varepsilon}_{0,\omega}(\mathbf{k}) = \frac{\varepsilon^2 \sqrt{\omega \lambda^{\varepsilon}_0(\mathbf{k})}}{2} \hat{\Psi}\Big(\omega, \mathbf{k} - \frac{\mathbf{k}_0}{\sqrt{\varepsilon}}\Big) e^{i\omega \lambda^{\varepsilon}_0(\mathbf{k}) z_{int}/\varepsilon}, \tag{23}$$

and

$$\hat{b}^{\varepsilon}_{0,\omega}(\mathbf{k}) = -\frac{\varepsilon^2}{2} \hat{\Psi}\Big(\omega, \mathbf{k} - \frac{\mathbf{k}_0}{\sqrt{\varepsilon}}\Big) + \hat{b}^{\varepsilon,ref}_{\omega}(\mathbf{k}) e^{i\omega \lambda^{\varepsilon}_0(\mathbf{k}) z_{int}/\varepsilon}.$$

Therefore, the incident wavefield at the interface can be written as

$$\hat{u}^{\varepsilon,inc}_{\omega}(\mathbf{k}, z_{int}) = \frac{\hat{a}^{\varepsilon}_{0,\omega}(\mathbf{k})}{\sqrt{\omega \lambda^{\varepsilon}_0(\mathbf{k})}} = \frac{\varepsilon^2}{2} \hat{\Psi}\Big(\omega, \mathbf{k} - \frac{\mathbf{k}_0}{\sqrt{\varepsilon}}\Big) e^{i\omega \lambda^{\varepsilon}_0(\mathbf{k}) z_{int}/\varepsilon},$$

and as expected, the up-going modes $\hat{b}^{\varepsilon}_{0,\omega}(\mathbf{k})$ are composed of a source component as well as the reflected part of the wavefield at the interface.

2.2 Reflection and transmission at the interface

Denoting

$$\hat{u}^{\varepsilon,ref}_{\omega}(\mathbf{k}, z) = \frac{\hat{b}^{\varepsilon,ref}_{\omega}(\mathbf{k})}{\sqrt{\omega \lambda^{\varepsilon}_0(\mathbf{k})}} e^{-i\omega \lambda^{\varepsilon}_0(\mathbf{k})(z - z_{int})/\varepsilon} \qquad 0 < z < z_{int},$$

the reflected wavefield at the interface and

$$\hat{u}^{\varepsilon,tr}_{\omega}(\mathbf{x}, z) = \frac{\hat{a}^{\varepsilon,tr}_{\omega}(\mathbf{k})}{\sqrt{\omega \lambda^{\varepsilon}_1(\mathbf{k})}} e^{i\omega \lambda^{\varepsilon}_1(\mathbf{k})(z - z_{int})/\varepsilon} \qquad z > z_{int},$$

the transmitted wavefield, the following continuity conditions across the interface $z = z_{int}$ are obtained from (8) for $V \equiv 0$:

$$\begin{aligned}\hat{u}^{\varepsilon,inc}_{\omega}(\mathbf{x}, z_{int}) + \hat{u}^{\varepsilon,ref}_{\omega}(\mathbf{x}, z_{int}) &= \hat{u}^{\varepsilon,tr}_{\omega}(\mathbf{x}, z_{int}),\\ \partial_z \hat{u}^{\varepsilon,inc}_{\omega}(\mathbf{x}, z_{int}) + \partial_z \hat{u}^{\varepsilon,ref}_{\omega}(\mathbf{x}, z_{int}) &= \partial_z \hat{u}^{\varepsilon,tr}_{\omega}(\mathbf{x}, z_{int}).\end{aligned}$$

These two conditions yield the system

$$\frac{\hat{a}^{\varepsilon}_{0,\omega}(\mathbf{k})}{\sqrt{\lambda^{\varepsilon}_0(\mathbf{k})}} + \frac{\hat{b}^{\varepsilon,ref}_{\omega}(\mathbf{k})}{\sqrt{\lambda^{\varepsilon}_0(\mathbf{k})}} = \frac{\hat{a}^{\varepsilon,tr}_{\omega}(\mathbf{k})}{\sqrt{\lambda^{\varepsilon}_1(\mathbf{k})}},$$
$$\sqrt{\lambda^{\varepsilon}_0(\mathbf{k})}\hat{a}^{\varepsilon}_{0,\omega}(\mathbf{k}) - \sqrt{\lambda^{\varepsilon}_0(\mathbf{k})}\hat{b}^{\varepsilon,ref}_{\omega}(\mathbf{k}) = \sqrt{\lambda^{\varepsilon}_1(\mathbf{k})}\hat{a}^{\varepsilon,tr}_{\omega}(\mathbf{k}),$$

with solutions

$$\hat{a}^{\varepsilon,tr}_{\omega}(\mathbf{k}) = \frac{1}{\tau^{\varepsilon}_+(\mathbf{k})}\hat{a}^{\varepsilon}_{0,\omega}(\mathbf{k}) \qquad \text{and} \qquad \hat{b}^{\varepsilon,ref}_{\omega}(\mathbf{k}) = \frac{\tau^{\varepsilon}_-(\mathbf{k})}{\tau^{\varepsilon}_+(\mathbf{k})}\hat{a}^{\varepsilon}_{0,\omega}(\mathbf{k}),$$

where

$$\tau^{\varepsilon}_{\pm}(\mathbf{k}) = \frac{1}{2}\left(\sqrt{\frac{\lambda^{\varepsilon}_0(\mathbf{k})}{\lambda^{\varepsilon}_1(\mathbf{k})}} \pm \sqrt{\frac{\lambda^{\varepsilon}_1(\mathbf{k})}{\lambda^{\varepsilon}_0(\mathbf{k})}}\right). \tag{24}$$

2.3 The reflected wave

From the above analysis, the reflected wave at the plane $z = 0$ can be expressed as

$$\begin{aligned} u^{\varepsilon}(t,\mathbf{x},z=0^-) &= \frac{1}{(2\pi)^3\varepsilon^2}\iint \hat{u}^{\varepsilon,ref}_{\omega}(\mathbf{k},z=0)e^{-i\omega(t/\varepsilon-\mathbf{x}\cdot\mathbf{k}/\sqrt{\varepsilon})}\omega^2 d\omega d\mathbf{k} \\ &= \frac{1}{(2\pi)^3\varepsilon^2}\iint e^{2i\omega\lambda^{\varepsilon}_0(\mathbf{k})z_{int}/\varepsilon}\frac{\tau^{\varepsilon}_-(\mathbf{k})\hat{a}^{\varepsilon}_{0,\omega}(\mathbf{k})}{\tau^{\varepsilon}_+(\mathbf{k})\sqrt{\omega\lambda^{\varepsilon}_0(\mathbf{k})}}e^{-i\omega(t/\varepsilon-\mathbf{x}\cdot\mathbf{k}/\sqrt{\varepsilon})}\omega^2 d\omega d\mathbf{k} \\ &= \frac{1}{2(2\pi)^3}\iint e^{2i\omega\lambda^{\varepsilon}_0(\mathbf{q}+\mathbf{k}_0/\sqrt{\varepsilon})z_{int}/\varepsilon}\frac{\tau^{\varepsilon}_-(\mathbf{q}+\mathbf{k}_0/\sqrt{\varepsilon})}{\tau^{\varepsilon}_+(\mathbf{q}+\mathbf{k}_0/\sqrt{\varepsilon})}e^{-i\omega(t/\varepsilon-\mathbf{x}\cdot\mathbf{k}_0/\varepsilon-\mathbf{x}\cdot\mathbf{q}/\sqrt{\varepsilon})}\hat{\Psi}(\omega,\mathbf{q})\omega^2 d\omega d\mathbf{q}, \end{aligned}$$

where the last line is obtained after the change of variable $\mathbf{k} = \mathbf{q} + \mathbf{k}_0/\sqrt{\varepsilon}$, corresponding to the argument of $\hat{\Psi}$ in (23). Considering the following position and time of observation

$$\mathbf{x} = \mathbf{x}_{obs,ref} + \sqrt{\varepsilon}\,\mathbf{y} \qquad \text{and} \qquad t = t^{\varepsilon}_{obs,ref}(\mathbf{y}) := t_{obs,ref} + \sqrt{\varepsilon}\,\mathbf{k}_0\cdot\mathbf{y}, \tag{25}$$

where

$$\mathbf{x}_{obs,ref} := \frac{2\mathbf{k}_0 z_{int}}{\lambda_0} \qquad \text{and} \qquad t_{obs,ref} := \frac{2z_{int}}{c_0^2\lambda_0}, \tag{26}$$

with λ_0 defined by (22), the asymptotic specular reflected wave is given by

$$\begin{aligned} U^{ref}(s,\mathbf{y}) &:= \lim_{\varepsilon\to 0} u^{\varepsilon}\big(t^{\varepsilon}_{obs,ref}(\mathbf{y}) + \varepsilon s, \mathbf{x}_{obs,ref} + \sqrt{\varepsilon}\,\mathbf{y}, z=0\big) \\ &= \frac{\mathcal{R}}{2(2\pi)^3}\int e^{-i\omega(s-\mathbf{y}\cdot\mathbf{q})}\hat{\mathcal{U}}_0(\omega,\mathbf{q},2z_{int})\hat{\Psi}(\omega,\mathbf{q})\omega^2 d\omega d\mathbf{q}. \end{aligned} \tag{27}$$

Here, U^{ref} corresponds to the asymptotic wave front observed in the frame of the source term at position $\mathbf{x}_{obs,ref}$ and time $t^{\varepsilon}_{obs,ref}(\mathbf{y})$. This travel time is influenced by the offset $\mathbf{y}$ since the beam width $\sqrt{\varepsilon}$ is larger than the pulse width ε and with the wave front traveling obliquely relative to the vertical direction. Note that $\mathbf{x}_{obs,ref}$ is twice the lateral position

$$\mathbf{x}_{int} := \frac{\mathbf{k}_0 z_{int}}{\lambda_0}, \tag{28}$$

where the incident pulse hit the interface. Therefore, the standard reflexion relation reads

$$\theta_{inc} = \theta^0_{ref} := \arctan\Big(\frac{|\mathbf{k}_0|}{\lambda_0}\Big), \tag{29}$$

where the incident and reflected angle are equal. We refer to Figure 5 as an illustration of the geometrical properties of the reflection.

Regarding the profile of the reflected wave, the reflection coefficient is given by

$$\mathcal{R} := \frac{\lambda_0 - \lambda_1}{\lambda_0 + \lambda_1}, \tag{30}$$

and

$$\hat{\mathcal{U}}_0(\omega,\mathbf{q},z) := e^{-i\omega z c_0 \mathbf{q}^T A_0 \mathbf{q}}, \tag{31}$$

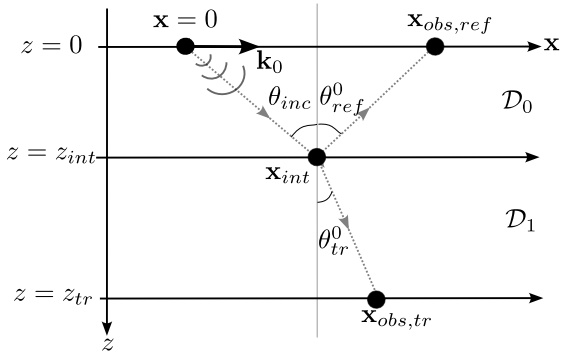

Figure 5: Illustration of the reflection and transmission in the context of a flat interface at $z = z_{int}$. The source is located at $\mathbf{x} = 0$ in the plan $z = 0$, and the emitted wave hit the interface at $\mathbf{x} = \mathbf{x}_{int}$, in the plan $z = z_{int}$, with an incident angle θ_{inc}. The reflected wave, with angle θ^0_{ref}, is observed in the plan $z = 0$ at $\mathbf{x} = \mathbf{x}_{obs,ref}$, while the transmitted wave, with angle θ^0_{tr}, is observed in the plan $z = z_{tr}$ at $\mathbf{x} = \mathbf{x}_{obs,tr}$.

where A_0 is defined by (21). The term $\hat{\mathcal{U}}_0$ leads to the following homogeneous semi-group

$$\check{\mathcal{U}}_0(\omega, \mathbf{y}, z) := \frac{\omega^2}{(2\pi)^2} \int e^{i\omega \mathbf{y}\cdot\mathbf{q}} e^{-i\omega z c_0 \mathbf{q}^T A_0 \mathbf{q}} d\mathbf{q}, \tag{32}$$

satisfying the Schrödinger type equation

$$i\partial_z \check{\mathcal{U}}_0(\omega, \mathbf{y}, z) + \frac{1}{k_{0,\omega}} \nabla_{\mathbf{y}} \cdot \Big(A_0 \nabla_{\mathbf{y}} \check{\mathcal{U}}_0 \Big)(\omega, \mathbf{y}, z) = 0 \qquad z > 0,$$

where

$$\check{\mathcal{U}}_0(\omega, \mathbf{y}, z = 0) = \delta(\mathbf{y}) \qquad \text{and} \qquad k_{0,\omega} = \omega / c_0,$$

which is characteristic of the paraxial approximation. Due to the initial lateral direction $\mathbf{k}_0$, we do not have the standard Schrödinger equation with a Laplacian term. Nevertheless, the standard Laplacian can be recovered by sending this direction to zero. In the time domain, the function

$$\mathcal{U}_0(s, \mathbf{y}, z) := \frac{1}{2(2\pi)^3} \int e^{-i\omega(s - \mathbf{y}\cdot\mathbf{q})} \hat{\mathcal{U}}_0(\omega, \mathbf{q}, z) \hat{\Psi}(\omega, \mathbf{q}) \omega^2 d\omega d\mathbf{q}, \tag{33}$$

corresponding to the pulse profile in (27), satisfies the following paraxial wave equation

$$\partial^2_{sz} \mathcal{U}_0 - c_0 \nabla_{\mathbf{y}} \cdot \Big(A_0 \nabla_{\mathbf{y}} \mathcal{U}_0 \Big) = 0, \qquad \text{with} \qquad \mathcal{U}_0(s, z = 0, \mathbf{y}) = \frac{1}{2} \Psi(s, \mathbf{y}). \tag{34}$$

As a result, the reflecting wave by a flat (unperturbed) interface can be expressed as

$$U^{ref}(s, \mathbf{y}) = \mathcal{R}\, \mathcal{U}_0(s, \mathbf{y}, 2z_{int}).$$

Under the paraxial wave model, this formulation corresponds to the travel of the emitted pulse from the source location to the interface, and back from the interface to the source location (yielding the $z = 2z_{int}$). The factor $\mathcal{R}$ accounts for the reflection at the interface.

2.4 The transmitted wave

Following the same strategy as for the reflected wave, the transmitted wave observed at $z = z_{tr}$ reads

$$\begin{aligned}
u^\varepsilon(t, \mathbf{x}, z = z_{tr}) &= \frac{1}{(2\pi)^3 \varepsilon^2} \iint \hat{u}^{\varepsilon,tr}_\omega(\mathbf{k}, z = z_{tr}) e^{-i\omega(t/\varepsilon - \mathbf{x}\cdot\mathbf{k}/\sqrt{\varepsilon})} \omega^2 d\omega d\mathbf{k} \\
&= \frac{1}{(2\pi)^3 \varepsilon^2} \iint \frac{\hat{a}^\varepsilon_{0,\omega}(\mathbf{k})}{\tau^\varepsilon_+(\mathbf{k}) \sqrt{\omega \lambda^\varepsilon_1(\mathbf{k})}} e^{i\omega \lambda^\varepsilon_1(\mathbf{k})(z_{tr} - z_{int})/\varepsilon} e^{-i\omega(t/\varepsilon - \mathbf{x}\cdot\mathbf{k}/\sqrt{\varepsilon})} \omega^2 d\omega d\mathbf{k} \\
&= \frac{1}{2(2\pi)^3} \iint e^{i\omega(\lambda^\varepsilon_0(\mathbf{q} + \mathbf{k}_0/\sqrt{\varepsilon}) z_{int} + \lambda^\varepsilon_1(\mathbf{q} + \mathbf{k}_0/\sqrt{\varepsilon})(z_{tr} - z_{int}))/\varepsilon} \frac{\sqrt{\lambda^\varepsilon_0(\mathbf{q} + \mathbf{k}_0/\sqrt{\varepsilon})}}{\tau^\varepsilon_+(\mathbf{q} + \mathbf{k}_0/\sqrt{\varepsilon}) \sqrt{\lambda^\varepsilon_1(\mathbf{q} + \mathbf{k}_0/\sqrt{\varepsilon})}} \\
&\qquad \times e^{-i\omega(t/\varepsilon - \mathbf{x}\cdot\mathbf{k}_0/\varepsilon - \mathbf{x}\cdot\mathbf{q}/\sqrt{\varepsilon})} \hat{\Psi}(\omega, \mathbf{q}) \omega^2 d\omega d\mathbf{q}.
\end{aligned}$$

Using the expansion (20), we obtain the following asymptotic specular transmitted wave

$$U^{tr}(s,\mathbf{y}) := \lim_{\varepsilon\to 0} u^{\varepsilon}\big(t^{\varepsilon}_{obs,tr}(\mathbf{y}) + \varepsilon s, \mathbf{x}_{obs,tr} + \sqrt{\varepsilon}\mathbf{y}, z = z_{tr}\big) \tag{35}$$
$$= \frac{\mathcal{T}}{2(2\pi)^3}\sqrt{\frac{\lambda_0}{\lambda_1}}\int e^{-i\omega(s-\mathbf{y}\cdot\mathbf{q})}\hat{\mathcal{U}}_1(\omega,\mathbf{q},z_{tr}-z_{int})\hat{\mathcal{U}}_0(\omega,\mathbf{q},z_{int})\hat{\Psi}(\omega,\mathbf{q})\omega^2 d\omega d\mathbf{q},$$

with

$$\mathbf{x}_{obs,tr} := \mathbf{x}_{int} + \mathbf{x}_{tr} := \mathbf{x}_{int} + \frac{\mathbf{k}_0(z_{tr}-z_{int})}{\lambda_1}, \tag{36}$$

where $\mathbf{x}_{int}$ is given by (28), the λ_j's by (22), and

$$t^{\varepsilon}_{obs,tr}(\mathbf{y}) := t_{obs,tr} + \sqrt{\varepsilon}\mathbf{y} \qquad \text{with} \qquad t_{obs,tr} := \frac{z_{int}}{c_0^2\lambda_0} + \frac{z_{tr}-z_{int}}{c_1^2\lambda_1}. \tag{37}$$

Here, U^{tr} corresponds to the wave front observed in the frame of the source term at position $\mathbf{x}_{obs,tr}$, and time $t^{\varepsilon}_{obs,tr}(\mathbf{y})$. The time $t_{obs,tr}$ for the pulse to reach the plan $z = z_{tr}$ is the sum of the time to reach the interface and the time to go from the interface to the plan $z = z_{tr}$. Again, the term $\sqrt{\varepsilon}\mathbf{y}$ in $t^{\varepsilon}_{obs,tr}(\mathbf{y})$ is due to the offset of the observation position, which is large compared to the pulse width and with the wave front traveling obliquely relative to the vertical direction. The lateral position $\mathbf{x}_{obs,tr}$, where the pulse hit the plan $z = z_{tr}$, corresponds to a sum of vectors, where the first one represents the lateral position where the pulse hit the interface, and the second one the additional lateral displacement once the pulse goes through the interface and reaches the plan $z = z_{tr}$. We refer to Figure 5 as an illustration for the geometrical properties of transmission. From this formulation, one has the Snell-Descartes law:

$$\frac{\sin(\theta_{inc})}{c_0} = \frac{\sin(\theta^0_{tr})}{c_1},$$

with θ_{inc} defined by (29), and

$$\theta^0_{tr} := \arctan\Big(\frac{|\mathbf{k}_0|}{\lambda_1}\Big). \tag{38}$$

Regarding the pulse profile, the transmission coefficient is defined as

$$\mathcal{T} := \frac{2\sqrt{\lambda_0\lambda_1}}{\lambda_0+\lambda_1},$$

so that we have the conservation relation $\mathcal{R}^2 + \mathcal{T}^2 = 1$, and $\hat{\mathcal{U}}_0$ is defined by (31). The term $\hat{\mathcal{U}}_1$ is defined in the same way:

$$\hat{\mathcal{U}}_1(\omega,\mathbf{q},z) := e^{-i\omega z c_1 \mathbf{q}^T A_1 \mathbf{q}}, \tag{39}$$

where A_1 is defined by (21). Considering $\mathcal{U}_1$, defined as (33) with c_1 and A_1 instead of c_0 and A_0, and satisfying the corresponding paraxial wave equation (34), the formulation (35) corresponds to the travel of the emitted pulse from the source location to the interface, and from the interface to the plane $z = z_{tr}$ under the paraxial approximation. The factor $\mathcal{T}$ accounts for the transmission at the interface.

3 The reflected and transmitted waves for a random interface

In this section, in presence of a random interface, explicit formulations for the reflected and transmitted waves are derived following the strategies described for a flat interface. Along the interface

$$z = z^{\varepsilon}_{int}(\mathbf{x}) := z_{int} + \varepsilon\, V\Big(\frac{\mathbf{x}}{\varepsilon^{\gamma}}\Big),$$

the incident, reflected and transmitted waves, evolving in homogeneous spaces, can be written as

$$u^{\varepsilon,inc}(t,\mathbf{x},z) = \frac{1}{(2\pi)^3\varepsilon^2}\iint e^{-i\omega(t/\varepsilon-\mathbf{x}\cdot\mathbf{k}/\sqrt{\varepsilon})}\frac{\hat{a}^{\varepsilon}_{0,\omega}(\mathbf{k})}{\sqrt{\omega\lambda^{\varepsilon}_0(\mathbf{k})}}e^{i\omega\lambda^{\varepsilon}_0(\mathbf{k})(z-z_{int})/\varepsilon}\omega^2 d\omega d\mathbf{k} \qquad 0 < z < z^{\varepsilon}_{int}(\mathbf{x})$$

$$u^{\varepsilon,ref}(t,\mathbf{x},z) = \frac{1}{(2\pi)^3\varepsilon^2}\iint e^{-i\omega(t/\varepsilon-\mathbf{x}\cdot\mathbf{k}/\sqrt{\varepsilon})}\frac{\hat{b}^{\varepsilon,ref}_{\omega}(\mathbf{k})}{\sqrt{\omega\lambda^{\varepsilon}_0(\mathbf{k})}}e^{-i\omega\lambda^{\varepsilon}_0(\mathbf{k})(z-z_{int})/\varepsilon}\omega^2 d\omega d\mathbf{k} \qquad 0 < z < z^{\varepsilon}_{int}(\mathbf{x}),$$

$$u^{\varepsilon,tr}(t,\mathbf{x},z) = \frac{1}{(2\pi)^3\varepsilon^2}\iint e^{-i\omega(t/\varepsilon-\mathbf{x}\cdot\mathbf{k}/\sqrt{\varepsilon})}\frac{\hat{a}^{\varepsilon,tr}_{\omega}(\mathbf{k})}{\sqrt{\omega\lambda^{\varepsilon}_1(\mathbf{k})}}e^{i\omega\lambda^{\varepsilon}_1(\mathbf{k})(z-z_{int})/\varepsilon}\omega^2 d\omega d\mathbf{k} \qquad z > z^{\varepsilon}_{int}(\mathbf{x}),$$

yielding from (8) the two continuity relations along the random interface $z = z^\varepsilon_{int}(\mathbf{x})$:

$$\begin{aligned} u^{\varepsilon,inc}(t,\mathbf{x},z^\varepsilon_{int}(\mathbf{x})^-) + u^{\varepsilon,ref}(t,\mathbf{x},z^\varepsilon_{int}(\mathbf{x})^-) &= u^{\varepsilon,tr}(t,\mathbf{x},z^\varepsilon_{int}(\mathbf{x})^+), \\ \partial_z u^{\varepsilon,inc}(t,\mathbf{x},z^\varepsilon_{int}(\mathbf{x})^-) + \partial_z u^{\varepsilon,ref}(t,\mathbf{x},z^\varepsilon_{int}(\mathbf{x})^-) &= \partial_z u^{\varepsilon,tr}(t,\mathbf{x},z^\varepsilon_{int}(\mathbf{x})^+). \end{aligned} \tag{40}$$

Now, we perform some algebra consisting in taking the Fourier transform w.r.t. time, making the change of variable $\mathbf{k} \to \mathbf{k}_0/\sqrt{\varepsilon} + \mathbf{q}$ (corresponding to the scaling of the source profile (23)) for all the terms of (40), then considering the following approximation from (20),

$$\lambda^\varepsilon_j\Big(\mathbf{q} + \frac{\mathbf{k}_0}{\sqrt{\varepsilon}}\Big) = \lambda_j + \mathcal{O}(\sqrt{\varepsilon}) \qquad \text{for } j = 0, 1, \tag{41}$$

and finally going back to the original variable $\mathbf{q} \to \mathbf{k} - \mathbf{k}_0/\sqrt{\varepsilon}$. All these steps yield the continuity relations at the leading order in ε:

$$\begin{aligned} \frac{1}{\sqrt{\lambda_0}}\breve{u}^{\varepsilon,inc}_\omega(\mathbf{x},z_{int})e^{i\omega\lambda_0 V(\mathbf{x}/\varepsilon^\gamma)} + \frac{1}{\sqrt{\lambda_0}}\breve{u}^{\varepsilon,ref}_\omega(\mathbf{x},z_{int})e^{-i\omega\lambda_0 V(\mathbf{x}/\varepsilon^\gamma)} &= \frac{1}{\sqrt{\lambda_1}}\breve{u}^{\varepsilon,tr}_\omega(\mathbf{x},z_{int})e^{i\omega\lambda_1 V(\mathbf{x}/\varepsilon^\gamma)}, \\ \sqrt{\lambda_0}\breve{u}^{\varepsilon,inc}_\omega(\mathbf{x},z_{int})e^{i\omega\lambda_0 V(\mathbf{x}/\varepsilon^\gamma)} - \sqrt{\lambda_0}\breve{u}^{\varepsilon,ref}_\omega(\mathbf{x},z_{int})e^{-i\omega\lambda_0 V(\mathbf{x}/\varepsilon^\gamma)} &= \sqrt{\lambda_1}\breve{u}^{\varepsilon,tr}_\omega(\mathbf{x},z_{int})e^{i\omega\lambda_1 V(\mathbf{x}/\varepsilon^\gamma)}, \end{aligned}$$

where

$$\begin{aligned} \breve{u}^{\varepsilon,inc}_\omega(\mathbf{x},z) &:= \frac{\omega^2}{(2\pi)^2\varepsilon}\int e^{i\omega\mathbf{x}\cdot\mathbf{k}/\sqrt{\varepsilon}}\frac{\hat{a}^\varepsilon_{0,\omega}(\mathbf{k})}{\sqrt{\omega}}e^{i\omega\lambda^\varepsilon_0(\mathbf{k})(z-z_{int})/\varepsilon}d\mathbf{k}, \\ \breve{u}^{\varepsilon,ref}_\omega(\mathbf{x},z) &:= \frac{\omega^2}{(2\pi)^2\varepsilon}\int e^{i\omega\mathbf{x}\cdot\mathbf{k}/\sqrt{\varepsilon}}\frac{\hat{b}^{\varepsilon,ref}_\omega(\mathbf{k})}{\sqrt{\omega}}e^{-i\omega\lambda^\varepsilon_0(\mathbf{k})(z-z_{int})/\varepsilon}d\mathbf{k}, \\ \breve{u}^{\varepsilon,tr}_\omega(\mathbf{x},z) &:= \frac{\omega^2}{(2\pi)^2\varepsilon}\int e^{i\omega\mathbf{x}\cdot\mathbf{k}/\sqrt{\varepsilon}}\frac{\hat{a}^{\varepsilon,tr}_\omega(\mathbf{k})}{\sqrt{\omega}}e^{i\omega\lambda^\varepsilon_1(\mathbf{k})(z-z_{int})/\varepsilon}d\mathbf{k}. \end{aligned}$$

The expansion (41) is critical to identify the mode amplitudes $\hat{a}^{\varepsilon,tr}_\omega(\mathbf{k})$ and $\hat{b}^{\varepsilon,ref}_\omega(\mathbf{k})$. In fact, the latter system can be solved to provide at the leading order

$$\begin{aligned} \breve{u}^{\varepsilon,ref}_\omega(\mathbf{x},z_{int}) &= \mathcal{R}\,\breve{u}^{\varepsilon,inc}_\omega(\mathbf{x},z_{int})e^{2i\omega\lambda_0 V(\mathbf{x}/\varepsilon^\gamma)}, \\ \breve{u}^{\varepsilon,tr}_\omega(\mathbf{x},z_{int}) &= \mathcal{T}\,\breve{u}^{\varepsilon,inc}_\omega(\mathbf{x},z_{int})e^{i\omega(\lambda_0-\lambda_1)V(\mathbf{x}/\varepsilon^\gamma)}, \end{aligned}$$

yielding for the reflection and transmission amplitudes in the Fourier domain:

$$\begin{aligned} \hat{b}^{\varepsilon,ref}_\omega(\mathbf{k}) = \frac{\varepsilon\mathcal{R}\omega^2}{2(2\pi)^2}\iint & e^{-i\omega\mathbf{x}'\cdot(\mathbf{k}-\mathbf{k}')/\sqrt{\varepsilon}}e^{i\omega\lambda^\varepsilon_0(\mathbf{k}')z_{int}/\varepsilon}e^{2i\omega\lambda_0 V(\mathbf{x}'/\varepsilon^\gamma)} \\ & \times\sqrt{\omega\lambda^\varepsilon_0(\mathbf{k}')}\hat{\Psi}\Big(\omega,\mathbf{k}'-\frac{\mathbf{k}_0}{\sqrt{\varepsilon}}\Big)d\mathbf{x}'d\mathbf{k}', \\ \hat{a}^{\varepsilon,tr}_\omega(\mathbf{k}) = \frac{\varepsilon\mathcal{T}\omega^2}{2(2\pi)^2}\iint & e^{-i\omega\mathbf{x}'\cdot(\mathbf{k}-\mathbf{k}')/\sqrt{\varepsilon}}e^{i\omega\lambda^\varepsilon_0(\mathbf{k}')z_{int}/\varepsilon}e^{i\omega(\lambda_0-\lambda_1)V(\mathbf{x}'/\varepsilon^\gamma)} \\ & \times\sqrt{\omega\lambda^\varepsilon_0(\mathbf{k}')}\hat{\Psi}\Big(\omega,\mathbf{k}'-\frac{\mathbf{k}_0}{\sqrt{\varepsilon}}\Big)d\mathbf{x}'d\mathbf{k}'. \end{aligned}$$

To get ride of the source profile scaling, we make the change of variables

$$\mathbf{k} \to \frac{\mathbf{k}_0}{\sqrt{\varepsilon}} + \mathbf{q} \qquad \text{and} \qquad \mathbf{k}' \to \frac{\mathbf{k}_0}{\sqrt{\varepsilon}} + \mathbf{q}',$$

so that at the leading order in ε, using (20), the reflected and transmitted wave read

$$\begin{aligned} u^{\varepsilon,ref}(t,\mathbf{x},z=0) \simeq \frac{\mathcal{R}}{2(2\pi)^5\varepsilon}\iiiint & e^{-i\omega(t-2\lambda_0 z_{int}-\mathbf{x}\cdot\mathbf{k}_0)/\varepsilon}e^{2i\omega\lambda_0 V(\mathbf{x}'/\varepsilon^\gamma)} \\ & \times e^{i\omega\mathbf{q}\cdot(\mathbf{x}-\mathbf{x}'-\mathbf{x}_{int})/\sqrt{\varepsilon}}e^{i\omega\mathbf{q}'\cdot(\mathbf{x}'-\mathbf{x}_{int})/\sqrt{\varepsilon}} \\ & \times\hat{\mathcal{U}}_0(\omega,\mathbf{q},z_{int})\hat{\mathcal{U}}_0(\omega,\mathbf{q}',z_{int})\hat{\Psi}(\omega,\mathbf{q}')\omega^4 d\omega d\mathbf{x}'d\mathbf{q}'d\mathbf{q}, \end{aligned} \tag{42}$$

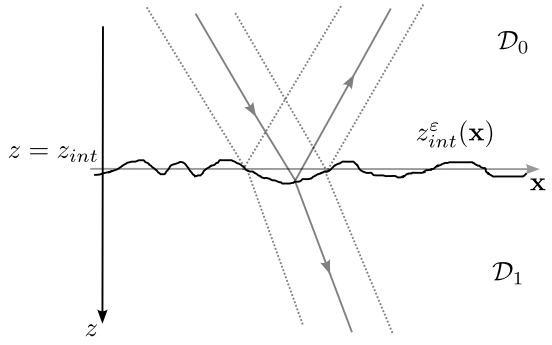

Figure 6: Illustration of the reflection and transmission in case of a random interface with $\gamma = 1/2$. The travel times of the reflected and transmitted waves are affected by the fluctuations V.

and

$$u^{\varepsilon,tr}(t,\mathbf{x},z=z_{tr}) \simeq \frac{\mathcal{T}}{2(2\pi)^5\varepsilon}\sqrt{\frac{\lambda_0}{\lambda_1}}\iiiint e^{-i\omega(t-\lambda_0 z_{int}-\lambda_1(z_{tr}-z_{int}))-\mathbf{x}\cdot\mathbf{k}_0)/\varepsilon}e^{i\omega(\lambda_0-\lambda_1)V(\mathbf{x}'/\varepsilon^\gamma)} \\ \times e^{i\omega\mathbf{q}\cdot(\mathbf{x}-\mathbf{x}'-\mathbf{x}_{tr})/\sqrt{\varepsilon}}e^{i\omega\mathbf{q}'\cdot(\mathbf{x}'-\mathbf{x}_{int})/\sqrt{\varepsilon}} \\ \times \hat{\mathcal{U}}_1(\omega,\mathbf{q},z_{tr}-z_{int})\hat{\mathcal{U}}_0(\omega,\mathbf{q}',z_{int})\hat{\Psi}(\omega,\mathbf{q}')\omega^4 d\omega d\mathbf{x}' d\mathbf{q}' d\mathbf{q}. \tag{43}$$

Here, the $\hat{\mathcal{U}}_j$'s are defined by (31) and (39), and $\mathbf{x}_{int}$ (resp. $\mathbf{x}_{tr}$), representing the lateral position where the incident pulse hit the interface (resp. the lateral displacement from $\mathbf{x}_{int}$ to the location where the transmitted wave is observed), by (28) (resp. by (36)).

Let us remark that the scattering operator, resulting from the random interface, is provided through the following Fourier representation:

$$K^{\varepsilon}(\omega,\mathbf{q}',\mathbf{q}) = \int e^{i\omega(\mathbf{q}'-\mathbf{q})\cdot(\mathbf{x}'-\mathbf{x}_{int})/\sqrt{\varepsilon}}e^{i\omega\tau V(\mathbf{x}'/\varepsilon^\gamma)}d\mathbf{x}', \tag{44}$$

for a given frequency ω, and centered around $\mathbf{x}_{int}$ with radius corresponding to the beam width $\sqrt{\varepsilon}$. This operator described how an incident plane wave with lateral direction $\mathbf{q}'$, supported by the source term $\hat{\Psi}$, is diffracted into a direction $\mathbf{q}$. For both the reflected (42) and transmitted waves (43), the plane wave with direction $\mathbf{q}'$, propagate according to $\hat{\mathcal{U}}_0(\mathbf{q}')$ under the paraxial approximation. Once it has been diffracted by the surface, the reflected wave still propagates according to $\hat{\mathcal{U}}_0(\mathbf{q})$, but the transmitted one propagates according to $\hat{\mathcal{U}}_1(\mathbf{q})$.

The remaining of the paper consists in describing the effective statistical behavior of this operator in the high-frequency limit $\varepsilon \to 0$. The two cases,

$$\gamma = 1/2 \qquad \text{and} \qquad \gamma > 1/2,$$

are analyzed separately as they provide two different statistical behaviors for the reflected and transmitted waves.

4 The case $\gamma = 1/2$

The case $\gamma = 1/2$ corresponds to a correlation length (of the interface fluctuations) and a beam width of the same order. Since the wavelength is also assumed to be of order the strength of the fluctuations, it is natural to expect a random arrival time for the reflected and transmitted waves, but no homogenization effect (see Figure 6 for an illustration). To describe mathematically this phenomenon on the reflected wave, the change of variable

$$\mathbf{x}' \to \mathbf{x}_{int} + \sqrt{\varepsilon}\,\mathbf{y}'$$

is applied to (42), so that at the leading order the observed reflected wave reads

$$u^{\varepsilon,ref}(t,\mathbf{x},z=0) \simeq \frac{\mathcal{R}}{2(2\pi)^5}\iiiint e^{-i\omega(t-2\lambda_0 z_{int}-\mathbf{x}\cdot\mathbf{k}_0)/\varepsilon}e^{i\omega(\mathbf{q}'-\mathbf{q})\cdot\mathbf{y}'}e^{2i\omega\lambda_0 V(\mathbf{x}_{int}/\sqrt{\varepsilon}+\mathbf{y}')} \\ \times e^{i\omega\mathbf{q}\cdot(\mathbf{x}-\mathbf{x}_{obs,ref})/\sqrt{\varepsilon}}\hat{\mathcal{U}}_0(\omega,\mathbf{q},z_{int})\hat{\mathcal{U}}_0(\omega,\mathbf{q}',z_{int}) \\ \times \hat{\Psi}(\omega,\mathbf{q}')\omega^4 d\omega d\mathbf{y}' d\mathbf{q}' d\mathbf{q}.$$

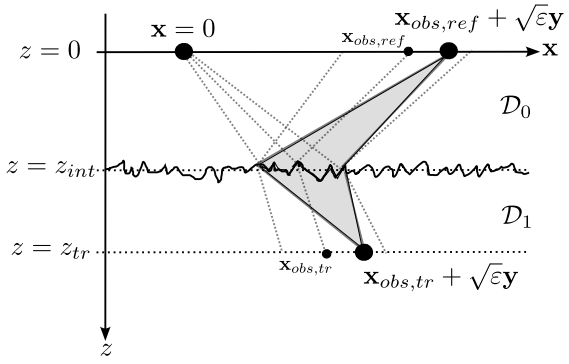

Figure 7: Illustration of the contributions to the reflected and transmitted waves observed at points $\mathbf{x}_{obs,ref}+\sqrt{\varepsilon}\mathbf{y}$ and $\mathbf{x}_{obs,tr}+\sqrt{\varepsilon}\mathbf{y}$ respectively.

Here, the lateral position $\mathbf{x}_{obs,ref}$, at which the specular reflected wave is observed, is defined by (25), λ_0 by (22), and $\hat{\mathcal{U}}_0$ by (31). The fast oscillating components suggest to consider

$$U^{\varepsilon,ref}(s,\mathbf{y}) := u^{\varepsilon,ref}\big(t^{\varepsilon}_{obs,ref}(\mathbf{y})+\varepsilon s, \mathbf{x}_{obs,ref}+\sqrt{\varepsilon}\mathbf{y}, z=0\big) \qquad (s,\mathbf{y})\in\mathbb{R}\times\mathbb{R}^2,$$

where $t^{\varepsilon}_{obs,ref}(\mathbf{y})$ is defined by (26) and corresponds to the expected travel time to observe the reflected wave at the plan $z=0$. The wave front $U^{\varepsilon,ref}$ is observed at the same lateral position and time frame as the specular reflected wave for a flat surface, and for which we have the following result.

Proposition 4.1 *The family $(U^{\varepsilon,ref})_\varepsilon$ converges in distribution in $L^2(\mathbb{R}\times\mathbb{R}^2)$ to*

$$U^{ref}(s,\mathbf{y}) := \frac{\mathcal{R}}{2(2\pi)^5}\iiiint e^{-i\omega(s-2\lambda_0\mathcal{V}(\mathbf{y}')-\mathbf{q}\cdot\mathbf{y})}e^{i\omega(\mathbf{q}'-\mathbf{q})\cdot\mathbf{y}'} \times\hat{\mathcal{U}}_0(\omega,\mathbf{q},z_{int})\hat{\mathcal{U}}_0(\omega,\mathbf{q}',z_{int})\hat{\Psi}(\omega,\mathbf{q}')\omega^4 d\omega d\mathbf{y}' d\mathbf{q}' d\mathbf{q},$$

where $\mathcal{V}$ is a random field with the same law as V.

The reflected wave front U^{ref} consists in a superposition of contribution observed at point $\mathbf{y}$. Each of these contributions result in waves emitted with initial lateral direction $\mathbf{q}'$, propagating according to $\hat{\mathcal{U}}_0(\mathbf{q}')$, and scattered into direction $\mathbf{q}$ at point $\mathbf{y}'$ before propagating back according to $\hat{\mathcal{U}}_0(\mathbf{q})$ (see Figure 7 for an illustration). Note that the specular reflected component has still a beam width of order $\sqrt{\varepsilon}$, and the observation point is still $\mathbf{x}_{obs,ref}$, meaning there is no significant perturbation of the specular reflected cone and angle θ^0_{ref} given by (29). Finally, at $z=0$, a random time correction $2\lambda_0\mathcal{V}(\mathbf{y}')$ is observed for contributions scattered at point $\mathbf{y}'$. In U^{ref}, the scattering operator

$$K_{ref}(\omega,\mathbf{q}',\mathbf{q}) := \int e^{i\omega(\mathbf{q}'-\mathbf{q})\cdot\mathbf{y}'}e^{2i\omega\lambda_0\mathcal{V}(\mathbf{y}')}d\mathbf{y}' \tag{45}$$

has the same law as $\varepsilon K^\varepsilon$ given by (44) (for $\tau=2\lambda_0$) after proper centerings thanks to the stationarity of V: for any $\varphi,\psi\in\mathcal{S}(\mathbb{R}^2)$, where $\mathcal{S}(\mathbb{R}^2)$ stands for the Schwartz class, the two random variables $K_{ref}(\omega,\varphi,\psi)$ and $\varepsilon K^\varepsilon(\omega,\varphi,\psi)$ have the same law.

Proof (of Proposition 4.1) The wave front $U^{\varepsilon,ref}$ reads at the leading order in ε as

$$U^{\varepsilon,ref}(s,\mathbf{y}) \simeq \frac{\mathcal{R}}{2(2\pi)^5}\iiiint e^{-i\omega(s-\mathbf{q}\cdot\mathbf{y})}e^{i\omega(\mathbf{q}'-\mathbf{q})\cdot\mathbf{y}'}e^{2i\omega\lambda_0 V(\mathbf{x}_{int}/\sqrt{\varepsilon}+\mathbf{y}')} \times\hat{\mathcal{U}}_0(\omega,\mathbf{q},z_{int})\hat{\mathcal{U}}_0(\omega,\mathbf{q}',z_{int})\hat{\Psi}(\omega,\mathbf{q}')\omega^4 d\omega d\mathbf{y}' d\mathbf{q}' d\mathbf{q},$$

for which we have

$$\lim_{\varepsilon\to0}\|U^{\varepsilon,ref}\|_{L^2(\mathbb{R}\times\mathbb{R}^2)} = \|U^{ref}\|_{L^2(\mathbb{R}\times\mathbb{R}^2)} = \frac{\mathcal{R}}{2}\|\Psi\|_{L^2(\mathbb{R}\times\mathbb{R}^2)}. \tag{46}$$

From this relation, it is enough to prove the convergence in $\mathcal{S}'(\mathbb{R}\times\mathbb{R}^2)$ as a tempered distribution. Using (46), the tightness is readily satisfied since for any $\varphi\in\mathcal{S}(\mathbb{R}\times\mathbb{R}^2)$

$$\limsup_{\varepsilon\to0}\big|\langle U^{\varepsilon,ref},\varphi\rangle_{L^2(\mathbb{R}\times\mathbb{R}^2)}\big| \le \frac{\mathcal{R}}{2}\|\Psi\|_{L^2(\mathbb{R}\times\mathbb{R}^2)}\|\varphi\|_{L^2(\mathbb{R}\times\mathbb{R}^2)}.$$

The convergence of the finite-dimensional distributions is obtained from the stationarity of V to remove the argument $\mathbf{x}_{int}/\sqrt{\varepsilon}$, yielding for any $n \geq 1$ and $\varphi_1, \ldots, \varphi_n \in \mathcal{S}(\mathbb{R} \times \mathbb{R}^2)$:

$$\lim_{\varepsilon \to 0} \mathbb{E}\Big[\prod_{j=1}^{n} \big\langle U^{\varepsilon,ref}, \varphi_j \big\rangle_{L^2(\mathbb{R}\times\mathbb{R}^2)} \Big] = \mathbb{E}\Big[\prod_{j=1}^{n} \big\langle U^{ref}, \varphi_j \big\rangle_{L^2(\mathbb{R}\times\mathbb{R}^2)} \Big].$$

This concludes the proof. □

The transmitted wave, observed at the same lateral position and time frame as the specular transmitted wave for a flat surface, reads

$$U^{\varepsilon,tr}(s,\mathbf{y}) := u^{\varepsilon,tr}\big(t^{\varepsilon}_{obs,tr}(\mathbf{y}) + \varepsilon s, \mathbf{x}_{obs,tr} + \sqrt{\varepsilon}\mathbf{y}, z = z_{tr}\big), \qquad (s,\mathbf{y}) \in \mathbb{R} \times \mathbb{R}^2,$$

where $\mathbf{x}_{obs,tr}$ and $t^{\varepsilon}_{obs,tr}(\mathbf{y})$ are respectively defined by (36) and (37), and $u^{\varepsilon,tr}$ by (43) at the leading order. The asymptotic behavior of this transmitted wave front is provided by the following result, whose proof follows similar lines as for the reflected wave and is therefore omitted.

Proposition 4.2 *The family $(U^{\varepsilon,tr})_\varepsilon$ converges in distribution in $L^2(\mathbb{R} \times \mathbb{R}^2)$ to*

$$U^{tr}(s,\mathbf{y}) := \frac{\mathcal{T}}{2(2\pi)^5}\sqrt{\frac{\lambda_0}{\lambda_1}} \iiiint e^{-i\omega(s-(\lambda_0-\lambda_1)\mathcal{V}(\mathbf{y}')-\mathbf{q}\cdot\mathbf{y})} e^{i\omega(\mathbf{q}'-\mathbf{q})\cdot\mathbf{y}'} \times \hat{\mathcal{U}}_1(\omega,\mathbf{q},z_{tr}-z_{int})\hat{\mathcal{U}}_0(\omega,\mathbf{q}',z_{int})\hat{\Psi}(\omega,\mathbf{q}')\omega^4 d\omega d\mathbf{y}' d\mathbf{q}' d\mathbf{q},$$

where $\mathcal{V}$ is a random field with the same distribution as V.

The transmitted wave front U^{tr} consists as well in a superposition of diffracted contributions observed at point $\mathbf{y}$. Each of these contribution results in waves emitted with initial lateral direction $\mathbf{q}'$, propagating according to $\hat{\mathcal{U}}_0$, scattered into direction $\mathbf{q}$ at point $\mathbf{y}'$ when going through the interface, and then propagates according to $\hat{\mathcal{U}}_1$ until it reaches $z = z_{tr}$ (see Figure 7 for an illustration). Again, the beam width of the transmitted wave is still $\sqrt{\varepsilon}$, and the observation point is still $\mathbf{x}_{obs,tr}$, meaning there is no significant perturbation of the specular transmitted cone and angle θ^0_{tr} given by (38). Also, a random time correction $(\lambda_0 - \lambda_1)\mathcal{V}(\mathbf{y}')$ is observed for contributions scattered at point $\mathbf{y}'$. For the transmitted wave, the scattering operator reads

$$K_{tr}(\omega,\mathbf{q}',\mathbf{q}) := \int e^{i\omega(\mathbf{q}'-\mathbf{q})\cdot\mathbf{y}'} e^{i\omega(\lambda_0-\lambda_1)\mathcal{V}(\mathbf{y}')} d\mathbf{y}', \tag{47}$$

which has the same law as $\varepsilon K^\varepsilon$ given by (44) (for $\tau = \lambda_0 - \lambda_1$) after proper centerings and thanks to the stationarity of V.

5 The case $\gamma > 1/2$: homogenized specular reflected and transmitted components

The case $\gamma > 1/2$ corresponds to a correlation length (of the interface fluctuations) smaller than the beam width. The incident wave is therefore strongly scattered and homogenization phenomena take place.

In this section, the following reflected wave front is considered

$$U^{\varepsilon,ref}(s,\mathbf{y},\widetilde{\mathbf{y}}) := u^{\varepsilon,ref}\big(t^{\varepsilon}_{obs,ref}(\mathbf{y}) + \varepsilon s, \mathbf{x}_{obs,ref} + \sqrt{\varepsilon}\mathbf{y} + \varepsilon^\gamma \widetilde{\mathbf{y}}, z = 0\big) \qquad (s,\mathbf{y},\widetilde{\mathbf{y}}) \in \mathbb{R} \times \mathbb{R}^2 \times \mathbb{R}^2,$$

where $u^{\varepsilon,ref}$ is given at the lead order by (42), $t^{\varepsilon}_{obs,ref}(\mathbf{y})$ and $\mathbf{x}_{obs,ref}$ are defined respectively by (25) and (26). The additional variable $\widetilde{\mathbf{y}}$ accounts here for variations at the scale of the correlation length. The asymptotic behavior to $U^{\varepsilon,ref}$ is described by the following result.

Proposition 5.1 *The family $(U^{\varepsilon,ref})_\varepsilon$ converges in probability in $\mathcal{S}'(\mathbb{R} \times \mathbb{R}^2 \times \mathbb{R}^2)$, the set of tempered distributions, to the deterministic pulse profile*

$$\begin{aligned} U^{ref}(s,\mathbf{y}) &= \frac{\mathcal{R}}{2(2\pi)^3} \iiint e^{-i\omega(s-\mathbf{q}\cdot\mathbf{y})} \hat{\mathcal{U}}_0(\omega,\mathbf{q},2z_{int})\phi_V(2\omega\lambda_0)\hat{\Psi}(\omega,\mathbf{q})\omega^2 d\omega d\mathbf{q} \\ &= \mathcal{R}\widetilde{\mathcal{U}}_0(s,\mathbf{y},2z_{int}). \end{aligned}$$

Here,

$$\phi_V(u) = \mathbb{E}\big[e^{iuV(0)}\big] \tag{48}$$

is the characteristic function to $V(0)$*,* $\hat{\mathcal{U}}_0$ *is defined by* (31)*. The function* $\widetilde{\mathcal{U}}_0$ *satisfies* (34) *with initial condition*

$$\widetilde{\mathcal{U}}_0(s, \mathbf{y}, z = 0) = \frac{1}{2}\Phi *_s \Psi(s, \mathbf{y}),$$

where $*_s$ *is the convolution operator acting on the* s*-variable, and*

$$\Phi(s) := \frac{1}{2\pi}\int e^{-i\omega s}\phi_V(2\omega\lambda_0)d\omega$$

corresponds to a scaled version to the probability density function of $V(0)$*.*

Let us make some comments on the homogenized specular reflected wave front. First, the asymptotic profile does not depend on $\widetilde{\mathbf{y}}$, so that this homogenized limit does not depend on fluctuations at the scale of the interface fluctuations. Second, through $\widetilde{\mathcal{U}}_0$, the impact of the interface fluctuations on the specular reflected wave can be described as the reflection problem with a flat interface where the homogenized scattering property are captured by the convolution in the initial condition $\Phi *_s \Psi/2$. Finally, compared to the case $\gamma = 1/2$, the scattering operator (45) is now homogenized:

$$\mathbb{E}[K_{ref}(\omega, \mathbf{q}', \mathbf{q})] = \int e^{i\omega(\mathbf{q}'-\mathbf{q})\cdot\mathbf{y}'}\mathbb{E}\Big[e^{2i\omega\lambda_0\mathcal{V}(\mathbf{y}')}\Big]d\mathbf{y}' = \delta(\omega(\mathbf{q}'-\mathbf{q}))\phi_V(2\omega\lambda_0).$$

This homogenized scattering operator acts as for a flat surface, it does not modify the incident direction $\mathbf{q}'$, and the effective contribution of the interface fluctuations produce only a low-pass filter in frequency through the characteristic function ϕ_V. In this situation as well, the specular reflected component has a beam width of order $\sqrt{\varepsilon}$, and the observation point remains $\mathbf{x}_{obs,ref}$. Therefore, there is still no significant perturbation of the specular reflected cone and angle θ^0_{ref} (29).

Proof (of Proposition 5.1) The proof is in two steps. The first step consists in evaluating the first order moment of $U^{\varepsilon,ref}$ to identify the homogenized limit, and then the second order moment to prove the convergence in probability thanks to the Chebyshev inequality.

Before evaluating the moment, let us make the change of variable

$$\mathbf{x}' \to \mathbf{x}_{int} + \sqrt{\varepsilon}\,\mathbf{y}' + \varepsilon^\gamma\widetilde{\mathbf{y}},$$

yielding at the leading order

$$U^{\varepsilon,ref}(s, \mathbf{y}, \widetilde{\mathbf{y}}) \simeq \frac{\mathcal{R}}{2(2\pi)^5}\iiiint e^{-i\omega(s-\mathbf{q}\cdot\mathbf{y})}e^{2i\omega\lambda_0 V(\mathbf{x}_{int}/\varepsilon^\gamma + \mathbf{y}'/\varepsilon^{\gamma-1/2} + \widetilde{\mathbf{y}})}$$
$$\times\, e^{i\omega(\mathbf{q}'-\mathbf{q})\cdot\mathbf{y}'}e^{i\omega\mathbf{q}'\cdot\widetilde{\mathbf{y}}\varepsilon^{\gamma-1/2}}\hat{\mathcal{U}}_0(\omega, \mathbf{q}, z_{int})\hat{\mathcal{U}}_0(\omega, \mathbf{q}', z_{int})\hat{\Psi}(\omega, \mathbf{q}')\omega^4 d\omega d\mathbf{y}' d\mathbf{q}' d\mathbf{q}.$$

First order moment. Taking the expectation to $U^{\varepsilon,ref}$ and using the stationarity of the fluctuations yield

$$\begin{aligned}
\lim_{\varepsilon\to 0}\mathbb{E}[U^{\varepsilon,ref}(s, \mathbf{y}, \widetilde{\mathbf{y}})] &= \frac{\mathcal{R}}{2(2\pi)^5}\iiiint e^{-i\omega(s-\mathbf{q}\cdot\mathbf{y})}\mathbb{E}\big[e^{2i\omega\lambda_0 V(0)}\big]e^{i\omega(\mathbf{q}'-\mathbf{q})\cdot\mathbf{y}'} \\
&\qquad \times \hat{\mathcal{U}}_0(\omega, \mathbf{q}, z_{int})\hat{\mathcal{U}}_0(\omega, \mathbf{q}', z_{int})\hat{\Psi}(\omega, \mathbf{q}')\omega^4 d\omega d\mathbf{y}' d\mathbf{q}' d\mathbf{q} \\
&= \frac{\mathcal{R}}{2(2\pi)^3}\iiiint e^{-i\omega(s-\mathbf{q}\cdot\mathbf{y})}\mathbb{E}\big[e^{2i\omega\lambda_0 V(0)}\big] \\
&\qquad \times \hat{\mathcal{U}}_0(\omega, \mathbf{q}, 2z_{int})\hat{\Psi}(\omega, \mathbf{q})\omega^2 d\omega d\mathbf{q} \\
&= \mathcal{R}\widetilde{\mathcal{U}}_0(s, \mathbf{y}, 2z_{int}).
\end{aligned}$$

Second order moment. At the leading order, the correlation function to $U^{\varepsilon,ref}$ reads

$$\begin{aligned}\mathbb{E}[U^{\varepsilon,ref}(s_1,\mathbf{y}_1,\widetilde{\mathbf{y}}_1)U^{\varepsilon,ref}(s_2,\mathbf{y}_2,\widetilde{\mathbf{y}}_2)]&\\ = \frac{\mathcal{R}^2}{4(2\pi)^{10}}\int\cdots\int e^{-i\omega_1(s_1-\mathbf{q}_1\cdot\mathbf{y}_1)}e^{-i\omega_2(s_2-\mathbf{q}_2\cdot\mathbf{y}_2)}&\\ \times\mathbb{E}\big[e^{2i\omega_1\lambda_0 V(\mathbf{x}_{int}/\varepsilon^\gamma+\mathbf{y}_1'/\varepsilon^{\gamma-1/2}+\widetilde{\mathbf{y}}_1)}e^{2i\omega_2\lambda_0 V(\mathbf{x}_{int}/\varepsilon^\gamma+\mathbf{y}_2'/\varepsilon^{\gamma-1/2}+\widetilde{\mathbf{y}}_2)}\big]&\\ \times e^{i\omega_1(\mathbf{q}_1'-\mathbf{q}_1)\cdot\mathbf{y}_1'}e^{i\omega_2(\mathbf{q}_2'-\mathbf{q}_2)\cdot\mathbf{y}_2'}&\\ \times\hat{\mathcal{U}}_0(\omega_1,\mathbf{q}_1,z_{int})\hat{\mathcal{U}}_0(\omega_1,\mathbf{q}_1',z_{int})\hat{\mathcal{U}}_0(\omega_2,\mathbf{q}_2,z_{int})\hat{\mathcal{U}}_0(\omega_2,\mathbf{q}_2',z_{int})&\\ \times\hat{\Psi}(\omega_1,\mathbf{q}_1')\overline{\hat{\Psi}(\omega_2,\mathbf{q}_2')}\omega_1^4\omega_2^4 d\omega_1 d\omega_2 d\mathbf{y}_1' d\mathbf{y}_2' d\mathbf{q}_1' d\mathbf{q}_2' d\mathbf{q}_1 d\mathbf{q}_2.&\end{aligned}$$

Using the stationary of the fluctuations together with Lemma 1.1 yields

$$\begin{aligned}\lim_{\varepsilon\to 0}\mathbb{E}\big[e^{2i\omega_1\lambda_0 V(\mathbf{x}_{int}/\varepsilon^\gamma+\mathbf{y}_1'/\varepsilon^{\gamma-1/2}+\widetilde{\mathbf{y}}_1)}e^{2i\omega_2\lambda_0 V(\mathbf{x}_{int}/\varepsilon^\gamma+\mathbf{y}_2'/\varepsilon^{\gamma-1/2}+\widetilde{\mathbf{y}}_2)}\big]&\\ =\lim_{\varepsilon\to 0}\mathbb{E}\big[e^{2i\omega_1\lambda_0 V(\mathbf{y}_1'/\varepsilon^{\gamma-1/2}+\widetilde{\mathbf{y}}_1)}e^{2i\omega_2\lambda_0 V(\mathbf{y}_2'/\varepsilon^{\gamma-1/2}+\widetilde{\mathbf{y}}_2)}\big]&\\ =\lim_{\varepsilon\to 0}\mathbb{E}\big[e^{2i\omega_1\lambda_0 V(\mathbf{y}_1'/\varepsilon^{\gamma-1/2}+\widetilde{\mathbf{y}}_1)}\big]\mathbb{E}\big[e^{2i\omega_2\lambda_0 V(\mathbf{y}_2'/\varepsilon^{\gamma-1/2}+\widetilde{\mathbf{y}}_2)}\big]&\\ =\mathbb{E}\big[e^{2i\omega_1\lambda_0 V(0)}\big]\mathbb{E}\big[e^{2i\omega_2\lambda_0 V(0)}\big],&\end{aligned}$$

so that

$$\lim_{\varepsilon\to 0}\mathbb{E}\big[\langle U^{\varepsilon,ref},\varphi\rangle^2_{\mathcal{S}',\mathcal{S}}\big]=\mathbb{E}\big[\langle U^{ref},\varphi\rangle_{\mathcal{S}',\mathcal{S}}\big]^2,$$

which concludes the proof. □

The same strategy applies for the transmitted wave front

$$U^{\varepsilon,tr}(s,\mathbf{y},\widetilde{\mathbf{y}}):=u^{\varepsilon,tr}\big(t^\varepsilon_{obs,tr}(\mathbf{y})+\varepsilon s,\mathbf{x}_{obs,tr}+\sqrt{\varepsilon}\mathbf{y}+\varepsilon^\gamma\widetilde{\mathbf{y}},z=0\big)\qquad(s,\mathbf{y})\in\mathbb{R}\times\mathbb{R}^2\times\mathbb{R}^2,$$

where $u^{\varepsilon,tr}$ is given at the leading order by (43), and $\mathbf{x}_{obs,tr}$ and $t^\varepsilon_{obs,tr}(\mathbf{y})$ are respectively defined by (36) and (37). The asymptotic behavior for $U^{\varepsilon,tr}$ is described by the following result.

Proposition 5.2 *The family $(U^{\varepsilon,tr})_\varepsilon$ converges in probability in $\mathcal{S}'(\mathbb{R}\times\mathbb{R}^2\times\mathbb{R}^2)$ to the deterministic pulse profile*

$$\begin{aligned}U^{tr}(s,\mathbf{y})=\frac{\mathcal{T}}{2(2\pi)^5}\sqrt{\frac{\lambda_0}{\lambda_1}}\iiint e^{-i\omega(s-\mathbf{q}\cdot y)}\hat{\mathcal{U}}_1(\omega,\mathbf{q},z_{tr}-z_{int})\hat{\mathcal{U}}_0(\omega,\mathbf{q},z_{int})&\\ \times\phi_V((\lambda_0-\lambda_1)\omega)\hat{\Psi}(\omega,\mathbf{q})\omega^2 d\omega d\mathbf{x}' d\mathbf{q},&\end{aligned}$$

where ϕ_V is defined by (48)*, the $\hat{\mathcal{U}}_j$'s by* (31) *and* (39)*.*

The proof of this result is omitted as it is similar to the one of Proposition 5.1. Note that the profile U^{tr} is similar to the one obtained for a flat surface (35) with a convolved initial condition traducing homogenization effects of the highly oscillating rough interface. Similarly to the reflected wave the scattering operator (47) becomes

$$\mathbb{E}[K_{tr}(\omega,\mathbf{q}',\mathbf{q})]=\int e^{i\omega(\mathbf{q}'-\mathbf{q})\cdot\mathbf{y}'}\mathbb{E}\Big[e^{i\omega(\lambda_0-\lambda_1)\mathcal{V}(\mathbf{y}')}\Big]d\mathbf{y}'=\delta(\omega(\mathbf{q}'-\mathbf{q}))\phi_V((\lambda_0-\lambda_1)\omega)$$

as a result of the homogenization. Thus, ϕ_V accounts for the homogenized diffraction effects for transmission by playing the role of a low-pass filter in frequency, while the Dirac mass articulates that the incident direction $\mathbf{q}'$ is not affected. As for the reflected wave, the specular transmitted component observed at point $\mathbf{x}_{obs,tr}$ has still a beam width of order $\sqrt{\varepsilon}$. Therefore, there is no significant perturbation of the specular transmitted cone and angle θ^0_{tr} (38).

6 The case $\gamma > 1/2$: incoherent wave fluctuations for the nonspecular reflected contributions

From the homogenization phenomena described in the previous section, an effective frequency-dependent attenuation is observed on the specular components through ϕ_V. This section aims at describing how the scattering

phenomena produce incoherent wave fluctuations accounting for the missing energy carried by the specular components.

In this section, the following reflected wavefield, referred to as the speckle profile, is analyzed:

$$S^{\varepsilon,ref}(\bar{s},\bar{\mathbf{y}},\mathbf{y},\widetilde{s},\widetilde{\mathbf{y}}) := \varepsilon^{-2(\gamma-1/2)}u^{\varepsilon,ref}(t^{\varepsilon}_{obs,ref}(\bar{s},\bar{\mathbf{y}},\mathbf{y},\widetilde{\mathbf{y}}) + \varepsilon\widetilde{s}, \mathbf{x}^{\varepsilon}_{obs,ref}(\bar{\mathbf{y}},\mathbf{y}) + \varepsilon^{\gamma}\widetilde{\mathbf{y}}, z=0), \tag{49}$$

where

$$\mathbf{x}^{\varepsilon}_{obs,ref}(\bar{\mathbf{y}},\mathbf{y}) := \mathbf{x}_{obs,ref} + \varepsilon^{1-\gamma}\bar{\mathbf{y}} + \sqrt{\varepsilon}\,\mathbf{y}, \tag{50}$$

and

$$t^{\varepsilon}_{obs,ref}(\bar{s},\bar{\mathbf{y}},\mathbf{y},\widetilde{\mathbf{y}}) := t_{obs,ref} + \varepsilon^{1-\gamma}\mathbf{k}_0\cdot\bar{\mathbf{y}} + \sqrt{\varepsilon}\,\mathbf{k}_0\cdot\mathbf{y} + \varepsilon^{\gamma}\mathbf{k}_0\cdot\widetilde{\mathbf{y}} + \varepsilon^{2(1-\gamma)}\bar{s}. \tag{51}$$

The proof of Proposition (6.1) below is implemented in a way that justifies the scaling in (49-51). Tracking the scales of interest throughout this derivation allows to provide physical interpretation of these scalings.

Recalling (9), the wavefield $u^{\varepsilon,ref}$ is observed around the observation location $\mathbf{x}_{obs,ref}$ (the position to observe the specular reflected component), but now on a neighborhood of order

$$\frac{r_0^2}{l_c L} \sim \frac{\lambda}{\pi l_c} \sim \varepsilon^{1-\gamma}$$

through the $\bar{\mathbf{y}}$-variable. The radius of the region over which the reflected speckle can be observed is of order the roughness parameter λ/l_c. We will see below that this radius is additionally proportional to the distance from the source plan to the interface. Note that this neighborhood is larger than the beam width (of order $\sqrt{\varepsilon}$) since $\gamma > 1/2$, and can be of order one for $\gamma = 1$. The variables $\mathbf{y}$ and $\widetilde{\mathbf{y}}$ account for variations at the scale of the beam width as well as fluctuations of order the correlation length respectively (see Figure 8 for an illustration). The time scale under consideration is around the travel time $t_{obs,ref}$, with three corrections depending on the observation offsets ($\bar{\mathbf{y}}$, $\mathbf{y}$, and $\widetilde{\mathbf{y}}$), and lying in a time window larger than the pulse duration (of order ε). This time window, described through the variable $\bar{s}$, is of order

$$\frac{r_0^2\lambda}{l_c^2 L} \sim \Big(\frac{\lambda}{l_c}\Big)^2 \sim \varepsilon^{2(1-\gamma)},$$

the square of the roughness parameter. The $\widetilde{s}$-variable in (49) accounts for fluctuations at the scale of the pulse width. Finally, the amplitude of the speckle profile is of order

$$\frac{l_c^2}{\sqrt{\lambda L} r_0} \sim \Big(\frac{l_c}{r_0}\Big)^2 \sim \varepsilon^{2(\gamma-1/2)}$$

leading to the large amplitude factor $\varepsilon^{-2(\gamma-1/2)} \gg 1$ in (49). Note that the more we increase γ the wider is the area around $\mathbf{x}_{obs,ref}$ where we can observe the speckle pattern, while its magnitude is reduced. The order of magnitude of the speckle can be understood as spreading a beam of order r_0 over a two dimensional spatial window of order r_0^2/l_c. Therefore, it is indeed expected that we observe a speckle of order

$$\Big(\frac{r_0}{r_0^2/l_c}\Big)^2 \sim \Big(\frac{l_c}{r_0}\Big)^2 \sim \varepsilon^{2(\gamma-1/2)}.$$

This section aims at describing the asymptotic behavior of the two-point statistics and intensity of $S^{\varepsilon,ref}$ and the self-averaging properties that are exhibited by these quantities. The expectation of $S^{\varepsilon,ref}$ will be discussed in Section 6.2, where the asymptotic of the speckle itself is characterized as a mean-zero Gaussian random field.

6.1 Correlation and intensity functions.

The above scalings in ε of the speckle profile $S^{\varepsilon,ref}$ can be naturally justified through a careful analysis of its correlation function. This correlation function is defined as the product of $S^{\varepsilon,ref}$ at two nearby points:

$$\mathcal{C}^{\varepsilon,ref}(\bar{s},\bar{\mathbf{y}},\mathbf{y},\widetilde{s}_1,\widetilde{\mathbf{y}}_1,\widetilde{s}_2,\widetilde{\mathbf{y}}_2) := S^{\varepsilon,ref}(\bar{s},\bar{\mathbf{y}},\mathbf{y},\widetilde{s}_1,\widetilde{\mathbf{y}}_1)S^{\varepsilon,ref}(\bar{s},\bar{\mathbf{y}},\mathbf{y},\widetilde{s}_2,\widetilde{\mathbf{y}}_2), \tag{52}$$

with associated intensity given by

$$\mathcal{I}^{\varepsilon,ref}(\bar{s},\bar{\mathbf{y}},\mathbf{y},\widetilde{s},\widetilde{\mathbf{y}}) := \big|S^{\varepsilon,ref}(\bar{s},\bar{\mathbf{y}},\mathbf{y},\widetilde{s},\widetilde{\mathbf{y}})\big|^2 = \mathcal{C}^{\varepsilon,ref}(\bar{s},\bar{\mathbf{y}},\mathbf{y},\widetilde{s},\widetilde{\mathbf{y}},\widetilde{s},\widetilde{\mathbf{y}}).$$

The following result characterizes the asymptotic mean correlation function.

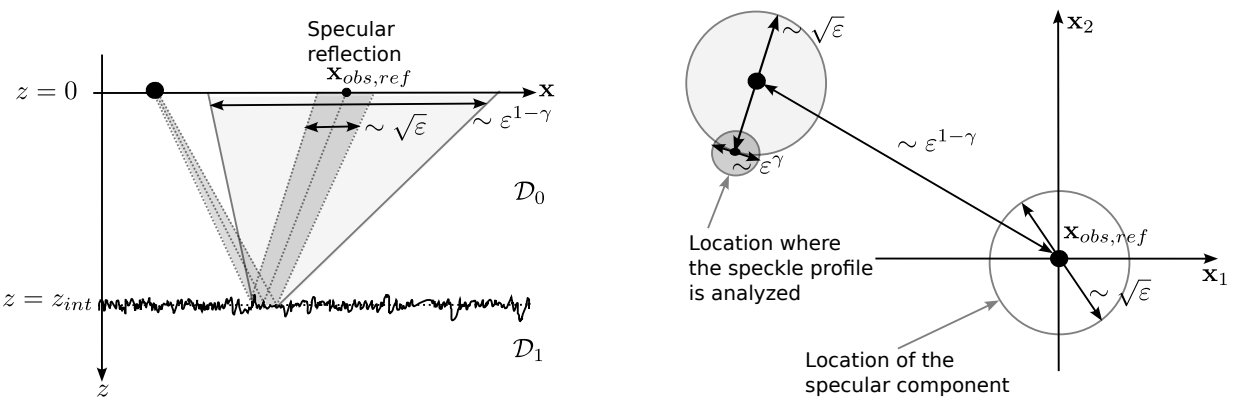

Figure 8: The left picture illustrates the zone where the speckle profile can be observed (in light gray) compared to the specular reflection component (in gray). The right picture illustrates the spatial windows over which the speckle profile is analyzed.

Proposition 6.1 *We have*

$$\lim_{\varepsilon\to 0} \mathbb{E}\big[\mathcal{C}^{\varepsilon,ref}(\bar{s},\bar{\mathbf{y}},\mathbf{y},\widetilde{s}_1,\widetilde{\mathbf{y}}_1,\widetilde{s}_2,\widetilde{\mathbf{y}}_2)\big] = \mathbf{C}^{ref}(\bar{s},\bar{\mathbf{y}},\widetilde{s}_1-\widetilde{s}_2,\widetilde{\mathbf{y}}_1-\widetilde{\mathbf{y}}_2), \tag{53}$$

in $\mathcal{S}'(\mathbb{R}\times\mathbb{R}^2\times\mathbb{R}^2\times\mathbb{R}\times\mathbb{R}^2\times\mathbb{R}\times\mathbb{R}^2)$*, where*

$$\mathbf{C}^{ref}(\bar{s},\bar{\mathbf{y}},\widetilde{s},\widetilde{\mathbf{y}}) := \frac{\mathcal{R}^2}{4(2\pi)^3}\iint e^{-i\omega(\widetilde{s}-\mathbf{p}\cdot\widetilde{\mathbf{y}})}\mathcal{A}(2\lambda_0,\omega,\mathbf{p})|\hat{\Psi}|_2^2(\omega)\delta(\bar{s}-z_{int}c_0\mathbf{p}^T A_0\mathbf{p})\delta(\bar{\mathbf{y}}-2z_{int}c_0A_0\mathbf{p})\omega^4 d\omega d\mathbf{p}, \tag{54}$$

with

$$\mathcal{A}(v,\omega,\mathbf{p}) := \int \mathbb{E}\big[e^{iv(V(\mathbf{y}')-V(0))}\big]e^{-i\omega\mathbf{p}\cdot\mathbf{y}'}d\mathbf{y}', \tag{55}$$

and

$$|\hat{\Psi}|_2^2(\omega) := \frac{1}{(2\pi)^2}\int |\hat{\Psi}(\omega,\mathbf{q})|^2 d\mathbf{q}. \tag{56}$$

The proof of Proposition (6.1) is postponed to Section 8.1. In this result $\mathbf{C}^{ref}(\bar{s},\bar{\mathbf{y}},\widetilde{s}_1-\widetilde{s}_2,\widetilde{\mathbf{y}}_1-\widetilde{\mathbf{y}}_2)$ corresponds to the mean correlation function at two nearby points in $\widetilde{s},\widetilde{\mathbf{y}}$, and showing asymptotic stationarity w.r.t. these variables. This correlation function does not depend on the variable $\mathbf{y}$ (corresponding to variation at the beam width scale), meaning the two point statistics are identical over regions of order the beam width. In a similar manner, the mean intensity carried by the speckle profile is given by

$$\lim_{\varepsilon\to 0}\mathbb{E}[\mathcal{I}^{\varepsilon,ref}(\bar{s},\bar{\mathbf{y}},\mathbf{y},\widetilde{s},\widetilde{\mathbf{y}})] = \mathbf{C}^{ref}(\bar{s},\bar{\mathbf{y}},0,0),$$

which does not depend on the variable $\mathbf{y}$ and the small scale fluctuations in $\widetilde{s}$ and $\widetilde{\mathbf{y}}$ (evolving at respectively the scale of the pulse width and correlation length). The intensity is therefore uniform over these scales.

In (54), the spatial window is larger than the beam width, and the contribution of the source in (54) is integrated over the supported lateral directions (see (56)). The term $\mathcal{A}(\cdot,\omega,\mathbf{p})$ corresponds to the distribution of scattered directions $\mathbf{p}$ produced by the random interface, for components at frequency ω, and are related to variations at the scale of the correlation length through $\mathbf{y}'$. From the Dirac masses in (54), the resulting speckle can be observed for a given direction $\mathbf{p}$ at position

$$\bar{\mathbf{y}} = \mathbf{y}_{\mathbf{p}}^{ref} := 2z_{int}c_0A_0\mathbf{p},$$

and corresponding time

$$\bar{s} = s_{\mathbf{p}}^{ref} := \mathbf{p}\cdot\mathbf{y}_{\mathbf{p}}^{ref}/2 = z_{int}c_0\mathbf{p}^T A_0\mathbf{p} \geq 0.$$

This latter time is nonnegative recalling (21). These two quantities depend on the distance z_{int} from the source term to the interface location. This distance influence therefore the cone size of the reflected speckle and the time widow to observe its evolution.

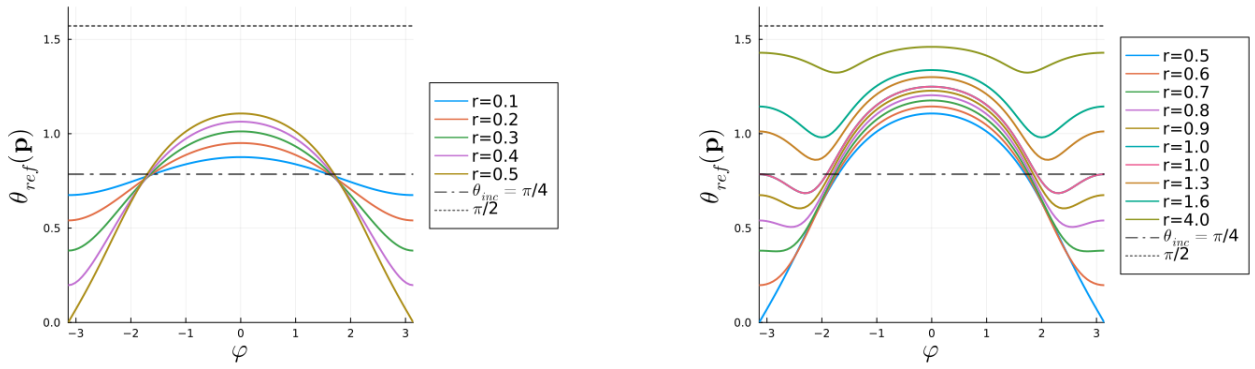

Figure 9: Illustration of the incident angle θ^0_{inc} (dash-dot line) and the reflected angle $\theta_{ref}(\mathbf{p}) \in (0, \pi/2)$ for $\gamma = 1$ and $\mathbf{p} = \beta_1 \mathbf{k}_0 + \beta_2 \mathbf{k}_0^\perp$ with $(\beta_1, \beta_2) = r\,(\cos(\varphi), \sin(\varphi))$.

Generalized Snell's law of refraction After some algebra, one can generalize the standard reflection relation between the incident and reflected angle (29) as follows. For a given frequency ω and nonnull slowness vector $\mathbf{k}_0$, $(\theta_{inc} > 0)$, we have

$$\frac{\tan(\theta_{ref}(\mathbf{p}))}{\tan(\theta_{inc})} = \frac{|\mathbf{x}_{int} + \varepsilon^{1-\gamma}\mathbf{y}^{ref}_{\mathbf{p}}|}{|\mathbf{x}_{int}|} = \sqrt{\Big(1 + \xi_\varepsilon \frac{\mathbf{p}\cdot\mathbf{k}_0}{\cos^2(\theta_{inc})}\Big)^2 + \xi_\varepsilon^2 (\mathbf{p}\cdot\mathbf{k}_0^\perp)^2}, \qquad \xi_\varepsilon = \varepsilon^{1-\gamma}\frac{c_0^2}{\sin^2(\theta_{inc})} \tag{57}$$

for $\mathbf{p}$ distributed according to the scattering operator $\mathcal{A}(2\lambda_0, \omega, \cdot)$, which corresponds to (1). The case $\gamma \in (1/2, 1)$ yields the perturbation formula

$$\theta_{ref}(\mathbf{p}) = \theta_{inc} + \xi_\varepsilon \tan(\theta_{inc})\mathbf{p}\cdot\mathbf{k}_0 + \mathcal{O}(\varepsilon^{2(1-\gamma)}|\mathbf{p}|^2).$$

We refer to Figure 9 for an illustration of $\theta_{ref}(\mathbf{p})$ when $\gamma = 1$, that is in the context of a rough interface $\lambda \sim l_c$. For null slowness vector $\mathbf{k}_0$, $(\theta_{inc} = 0)$, the refraction formula is simply given by $\tan(\theta_{ref}(\mathbf{p})) = \varepsilon^{1-\gamma} c_0 |\mathbf{p}|$, that is

$$\theta_{ref}(\mathbf{p}) = \arctan(\varepsilon^{1-\gamma} c_0 |\mathbf{p}|).$$

The following result describes the statistical stabilization of $\mathcal{C}^{\varepsilon,ref}$ as $\varepsilon \to 0$. In other words, when correlating the speckle profile at two nearby points w.r.t. the variables $\widetilde{s}$ and $\widetilde{\mathbf{y}}$, its limit, in the high-frequency regime $\varepsilon \to 0$, becomes deterministic and corresponds to the mean correlation function given in Proposition 6.2.

Proposition 6.2 *We have*

$$\lim_{\varepsilon\to 0} \mathcal{C}^{\varepsilon,ref}(\bar{s}, \bar{\mathbf{y}}, \mathbf{y}, \widetilde{s}_1, \widetilde{\mathbf{y}}_1, \widetilde{s}_2, \widetilde{\mathbf{y}}_2) = \mathbf{C}^{ref}(\bar{s}, \bar{\mathbf{y}}, \widetilde{s}_1 - \widetilde{s}_2, \widetilde{\mathbf{y}}_1 - \widetilde{\mathbf{y}}_2)$$

in probability in $\mathcal{S}'(\mathbb{R}\times\mathbb{R}^2\times\mathbb{R}^2\times\mathbb{R}\times\mathbb{R}^2\times\mathbb{R}\times\mathbb{R}^2)$, *where the deterministic limit* $\mathbf{C}^{ref}$ *is defined by* (54).

The same result holds for the intensity function, which also converges in probability in $\mathcal{S}'(\mathbb{R}\times\mathbb{R}^2\times\mathbb{R}^2\times\mathbb{R}\times\mathbb{R}^2)$:

$$\lim_{\varepsilon\to 0} \mathcal{I}^{\varepsilon,ref}(\bar{s}, \bar{\mathbf{y}}, \mathbf{y}, \widetilde{s}, \widetilde{\mathbf{y}}) = \mathbf{C}^{ref}(\bar{s}, \bar{\mathbf{y}}, 0, 0).$$

The proof of Position 6.2 is provided in Section 8.2.

6.2 Statistics of the incoherent wave fluctuations

A precise analysis to the statistics of the reflected speckle profile is provided in the Fourier domain at the scale of the pulse width and correlation length through

$$\hat{S}^{\varepsilon,ref}(\bar{s}, \bar{\mathbf{y}}, \mathbf{y}, \omega, \mathbf{p}) := \varepsilon^{-2(\gamma-1/2)} \iint e^{i\omega(\widetilde{s}-\mathbf{p}\cdot\widetilde{\mathbf{y}})} u^{\varepsilon,ref}\big(t^\varepsilon_{obs,ref}(\bar{s}, \bar{\mathbf{y}}, \mathbf{y}, \widetilde{\mathbf{y}}) + \varepsilon\widetilde{s}, \mathbf{x}^\varepsilon_{obs,ref}(\bar{\mathbf{y}}, \mathbf{y}) + \varepsilon^\gamma \widetilde{\mathbf{y}}\big) d\widetilde{s} d\widetilde{\mathbf{y}}.$$

where $\mathbf{x}^{\varepsilon}_{obs,ref}$ and $t^{\varepsilon}_{obs,ref}$ are respectively given by (50) and (51). As described by (54), the position and time where we observe the incoherent wave fluctuations away from the position of the specular component are given in terms of the scattered directions $\mathbf{p}$:

$$\mathbf{y}^{ref}_{\mathbf{p}} = 2z_{int}c_0 A_0\mathbf{p} \qquad \text{and} \qquad s^{ref}_{\mathbf{p}} := z_{int}c_0\mathbf{p}^T A_0\mathbf{p}. \tag{58}$$

Due to the singular nature of the correlation function, involving Dirac masses at $\mathbf{y}^{ref}_{\mathbf{p}}$ and $s^{ref}_{\mathbf{p}}$, we do not directly study $\hat{S}^{\varepsilon,ref}$ but rather a smoothed version

$$\hat{\mathcal{S}}^{\varepsilon,ref}_{\mathbf{y}}(\bar{s},\bar{\mathbf{y}},\omega,\mathbf{p}) := \hat{S}^{\varepsilon,ref}(\bar{s},\bar{\mathbf{y}},\mathbf{y},\omega,\mathbf{p})\frac{1}{\varepsilon^{3(\gamma-1/2)}}\varphi^{1/2}\Big(2\frac{\bar{s}-s^{ref}_{\mathbf{p}}}{\varepsilon^{2(\gamma-1/2)}}, 2\frac{\bar{\mathbf{y}}-\mathbf{y}^{ref}_{\mathbf{p}}}{\varepsilon^{2(\gamma-1/2)}}\Big), \tag{59}$$

where we have added the square root of a symmetric mollifier to smooth its correlation function around $s = s^{ref}_{\mathbf{p}}$ and $\mathbf{y} = \mathbf{y}^{ref}_{\mathbf{p}}$. Here $\mathbf{y}$ is fixed, and $\hat{\mathcal{S}}^{\varepsilon,ref}_{\mathbf{y}}$ is here localized in a small neighborhood of $\mathbf{y}^{ref}_{\mathbf{p}} + \varepsilon^{2(\gamma-1/2)}\mathbf{y}$ of order the correlation length (recalling that $\bar{\mathbf{y}}$ scales at $\varepsilon^{1-\gamma}$). In this section, we focus on the speckle pattern seen as a random field in the scattered direction $\mathbf{p}$, and aim at describing its statistical behavior at the scale of the correlation length.

At the leading order $\hat{\mathcal{S}}^{\varepsilon,ref}_{\mathbf{y}}$ reads

$$\begin{aligned}\hat{\mathcal{S}}^{\varepsilon,ref}_{\mathbf{y}}(\bar{s},\bar{\mathbf{y}},\omega,\mathbf{p}) \simeq \frac{\mathcal{R}}{2(2\pi)^2\varepsilon^{7(\gamma-1/2)+1}}\iint e^{-i\omega\bar{s}/\varepsilon^{2\gamma-1}}e^{i\omega\mathbf{p}\cdot\bar{\mathbf{y}}/\varepsilon^{2\gamma-1}}e^{i\omega\mathbf{p}\cdot\mathbf{y}/\varepsilon^{\gamma-1/2}}e^{i\omega(\mathbf{q}'-\mathbf{p}/\varepsilon^{\gamma-1/2})\cdot(\mathbf{x}'-\mathbf{x}_{int})/\sqrt{\varepsilon}} \\ \times e^{2i\omega\lambda_0 V(\mathbf{x}'/\varepsilon^{\gamma})}\hat{\mathcal{U}}_0(\omega,\mathbf{p}/\varepsilon^{\gamma-1/2},z_{int})\hat{\mathcal{U}}_0(\omega,\mathbf{q}',z_{int})\hat{\Psi}(\omega,\mathbf{q}') \\ \times \omega^2 d\mathbf{x}' d\mathbf{q}'\varphi^{1/2}\Big(2\frac{\bar{s}-s_{\mathbf{p}}}{\varepsilon^{2(\gamma-1/2)}}, 2\frac{\bar{\mathbf{y}}-\mathbf{y}_{\mathbf{p}}}{\varepsilon^{2(\gamma-1/2)}}\Big).\end{aligned} \tag{60}$$

Note that taking its expectation leads to

$$\begin{aligned}\mathbb{E}\big[\hat{\mathcal{S}}^{\varepsilon,ref}_{\mathbf{y}}(\bar{s},\bar{\mathbf{y}},\omega,\mathbf{p})\big] \simeq \frac{\mathcal{R}}{2\varepsilon^{7(\gamma-1/2)}}e^{-i\omega\bar{s}/\varepsilon^{2\gamma-1}}e^{i\omega\mathbf{p}\cdot\bar{\mathbf{y}}/\varepsilon^{2\gamma-1}}e^{i\omega\mathbf{p}\cdot\mathbf{y}/\varepsilon^{\gamma-1/2}}\mathbb{E}\big[e^{2i\omega\lambda_0 V(0)}\big] \\ \times \hat{\mathcal{U}}_0(\omega,\mathbf{p}/\varepsilon^{\gamma-1/2},2z_{int})\hat{\Psi}(\omega,\mathbf{p}/\varepsilon^{\gamma-1/2})\varphi^{1/2}\Big(2\frac{\bar{s}-s_{\mathbf{p}}}{\varepsilon^{2(\gamma-1/2)}}, 2\frac{\bar{\mathbf{y}}-\mathbf{y}_{\mathbf{p}}}{\varepsilon^{2(\gamma-1/2)}}\Big),\end{aligned}$$

so that applying a test function $\phi \in \mathcal{S}(\mathbb{R}\times\mathbb{R}^2\times\mathbb{R}\times\mathbb{R}^2)$ gives

$$\mathbb{E}\big[\big\langle\hat{\mathcal{S}}^{\varepsilon,ref}_{\mathbf{y}},\phi\big\rangle_{\mathcal{S}',\mathcal{S}}\big] \simeq \frac{\varepsilon^{\gamma-1/2}\mathcal{R}}{2}\iiiint e^{-i\omega s_{\mathbf{q}}}e^{-i\omega\widetilde{s}}e^{i\omega\mathbf{q}\cdot\mathbf{y}}\mathbb{E}\big[e^{2i\omega\lambda_0 V(0)}\big]\hat{\Psi}(\omega,\mathbf{q})\varphi^{1/2}(2\widetilde{s},2\widetilde{\mathbf{y}})\overline{\phi(0,0,\omega,0)}\omega^2 d\widetilde{s}d\widetilde{\mathbf{y}}d\omega d\mathbf{q}, \tag{61}$$

after the change of variable $\bar{s} \to s_{\mathbf{p}} + \varepsilon^{2(\gamma-1/2)}\widetilde{s}$, $\bar{\mathbf{y}} \to \mathbf{y}_{\mathbf{p}} + \varepsilon^{2(\gamma-1/2)}\widetilde{\mathbf{y}}$, and $\mathbf{p} \to \varepsilon^{\gamma-1/2}\mathbf{q}$. In other words, we have

$$\lim_{\varepsilon\to 0}\mathbb{E}\big[\hat{\mathcal{S}}^{\varepsilon,ref}_{\mathbf{y}}(\bar{s},\bar{\mathbf{y}},\omega,\mathbf{p})\big] = 0.$$

in $\mathcal{S}'(\mathbb{R}\times\mathbb{R}^2\times\mathbb{R}\times\mathbb{R}^2)$.

Theorem 6.1 *For any fixed $\mathbf{y}\in\mathbb{R}^2$, the family $(\hat{\mathcal{S}}^{\varepsilon,ref}_{\mathbf{y}})_{\varepsilon}$ converges in distribution in $\mathcal{S}'(\mathbb{R}\times\mathbb{R}^2\times\mathbb{R}\times\mathbb{R}^2,\mathbb{C})$ to a complex mean-zero Gaussian random field $\hat{\mathcal{S}}^{ref}$, which does not depend on $\mathbf{y}$, and with covariance functions given by*

$$\begin{aligned}\mathbb{E}[\hat{\mathcal{S}}^{ref}(\phi)\hat{\mathcal{S}}^{ref}(\psi)] = \int\cdots\int\hat{\mathcal{K}}_{ref}(\bar{s}_1,\bar{s}_2,\bar{\mathbf{y}}_1,\bar{\mathbf{y}}_2,\omega_1,-\omega_2,\mathbf{p}_1,\mathbf{p}_2) \\ \times\overline{\phi(\bar{s}_1,\bar{\mathbf{y}}_1,\omega_1,\mathbf{p}_1)\psi(\bar{s}_2,\bar{\mathbf{y}}_2,\omega_2,\mathbf{p}_2)}d\bar{s}_1 d\bar{s}_2 d\bar{\mathbf{y}}_1 d\bar{\mathbf{y}}_2 d\omega_1 d\omega_2 d\mathbf{p}_1 d\mathbf{p}_2,\end{aligned} \tag{62}$$

$$\begin{aligned}\mathbb{E}[\hat{\mathcal{S}}^{ref}(\phi)\overline{\hat{\mathcal{S}}^{ref}(\psi)}] = \int\cdots\int\hat{\mathcal{K}}_{ref}(\bar{s}_1,\bar{s}_2,\bar{\mathbf{y}}_1,\bar{\mathbf{y}}_2,\omega_1,\omega_2,\mathbf{p}_1,\mathbf{p}_2) \\ \times\overline{\phi(\bar{s}_1,\bar{\mathbf{y}}_1,\omega_1,\mathbf{p}_1)}\psi(\bar{s}_2,\bar{\mathbf{y}}_2,\omega_2,\mathbf{p}_2)d\bar{s}_1 d\bar{s}_2 d\bar{\mathbf{y}}_1 d\bar{\mathbf{y}}_2 d\omega_1 d\omega_2 d\mathbf{p}_1 d\mathbf{p}_2,\end{aligned} \tag{63}$$

for $\phi,\psi\in\mathcal{S}(\mathbb{R}\times\mathbb{R}^2\times\mathbb{R}\times\mathbb{R}^2,\mathbb{C})$. The kernel $\hat{\mathcal{K}}$ is given by

$$\begin{aligned}\hat{\mathcal{K}}_{ref}(\bar{s}_1,\bar{s}_2,\bar{\mathbf{y}}_1,\bar{\mathbf{y}}_2,\omega_1,\omega_2,\mathbf{p}_1,\mathbf{p}_2) = \frac{(2\pi)^3\mathcal{R}^2}{4}\mathcal{A}(2\lambda_0,\omega_1,\mathbf{p}_1)|\hat{\Psi}|_2^2(\omega_1)\hat{\varphi}(\omega_1,\mathbf{p}_1) \\ \times\delta(\omega_1-\omega_2)\delta(\mathbf{p}_1-\mathbf{p}_2)\delta(\bar{s}_1-s^{ref}_{\mathbf{p}_1})\delta(\bar{s}_2-s^{ref}_{\mathbf{p}_1})\delta(\bar{\mathbf{y}}_1-\mathbf{y}^{ref}_{\mathbf{p}_1})\delta(\bar{\mathbf{y}}_2-\mathbf{y}^{ref}_{\mathbf{p}_1}).\end{aligned}$$

The proof of Theorem 6.1 is provided in Section 9.

The difference with the correlation function (52), exhibiting a self-averaging property, with the speckle (59) in the Fourier domain is the following. For the correlation function, the speckle profile is correlated around given $\bar{s}$ and $\bar{\mathbf{y}}$. Hence, looking at the second order moment of the correlation function in $\mathcal{S}'$ corresponds to look at the fourth order moment of the speckle, but with two elements around some $\bar{s}_1, \bar{\mathbf{y}}_1$ and two others around some $\bar{s}_2, \bar{\mathbf{y}}_2$. These two observation points being far apart from each other the correlated speckles around each of these points become statistically independent:

$$\mathbb{E}[\mathcal{C}^{\varepsilon,ref}(\bar{s}_1,\bar{\mathbf{y}}_1)\mathcal{C}^{\varepsilon,ref}(\bar{s}_2,\bar{\mathbf{y}}_2)] \simeq \mathbb{E}[\mathcal{C}^{\varepsilon,ref}(\bar{s}_1,\bar{\mathbf{y}}_1)]\mathbb{E}[\mathcal{C}^{\varepsilon,ref}(\bar{s}_2,\bar{\mathbf{y}}_2)].$$

In this section, the speckle itself is studied as a random field in the scattered direction $\mathbf{p}$, with, for each $\mathbf{p}$, the corresponding time $s^{ref}_{\mathbf{p}}$ and position $\mathbf{y}^{ref}_{\mathbf{p}}$ of observation. Theorem 6.1 described the statistical interactions between the diffracted directions $\mathbf{p}$ through a Gaussian random field. Nevertheless, Theorem 6.1 holds for a fixed $\mathbf{y}$. For two differents $\mathbf{y}$, the following result holds as we can prove that

$$\lim_{\varepsilon\to 0}\mathbb{E}\big[\langle\hat{\mathcal{S}}^{\varepsilon,ref}_{\mathbf{y}_1},\phi_1\rangle_{\mathcal{S}',\mathcal{S}}\langle\hat{\mathcal{S}}^{\varepsilon,ref}_{\mathbf{y}_2},\phi_2\rangle_{\mathcal{S}',\mathcal{S}}\big] = 0,$$

for any $\mathbf{y}_1$, $\mathbf{y}_2$ and any test function ϕ_1, ϕ_2 in $\mathcal{S}'(\mathbb{R}\times\mathbb{R}^2\times\mathbb{R}\times\mathbb{R}^2,\mathbb{C})$.

Corollary 6.1 *For $n \geq 1$ and any fixed $\mathbf{y}_1,\ldots,\mathbf{y}_n,\in\mathbb{R}^2$, the family $(\hat{\mathcal{S}}^{\varepsilon,ref}_{\mathbf{y}_1},\ldots,\hat{\mathcal{S}}^{\varepsilon,ref}_{\mathbf{y}_n})_\varepsilon$ converges in distribution in $\mathcal{S}'_n$ (which is n times the Cartesian product of $\mathcal{S}'(\mathbb{R}\times\mathbb{R}^2\times\mathbb{R}\times\mathbb{R}^2,\mathbb{C})$) to a limit $(\hat{\mathcal{S}}^{ref}_1,\ldots,\hat{\mathcal{S}}^{ref}_n)$ made of n independent copies of the Gaussian random field $\hat{\mathcal{S}}^{ref}$ defined in Theorem 7.1.*

The real valued random field

$$\mathcal{S}^{\varepsilon,ref}_{\bar{\mathbf{y}}}(\bar{s},\bar{\mathbf{y}},\widetilde{s},\widetilde{\mathbf{y}}) := \frac{1}{(2\pi)^3}\iint e^{-i\omega(\widetilde{s}-\mathbf{p}\cdot\widetilde{\mathbf{y}})}\hat{\mathcal{S}}^{\varepsilon,ref}_{\mathbf{y}}(\bar{s},\bar{\mathbf{y}},\omega,\mathbf{p})d\omega d\mathbf{p},$$

corresponds to the speckle signal around time $\bar{s} = s^{ref}_{\mathbf{p}}$ and position $\bar{\mathbf{y}} = \mathbf{y}^{ref}_{\mathbf{p}}$, for which we have the following result.

Corollary 6.2 *For $n \geq 1$ and any fixed $\mathbf{y}_1,\ldots,\mathbf{y}_n \in \mathbb{R}^2$, the family $(\mathcal{S}^{\varepsilon,ref}_{\mathbf{y}_1},\ldots,\mathcal{S}^{\varepsilon,ref}_{\mathbf{y}_n})_\varepsilon$ converges in distribution in $\mathcal{S}'_n$ to $(\mathcal{S}^{ref}_1,\ldots,\mathcal{S}^{ref}_n)$ made of n independent copies of a real-valued mean-zero stationary Gaussian random field $\mathcal{S}^{ref}$ with covariance function given by*

$$\mathbb{E}[\mathcal{S}^{ref}(\phi)\mathcal{S}^{ref}(\psi)] = \int\cdots\int \mathcal{K}_{ref}(\bar{s}_1,\bar{s}_2,\bar{\mathbf{y}}_1,\bar{\mathbf{y}}_2,\widetilde{s}_1-\widetilde{s}_2,\widetilde{\mathbf{y}}_1-\widetilde{\mathbf{y}}_2)$$
$$\times\,\phi(\bar{s}_1,\bar{\mathbf{y}}_1,\widetilde{s}_1,\widetilde{\mathbf{y}}_1)\psi(\bar{s}_2,\bar{\mathbf{y}}_2,\widetilde{s}_2,\widetilde{\mathbf{y}}_2)d\bar{s}_1 d\bar{s}_2 d\bar{\mathbf{y}}_1 d\bar{\mathbf{y}}_2 d\widetilde{s}_1 d\widetilde{s}_2 d\widetilde{\mathbf{y}}_1 d\widetilde{\mathbf{y}}_2 \qquad (64)$$

for $\phi,\psi\in\mathcal{S}(\mathbb{R}\times\mathbb{R}^2\times\mathbb{R}\times\mathbb{R}^2)$. The kernel $\mathcal{K}$ is given by

$$\mathcal{K}_{ref}(\bar{s}_1,\bar{s}_2,\bar{\mathbf{y}}_1,\bar{\mathbf{y}}_2,\widetilde{s},\widetilde{\mathbf{y}}) = \frac{\mathcal{R}^2}{4(2\pi)^3}\iint e^{-i\omega(\widetilde{s}-\mathbf{p}\cdot\widetilde{\mathbf{y}})}\mathcal{A}(2\lambda_0,\omega,\mathbf{p})|\hat{\Psi}|_2^2(\omega)\hat{\varphi}(\omega,\mathbf{p})$$
$$\times\,\delta(\bar{s}_1-s^{ref}_{\mathbf{p}})\delta(\bar{s}_2-s^{ref}_{\mathbf{p}})\delta(\bar{\mathbf{y}}_1-\mathbf{y}^{ref}_{\mathbf{p}})\delta(\mathbf{y}_2-\mathbf{y}^{ref}_{\mathbf{p}})\omega^4 d\omega d\mathbf{p}.$$

7 The case $\gamma > 1/2$: incoherent wave fluctuations for the nonspecular transmitted contributions

The transmitted speckle profile is given by

$$S^{\varepsilon,tr}(\bar{s},\bar{\mathbf{y}},\mathbf{y},\widetilde{s},\widetilde{\mathbf{y}}) := \varepsilon^{-2(\gamma-1/2)}u^{\varepsilon,tr}(t^{\varepsilon}_{obs,tr}(\bar{s},\bar{\mathbf{y}},\mathbf{y},\widetilde{\mathbf{y}}) + \varepsilon\widetilde{s},\mathbf{x}^{\varepsilon}_{obs,tr}(\bar{\mathbf{y}},\mathbf{y}) + \varepsilon^{\gamma}\widetilde{\mathbf{y}},z=z_{tr}), \qquad (65)$$

where $u^{\varepsilon,tr}$ is given by (43) at the leading order,

$$\mathbf{x}^{\varepsilon}_{obs,tr}(\mathbf{y},\bar{\mathbf{y}}) := \mathbf{x}_{obs,tr} + \varepsilon^{1-\gamma}\bar{\mathbf{y}} + \sqrt{\varepsilon}\,\mathbf{y},$$

and

$$t^{\varepsilon}_{obs,tr}(\bar{s},\bar{\mathbf{y}},\mathbf{y},\widetilde{\mathbf{y}}) := t_{obs,tr} + \varepsilon^{1-\gamma}\mathbf{k}_0\cdot\bar{\mathbf{y}} + \sqrt{\varepsilon}\,\mathbf{k}_0\cdot\mathbf{y} + \varepsilon^{\gamma}\mathbf{k}_0\cdot\widetilde{\mathbf{y}} + \varepsilon^{2(1-\gamma)}\bar{s}.$$

As for the reflected wavefield, the transmitted wavefield $u^{\varepsilon,tr}$ is therefore observed in a neighborhood, of order the roughness parameter λ/l_c which is larger than the beam width (since $\gamma > 1/2$), around the location $\mathbf{x}_{obs,tr}$

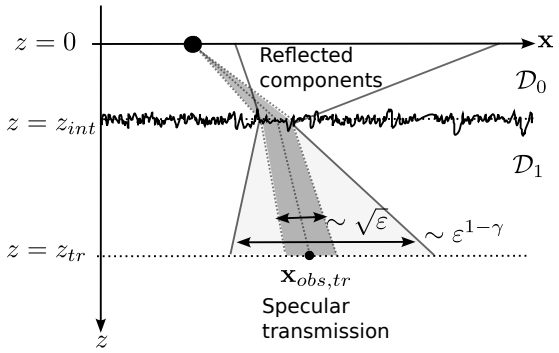

Figure 10: Illustration to the zone where the transmitted speckle profile can be observed (in light gray) compared to the specular reflection component (in gray).

to observe the specular transmitted component. We also look for variations at the beam width scale as well as fluctuations of order the correlation length through respectively $\mathbf{y}$ and $\widetilde{\mathbf{y}}$ (see the right picture of Figure 8 for an illustration). The speckle profile $S^{\varepsilon,tr}$ is observed in a time scale around the travel time $t_{obs,ref}$ with three corrections depending on the observation locations ($\bar{\mathbf{y}}$, $\mathbf{y}$, and $\widetilde{\mathbf{y}}$). The overall time window is larger than the pulse width (given by $\varepsilon^{2(1-\gamma)}\bar{s}$), of order the square of the roughness parameter, and we also look for fluctuations at the scale of the pulse width through the variable $\widetilde{s}$. Finally, the factor $\varepsilon^{2(\gamma-1/2)} \gg 1$ characterizes the amplitude of the speckle component. Recall that as the parameter γ increases (that is the roughness increases) the area where the speckle pattern is observed around $\mathbf{x}_{obs,tr}$ increases, as does the speckle signal duration, however the magnitude of the speckle decreases.

As for the reflected speckle, the first order moment of $S^{\varepsilon,tr}$ goes to zero in the high-frequency limit and we only focus on its two-point statistics and on the intensity.

7.1 Correlation function and intensity.

This correlation function at two nearby points to $S^{\varepsilon,tr}$ is defined as:

$$\mathcal{C}^{\varepsilon,tr}(\bar{s},\bar{\mathbf{y}},\mathbf{y},\widetilde{s}_1,\widetilde{\mathbf{y}}_1,\widetilde{s}_2,\widetilde{\mathbf{y}}_2) := S^{\varepsilon,tr}(\bar{s},\bar{\mathbf{y}},\mathbf{y},\widetilde{s}_1,\widetilde{\mathbf{y}}_1)S^{\varepsilon,tr}(\bar{s},\bar{\mathbf{y}},\mathbf{y},\widetilde{s}_2,\widetilde{\mathbf{y}}_2),$$

and the associated intensity is given by

$$\mathcal{I}^{\varepsilon,tr}(\bar{s},\bar{\mathbf{y}},\mathbf{y},\widetilde{s},\widetilde{\mathbf{y}}) := \left|S^{\varepsilon,tr}(\bar{s},\bar{\mathbf{y}},\mathbf{y},\widetilde{s},\widetilde{\mathbf{y}})\right|^2 = \mathcal{C}^{\varepsilon,tr}(\bar{s},\bar{\mathbf{y}},\mathbf{y},\widetilde{s},\widetilde{\mathbf{y}},\widetilde{s},\widetilde{\mathbf{y}}).$$

The following result characterizes the asymptotic mean correlation function.

Proposition 7.1 *We have*

$$\lim_{\varepsilon\to 0} \mathcal{C}^{\varepsilon,tr}(\bar{s},\bar{\mathbf{y}},\mathbf{y},\widetilde{s}_1,\widetilde{\mathbf{y}}_1,\widetilde{s}_2,\widetilde{\mathbf{y}}_2) = \mathbf{C}^{tr}(\bar{s},\bar{\mathbf{y}},\widetilde{s}_1-\widetilde{s}_2,\widetilde{\mathbf{y}}_1-\widetilde{\mathbf{y}}_2),$$

in probability in $\mathcal{S}'(\mathbb{R}\times\mathbb{R}^2\times\mathbb{R}^2\times\mathbb{R}\times\mathbb{R}^2\times\mathbb{R}\times\mathbb{R}^2)$*, where*

$$\mathbf{C}^{tr}(\bar{s},\bar{\mathbf{y}},\mathbf{y},\widetilde{s},\widetilde{\mathbf{y}}) := \frac{\mathcal{T}^2\lambda_0}{4\lambda_1(2\pi)^3}\iint e^{-i\omega(\widetilde{s}-\mathbf{p}\cdot\widetilde{\mathbf{y}})}\mathcal{A}(\lambda_0-\lambda_1,\omega,\mathbf{p})|\hat{\Psi}|_2^2(\omega)\delta(\bar{s}-s_{\mathbf{p}}^{tr})\delta(\bar{\mathbf{y}}-\mathbf{y}_{\mathbf{p}}^{tr})\omega^4 d\omega d\mathbf{p}. \tag{66}$$

with $\mathcal{A}$ *defined by* (55), $|\hat{\Psi}|_2^2$ *by* (56)*, and*

$$s_{\mathbf{p}}^{tr} = (z_{tr}-z_{int})c_1\mathbf{p}^T A_1\mathbf{p} \geq 0, \qquad \textit{and} \qquad \mathbf{y}_{\mathbf{p}}^{tr} = 2(z_{tr}-z_{int})c_1 A_1\mathbf{p}.$$

The stationarity property is also observed for $\mathbf{C}^{tr}$ w.r.t. its variables $\widetilde{s}$ and $\widetilde{\mathbf{y}}$, and does not depend on the variable $\mathbf{y}$ corresponding to variation at the scale of the beam width. In the same way, the mean intensity carried by the speckle profile is given by

$$\lim_{\varepsilon\to 0} \mathcal{I}^{\varepsilon,tr}(\bar{s},\bar{\mathbf{y}},\mathbf{y},\widetilde{s},\widetilde{\mathbf{y}}) = \mathbf{C}^{tr}(\bar{s},\bar{\mathbf{y}},0,0),$$

in probability, which does not depend on the variable $\mathbf{y}$ and the small scale fluctuations in $\widetilde{s}$ and $\widetilde{\mathbf{y}}$. The intensity is therefore uniform over these scales.

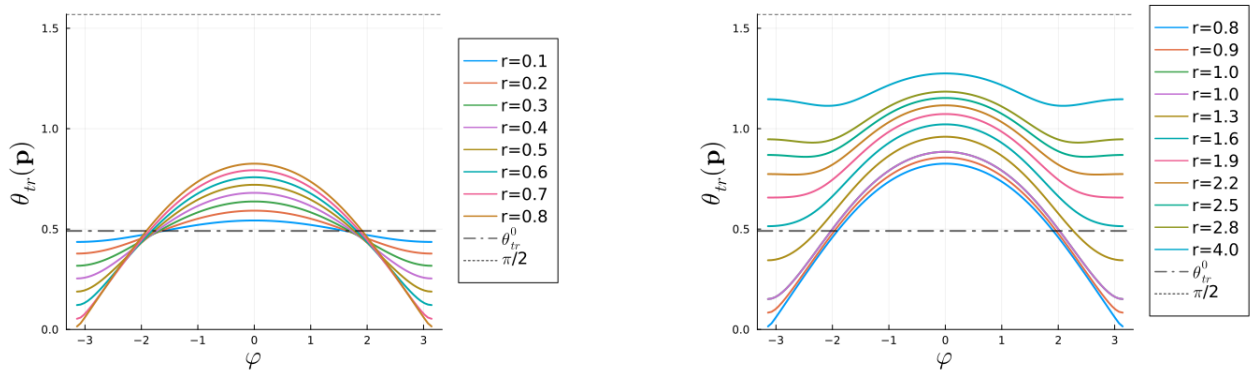

Figure 11: Illustration of the specular transmission angle θ^0_{tr} (dash-dot line) and the transmission angle $\theta_{ref}(\mathbf{p}) \in (0, \pi/2)$ for $\gamma = 1$, $c_0 = 1.5$, $c_1 = 1$, and $\mathbf{p} = \beta_1 \mathbf{k}_0 + \beta_2 \mathbf{k}_0^\perp$ with $(\beta_1, \beta_2) = r(\cos(\varphi), \sin(\varphi))$.

As already mentioned, in (54), the spatial window is now larger than the beam width. For a given direction $\mathbf{p}$, the resulting speckle at position

$$\bar{\mathbf{y}} = \mathbf{y}^{tr}_{\mathbf{p}}$$

is observed at the corresponding time

$$\bar{s} = s^{tr}_{\mathbf{p}} \geq 0,$$

which is nonnegative recalling (21) and that $|\mathbf{k}_0| < 1/c_0 < 1/c_1$. Note that for $\gamma = 1$, corresponding to a correlation length of order the wavelength, the speckle can be observed at distance of order one from $\mathbf{x}_{obs,tr}$.

Generalized Snell's law of transmission In term of reflection angle, for a given frequency ω and nonnull slowness vector $\mathbf{k}_0$ ($\theta_{inc} > 0$), we have, after some algebra, the following relation between the transmission angle and the specular transmission angle θ^0_{tr}

$$\begin{aligned}\frac{\tan(\theta_{tr}(\mathbf{p}))}{\tan(\theta^0_{tr})} &= \frac{|\mathbf{x}_{obs,tr} - \mathbf{x}_{int} + \varepsilon^{1-\gamma}\mathbf{y}^{tr}_{\mathbf{p}}|}{|\mathbf{x}_{obs,tr} - \mathbf{x}_{int}|} \\ &= \sqrt{\Big(1 + \xi_\varepsilon \frac{\mathbf{p}\cdot\mathbf{k}_0}{\cos^2(\theta_{tr})}\Big)^2 + \xi^2(\mathbf{p}\cdot\mathbf{k}_0^\perp)^2}, \qquad \xi_\varepsilon = \varepsilon^{1-\gamma}\frac{c_0^2}{\sin^2(\theta_{inc})},\end{aligned}$$

for $\mathbf{p}$ distributed according to the scattering operator $\mathcal{A}(\lambda_0 - \lambda_1, \omega, \cdot)$. From this relation, the standard Snell's relation of transmission can be generalized as follow

$$\frac{\sin(\theta_{tr}(\mathbf{p}))}{c_1} = \frac{\sin(\theta_{inc})}{c_0}\sqrt{\frac{\Xi}{1 + \sin^2(\theta^0_{tr})\big(\Xi - 1\big)}}, \qquad \Xi = \Big(1 + \xi_\varepsilon \frac{\mathbf{p}\cdot\mathbf{k}_0}{\cos^2(\theta_{tr})}\Big)^2 + \xi^2(\mathbf{p}\cdot\mathbf{k}_0^\perp)^2,$$

corresponding to (2), and leading for $\gamma \in (1/2, 1)$ to the perturbed relation

$$\frac{\sin(\theta_{tr}(\mathbf{p}))}{c_1} = \frac{\sin(\theta_{inc})}{c_0}\Big(1 + \xi_\varepsilon \frac{\mathbf{p}\cdot\mathbf{k}_0}{\cos^2(\theta^0_{tr})} + \mathcal{O}(\varepsilon^{2(1-\gamma)}|\mathbf{p}|^2)\Big).$$

This latter relation provides the approximation

$$\theta_{tr}(\mathbf{p}) = \theta^0_{tr} + \xi_\varepsilon \frac{\tan(\theta_{tr})}{\cos^2(\theta_{tr})}\mathbf{p}\cdot\mathbf{k}_0 + \mathcal{O}(\varepsilon^{2(1-\gamma)}|\mathbf{p}|^2).$$

Finally, for a null slowness vector $\mathbf{k}_0 = 0$ ($\theta_{inc} = 0$), the transmission angle satisfies $\tan(\theta_{tr}(\mathbf{p})) = \varepsilon^{1-\gamma}c_1|\mathbf{p}|$, so that

$$\theta_{tr}(\mathbf{p}) = \arctan(\varepsilon^{1-\gamma}c_1|\mathbf{p}|).$$

7.2 Statistics of the incoherent wave fluctuations

The transmitted speckle in the Fourier domain is given by

$$\hat{S}^{\varepsilon,tr}(\bar{s},\bar{\mathbf{y}},\mathbf{y},\omega,\mathbf{p}) := \varepsilon^{-2(\gamma-1/2)} \iint e^{i\omega(\widetilde{s}-\mathbf{p}\cdot\widetilde{\mathbf{y}})} u^{\varepsilon,tr}\big(t^{\varepsilon}_{obs,tr}(\bar{s},\bar{\mathbf{y}},\mathbf{y},\widetilde{\mathbf{y}}) + \varepsilon\widetilde{s}, \mathbf{x}^{\varepsilon}_{obs,tr}(\bar{\mathbf{y}},\mathbf{y}) + \varepsilon^{\gamma}\widetilde{\mathbf{y}}\big) d\widetilde{s} d\widetilde{\mathbf{y}}.$$

As described by (66), the position and time where we observe the incoherent wave fluctuations away from the position of the specular component are given in terms of the scattered directions $\mathbf{p}$:

$$\mathbf{y}^{tr}_{\mathbf{p}} := 2z_{int}c_0 A_0 \mathbf{p} \qquad \text{and} \qquad s^{tr}_{\mathbf{p}} := \mathbf{p}\cdot\mathbf{y}^{tr}_{\mathbf{p}}/2 = z_{int}c_1 \mathbf{p}^T A_1 \mathbf{p}. \tag{67}$$

As for the reflected speckle profile, due to the singular nature of the correlation function, involving Dirac masses at the observation time and position, we rather study a smoothed version of $\hat{S}^{\varepsilon,tr}$:

$$\hat{\mathcal{S}}^{\varepsilon,tr}_{\mathbf{y}}(\bar{s},\bar{\mathbf{y}},\omega,\mathbf{p}) := \hat{S}^{\varepsilon,tr}(\bar{s},\bar{\mathbf{y}},\mathbf{y},\omega,\mathbf{p}) \frac{1}{\varepsilon^{3(\gamma-1/2)}} \varphi^{1/2}\Big(2\frac{\bar{s}-s^{tr}_{\mathbf{p}}}{\varepsilon^{2(\gamma-1/2)}}, 2\frac{\bar{\mathbf{y}}-\mathbf{y}^{tr}_{\mathbf{p}}}{\varepsilon^{2(\gamma-1/2)}}\Big),$$

for a fixed $\mathbf{y}$, and where a square root of a symmetric mollifier is added to smooth its correlation function around $\bar{s} = s^{tr}_{\mathbf{p}}$ and $\bar{\mathbf{y}} = \mathbf{y}^{tr}_{\mathbf{p}}$.

Theorem 7.1 *For $n \geq 1$ and any fixed $\mathbf{y}_1,\dots,\mathbf{y}_n \in \mathbb{R}^2$, the family $(\hat{\mathcal{S}}^{\varepsilon,tr}_{\mathbf{y}_1},\dots,\hat{\mathcal{S}}^{\varepsilon,tr}_{\mathbf{y}_n})_\varepsilon$ converges in distribution in $\mathcal{S}'_n$ to $(\hat{\mathcal{S}}^{tr}_{\mathbf{y}_1},\dots,\hat{\mathcal{S}}^{tr}_{\mathbf{y}_n})_\varepsilon$ made of n independent copies of a complex mean-zero Gaussian random field $\hat{\mathcal{S}}^{ref}$ with covariance functions similar to* (62) *and* (63) *but with kernel*

$$\begin{aligned}\hat{\mathcal{K}}_{tr}(\bar{s}_1,\bar{s}_2,\bar{\mathbf{y}}_1,\bar{\mathbf{y}}_2,\omega_1,\omega_2,\mathbf{p}_1,\mathbf{p}_2) = \frac{(2\pi)^3\mathcal{T}^2\lambda_0}{4\lambda_1}\mathcal{A}(\lambda_0-\lambda_1,\omega_1,\mathbf{p}_1)|\hat{\Psi}|^2_2(\omega_1)\hat{\varphi}(\omega_1,\mathbf{p}_1)\\ \times \delta(\omega_1-\omega_2)\delta(\mathbf{p}_1-\mathbf{p}_2)\delta(\bar{s}_1-s_{\mathbf{p}_1})\delta(\bar{s}_2-s_{\mathbf{p}_1})\delta(\bar{\mathbf{y}}_1-\mathbf{y}_{\mathbf{p}_1})\delta(\bar{\mathbf{y}}_2-\mathbf{y}_{\mathbf{p}_1}).\end{aligned}$$

The real valued random field

$$\mathcal{S}^{\varepsilon,tr}_{\mathbf{y}}(\bar{s},\bar{\mathbf{y}},\widetilde{s},\widetilde{\mathbf{y}}) := \frac{1}{(2\pi)^3}\iint e^{-i\omega(\widetilde{s}-\mathbf{p}\cdot\widetilde{\mathbf{y}})}\hat{\mathcal{S}}^{\varepsilon,tr}_{\mathbf{y}}(\bar{s},\bar{\mathbf{y}},\omega,\mathbf{p})d\omega d\mathbf{p},$$

corresponds to the speckle signal around time $\bar{s} = s^{tr}_{\mathbf{p}}$ and position $\bar{\mathbf{y}} = \mathbf{y}^{tr}_{\mathbf{p}}$, for which we have the following result. The proof of Theorem 7.1 is omitted as it follows the same lines as the one of Theorem 6.1 provided in Section 9 together with

$$\lim_{\varepsilon\to 0}\mathbb{E}\big[\langle\hat{\mathcal{S}}^{\varepsilon,tr}_{\mathbf{y}_1},\phi_1\rangle_{\mathcal{S}',\mathcal{S}}\langle\hat{\mathcal{S}}^{\varepsilon,tr}_{\mathbf{y}_2},\phi_2\rangle_{\mathcal{S}',\mathcal{S}}\big] = 0,$$

for any $\mathbf{y}_1$, $\mathbf{y}_2$ and any test function ϕ_1, ϕ_2 in $\mathcal{S}'(\mathbb{R}\times\mathbb{R}^2\times\mathbb{R}\times\mathbb{R}^2,\mathbb{C})$, to obtain the convergence of the vector.

Corollary 7.1 *For $n \geq 1$ and any fixed $\mathbf{y}_1,\dots,\mathbf{y}_n \in \mathbb{R}^2$, the family $(\mathcal{S}^{\varepsilon,tr}_{\mathbf{y}_1},\dots,\mathcal{S}^{\varepsilon,tr}_{\mathbf{y}_n})_\varepsilon$ converges in distribution in $\mathcal{S}'_n$ to $(\mathcal{S}^{tr}_1,\dots,\mathcal{S}^{tr}_n)$ made of n independent copies of a real valued mean-zero Gaussian random field $\mathcal{S}^{ref}$ with a covariance function similar to* (64)*, but with kernel*

$$\begin{aligned}\mathcal{K}_{tr}(\bar{s}_1,\bar{s}_2,\bar{\mathbf{y}}_1,\bar{\mathbf{y}}_2,\widetilde{s},\widetilde{\mathbf{y}}) = \frac{\mathcal{T}^2\lambda_0}{4\lambda_1(2\pi)^3}\iint e^{-i\omega(\widetilde{s}-\mathbf{p}\cdot\widetilde{\mathbf{y}})}\mathcal{A}(\lambda_0-\lambda_1,\omega,\mathbf{p})|\hat{\Psi}|^2_2(\omega)\hat{\varphi}(\omega,\mathbf{p})\\ \times\delta(\bar{s}_1-s_{\mathbf{p}})\delta(\bar{s}_2-s_{\mathbf{p}})\delta(\bar{\mathbf{y}}_1-\mathbf{y}_{\mathbf{p}})\delta(\bar{\mathbf{y}}_2-\mathbf{y}_{\mathbf{p}})\omega^4 d\omega d\mathbf{p}.\end{aligned}$$

8 Proof of Propositions 6.1 and 6.2

This section is dedicated to the proof of the convergence of the expected correlation function, as well as its statistical stability. The following proof is presented in a way that naturally justifies the scaling considered in (49,50, 51)

8.1 Proof of Proposition 6.1

Recalling (42), the expected correlation function for the reflected wavefield reads at the leading order

$$\begin{aligned}
C_\varepsilon &:= \mathbb{E}[u^{\varepsilon,ref}(t_1,\mathbf{x}_1,z=0)u^{\varepsilon,ref}(t_2,\mathbf{x}_2,z=0)]\\
&\simeq \frac{\mathcal{R}^2}{4(2\pi)^{10}\varepsilon^2}\int\cdots\int e^{-i\omega_1(t_1-2\lambda_0 z_{int}-\mathbf{x}_1\cdot\mathbf{k}_0)/\varepsilon}e^{i\omega_2(t_2-2\lambda_0-\mathbf{x}_2\cdot\mathbf{k}_0)/\varepsilon}\\
&\qquad\times\mathbb{E}\big[e^{2i\omega_1\lambda_0 V(\mathbf{x}_1'/\varepsilon^\gamma)}e^{-2i\omega_2\lambda_0 V(\mathbf{x}_2'/\varepsilon^\gamma)}\big]\\
&\qquad\times e^{i\omega_1\mathbf{q}_1\cdot(\mathbf{x}_1-\mathbf{x}_1'-\mathbf{x}_{int})/\sqrt{\varepsilon}}e^{i\omega_1\mathbf{q}_1'\cdot(\mathbf{x}_1'-\mathbf{x}_{int})/\sqrt{\varepsilon}}\\
&\qquad\times e^{-i\omega_2\mathbf{q}_2\cdot(\mathbf{x}_2-\mathbf{x}_2'-\mathbf{x}_{int})/\sqrt{\varepsilon}}e^{-i\omega_2\mathbf{q}_2'\cdot(\mathbf{x}_2'-\mathbf{x}_{int})/\sqrt{\varepsilon}}\\
&\qquad\times\hat{\mathcal{U}}_0(\omega_1,\mathbf{q}_1,z_{int})\hat{\mathcal{U}}_0(\omega_1,\mathbf{q}_1',z_{int})\overline{\hat{\mathcal{U}}_0(\omega_2,\mathbf{q}_2,z_{int})\hat{\mathcal{U}}_0(\omega_2,\mathbf{q}_2',z_{int})}\\
&\qquad\times\hat{\Psi}(\omega_1,\mathbf{q}_1')\overline{\hat{\Psi}(\omega_2,\mathbf{q}_2')}\omega_1^4\omega_2^4 d\omega_1 d\omega_2 d\mathbf{x}_1' d\mathbf{x}_2' d\mathbf{q}_1' d\mathbf{q}_2' d\mathbf{q}_1 d\mathbf{q}_2\\
&\simeq \frac{\mathcal{R}^2}{4(2\pi)^{10}\varepsilon^2}\int\cdots\int L_1\times L_2\times L_3\times L_4\times L_5\times L_6\,\omega_1^4\omega_2^4 d\omega_1 d\omega_2 d\mathbf{x}_1' d\mathbf{x}_2' d\mathbf{q}_1' d\mathbf{q}_2' d\mathbf{q}_1 d\mathbf{q}_2,
\end{aligned}$$

where each L_j corresponds to one line in C_ε. In order to obtain a nontrivial limit for L_2, we consider the changes of variables

$$\mathbf{x}_1'\to\mathbf{x}_{int}+\mathbf{r}'+\varepsilon^\gamma\mathbf{y}'/2\qquad\text{and}\qquad\mathbf{x}_2'\to\mathbf{x}_{int}+\mathbf{r}'-\varepsilon^\gamma\mathbf{y}'/2, \tag{68}$$

so that by stationarity

$$L_2=\varepsilon^{2\gamma}\mathbb{E}\Big[e^{2i\omega_1\lambda_0 V((\mathbf{x}_{int}+\mathbf{r}')/\varepsilon^\gamma+\mathbf{y}'/2)}e^{-2i\omega_2\lambda_0 V((\mathbf{x}_{int}+\mathbf{r}')/\varepsilon^\gamma-\mathbf{y}'/2)}\Big]=\varepsilon^{2\gamma}\mathbb{E}\Big[e^{2i\omega_1\lambda_0 V(\mathbf{y}'/2)}e^{-2i\omega_2\lambda_0 V(-\mathbf{y}'/2)}\Big], \tag{69}$$

where the term $\varepsilon^{2\gamma}$ comes from the changes of variables. With this changes of variables, $L_3\times L_4$ now reads

$$\begin{aligned}
L_3\times L_4 &= e^{i\mathbf{r}'\cdot(\omega_1(\mathbf{q}_1'-\mathbf{q}_1)-\omega_2(\mathbf{q}_2'-\mathbf{q}_2))/\sqrt{\varepsilon}}\\
&\qquad\times e^{i\varepsilon^{\gamma-1/2}\mathbf{y}'\cdot(\omega_1(\mathbf{q}_1'-\mathbf{q}_1)+\omega_2(\mathbf{q}_2'-\mathbf{q}_2))/2}\\
&\qquad\times e^{i\omega_1\mathbf{q}_1\cdot(\mathbf{x}_1-\mathbf{x}_{int})/\sqrt{\varepsilon}}e^{-i\omega_1\mathbf{q}_1'\cdot\mathbf{x}_{int}/\sqrt{\varepsilon}}e^{-i\omega_2\mathbf{q}_2\cdot(\mathbf{x}_2-\mathbf{x}_{int})/\sqrt{\varepsilon}}e^{i\omega_2\mathbf{q}_2'\cdot\mathbf{x}_{int}/\sqrt{\varepsilon}}.
\end{aligned}$$

The term $e^{i\mathbf{r}'\cdot(\omega_1(\mathbf{q}_1'-\mathbf{q}_1)-\omega_2(\mathbf{q}_2'-\mathbf{q}_2))/\sqrt{\varepsilon}}$, being the only one involving the variable $\mathbf{r}'$ in C_ε, provides a Dirac mass once integrated in $\mathbf{r}'$:

$$(2\pi)^2\varepsilon\delta(\omega_1(\mathbf{q}_1'-\mathbf{q}_1)-\omega_2(\mathbf{q}_2'-\mathbf{q}_2)).$$

To keep the $\mathbf{y}'$-variable that integrates L_2, we make the changes of variables

$$\mathbf{q}_j\to\mathbf{q}_j'-\mathbf{p}_j/\varepsilon^{\gamma-1/2}\qquad j=1,2, \tag{70}$$

yielding

$$\begin{aligned}
\int L_3\times L_4\,d\mathbf{r}' &= (2\pi)^2\varepsilon^{-2\gamma+2}\delta(\omega_1\mathbf{p}_1-\omega_2\mathbf{p}_2)\,e^{i\mathbf{y}'\cdot(\omega_1\mathbf{p}_1+\omega_2\mathbf{p}_2)/2}e^{-i(\omega_1\mathbf{p}_1\cdot\mathbf{x}_1-\omega_2\mathbf{p}_2\cdot\mathbf{x}_2)/\varepsilon^\gamma}\\
&\qquad\times e^{i\omega_1\mathbf{q}_1'\cdot(\mathbf{x}_1-\mathbf{x}_{obs,ref})/\sqrt{\varepsilon}}e^{-i\omega_2\mathbf{q}_2'\cdot(\mathbf{x}_2-\mathbf{x}_{obs,ref})/\sqrt{\varepsilon}},
\end{aligned}$$

where we have used the presence of the Dirac mass to write

$$e^{-i\omega_1\mathbf{p}_1\cdot(\mathbf{x}_1-\mathbf{x}_{int})/\varepsilon^\gamma}e^{i\omega_2\mathbf{p}_2\cdot(\mathbf{x}_2-\mathbf{x}_{int})/\varepsilon^\gamma}=e^{-i\omega_1\mathbf{p}_1\cdot\mathbf{x}_1/\varepsilon^\gamma}e^{i\omega_2\mathbf{p}_2\cdot\mathbf{x}_2/\varepsilon^\gamma}.$$

Hence, making the changes of variables $\omega_j\mathbf{p}_j\to\mathbf{p}_j$, turning $\omega_1^4\omega_2^4$ in C_ε into $\omega_1^2\omega_2^2$, gives

$$\begin{aligned}
\int L_3\times L_4\,d\mathbf{r}' &= (2\pi)^2\varepsilon^{-2\gamma+2}\delta(\mathbf{p}_1-\mathbf{p}_2)\,e^{i\mathbf{y}'\cdot\mathbf{p}_1}e^{-i\mathbf{p}_1\cdot(\mathbf{x}_1-\mathbf{x}_2)/\varepsilon^\gamma}\\
&\qquad\times e^{i\omega_1\mathbf{q}_1'\cdot(\mathbf{x}_1-\mathbf{x}_{obs,ref})/\sqrt{\varepsilon}}e^{-i\omega_2\mathbf{q}_2'\cdot(\mathbf{x}_2-\mathbf{x}_{obs,ref})/\sqrt{\varepsilon}}.
\end{aligned}$$

The rapid phase $e^{-i\mathbf{p}_1\cdot(\mathbf{x}_1-\mathbf{x}_2)/\varepsilon^\gamma}$ yields the choice

$$\mathbf{x}_j=\mathbf{x}+\varepsilon^\gamma\widetilde{\mathbf{y}}_j\qquad\text{and then}\qquad t_j=t+\varepsilon^\gamma\mathbf{k}_0\cdot\widetilde{\mathbf{y}}_j+\varepsilon\widetilde{s}_j\qquad j=1,2, \tag{71}$$

to compensate in L_1. Here, t and $\mathbf{x}$ will be specified later on. With this choice,

$$\int L_3 \times L_4 \, d\mathbf{r}' = (2\pi)^2 \varepsilon^{-2\gamma+2} \delta(\mathbf{p}_1 - \mathbf{p}_2)\, e^{i\mathbf{p}_1\cdot\mathbf{y}'} e^{-i\mathbf{p}_1\cdot(\widetilde{\mathbf{y}}_1 - \widetilde{\mathbf{y}}_2)} \\ \times e^{i(\mathbf{x}-\mathbf{x}_{obs,ref})\cdot(\omega_1\mathbf{q}_1' - \omega_2\mathbf{q}_2')/\sqrt{\varepsilon}} e^{i\varepsilon^{\gamma-1/2}(\omega_1\mathbf{q}_1'\cdot\widetilde{\mathbf{y}}_1 - \omega_2\mathbf{q}_2'\cdot\widetilde{\mathbf{y}}_2)},$$

and L_1 becomes

$$L_1 = e^{-i(\omega_1-\omega_2)(t-2\lambda_0 z_{int} - \mathbf{x}\cdot\mathbf{k}_0)/\varepsilon} e^{-i(\omega_1\widetilde{s}_1 - \omega_2\widetilde{s}_2)}.$$

Regarding L_5, after all the changes of variables, we have

$$\begin{aligned} L_5 &= \hat{\mathcal{U}}_0\Big(\omega_1, \mathbf{q}_1' - \frac{\mathbf{p}_1}{\omega_1\varepsilon^{\gamma-1/2}}, z_{int}\Big)\hat{\mathcal{U}}_0(\omega_1, \mathbf{q}_1', z_{int}) \\ &\quad \times \overline{\hat{\mathcal{U}}_0\Big(\omega_2, \mathbf{q}_2' - \frac{\mathbf{p}_1}{\omega_2\varepsilon^{\gamma-1/2}}, z_{int}\Big)\hat{\mathcal{U}}_0(\omega_2, \mathbf{q}_2', z_{int})} \\ &= e^{-iz_{int}c_0\mathbf{p}_1^T A_0\mathbf{p}_1(1/\omega_1 - 1/\omega_2)/\varepsilon^{2\gamma-1}} e^{2iz_{int}c_0(\mathbf{q}_1'/\omega_1 - \mathbf{q}_2'/\omega_2)^T A_0\mathbf{p}_1/\varepsilon^{\gamma-1/2}}\, \hat{\mathcal{U}}_0(\omega_1, \mathbf{q}_1', 2z_{int})\overline{\hat{\mathcal{U}}_0(\omega_2, \mathbf{q}_2', 2z_{int})}. \end{aligned}$$

The two rapid phases in the last line suggests the changes of variables

$$\omega_1 = \omega + \varepsilon^{2\gamma-1}h/2, \qquad \omega_2 = \omega - \varepsilon^{2\gamma-1}h/2, \tag{72}$$

and

$$\mathbf{q}_1' = \mathbf{q} + \varepsilon^{\gamma-1/2}\mathbf{r}/2, \qquad \mathbf{q}_2' = \mathbf{q} - \varepsilon^{\gamma-1/2}\mathbf{r}/2, \tag{73}$$

so that at the leading order in ε:

$$\begin{aligned} L_5 \times L_6 &\simeq \varepsilon^{4\gamma-2} e^{ihz_{int}c_0\mathbf{p}_1^T A_0\mathbf{p}_1/\omega^2} e^{2iz_{int}c_0\mathbf{r}^T A_0\mathbf{p}_1/\omega} |\hat{\Psi}(\omega, \mathbf{q})|^2\omega^4, \\ L_2 &\simeq \varepsilon^{2\gamma}\mathbb{E}\big[e^{2i\omega\lambda_0(V(\mathbf{y}')-V(0))}\big], \\ \int L_3 \times L_4 \, d\mathbf{r}' &\simeq (2\pi)^2\varepsilon^{-2\gamma+2}\delta(\mathbf{p}_1-\mathbf{p}_2)\, e^{i\mathbf{p}_1\cdot\mathbf{y}'} e^{-i\mathbf{p}_1\cdot(\widetilde{\mathbf{y}}_1-\widetilde{\mathbf{y}}_2)} e^{i\omega(\mathbf{x}-\mathbf{x}_{obs,ref})\cdot\mathbf{r}/\varepsilon^{1-\gamma}} e^{ih\varepsilon^{2\gamma-3/2}(\mathbf{x}-\mathbf{x}_{obs,ref})\cdot\mathbf{q}}, \\ L_1 &\simeq e^{-ih(t-2\lambda_0 z_{int}-\mathbf{x}\cdot\mathbf{k}_0)/\varepsilon^{2(1-\gamma)}} e^{-i\omega(\widetilde{s}_1-\widetilde{s}_2)}, \end{aligned}$$

using the stationarity of V in (69) for L_2. The two latter relations naturally lead to the choice

$$\mathbf{x} = \mathbf{x}_{obs,ref} + \varepsilon^{1-\gamma}\bar{\mathbf{y}} + \sqrt{\varepsilon}\,\mathbf{y} \qquad \text{and} \qquad t = t_{obs,ref} + \varepsilon^{1-\gamma}\mathbf{k}_0\cdot\bar{\mathbf{y}} + \sqrt{\varepsilon}\,\mathbf{k}_0\cdot\mathbf{y} + \varepsilon^{2(1-\gamma)}\bar{s}, \tag{74}$$

so that gathering all this term yields

$$C_\varepsilon \simeq \frac{\varepsilon^{4(\gamma-1/2)}\mathcal{R}^2}{4(2\pi)^8}\int\cdots\int e^{-i\omega(\widetilde{s}_1-\widetilde{s}_2-\mathbf{p}\cdot(\widetilde{\mathbf{y}}_1-\widetilde{\mathbf{y}}_2))} e^{i\omega\mathbf{r}\cdot\bar{\mathbf{y}}} e^{-ih\bar{s}} e^{-i\omega\mathbf{p}\cdot\mathbf{y}'}\mathbb{E}\big[e^{2i\omega\lambda_0(V(\mathbf{y}')-V(0))}\big] \\ \times e^{-2i\omega z_{int}c_0\mathbf{r}^T A_0\mathbf{p}} e^{ihz_{int}c_0\mathbf{p}^T A_0\mathbf{p}} |\hat{\Psi}(\omega,\mathbf{q})|^2\,\omega^6 dh d\omega d\mathbf{q} d\mathbf{y}' d\mathbf{r} d\mathbf{p},$$

after the change of variable $\mathbf{p} \to -\omega\mathbf{p}$. As a result, the limit does not depend on the $\mathbf{y}$-variable, and for any test function φ, ψ, ϕ, we obtain

$$\lim_{\varepsilon\to 0}\iint \mathbb{E}\big[\big\langle S^{\varepsilon,ref}(\bar{s},\bar{\mathbf{y}},\mathbf{y}),\varphi\big\rangle_{\mathcal{S}',\mathcal{S}}\big\langle S^{\varepsilon,ref}(\bar{s},\bar{\mathbf{y}},\mathbf{y}),\psi\big\rangle_{\mathcal{S}',\mathcal{S}}\big]\phi(\bar{s},\bar{\mathbf{y}},\mathbf{y})d\bar{s}d\bar{\mathbf{y}}d\mathbf{y} \\ = \int\cdots\int \mathbf{C}^{ref}(\bar{s},\bar{\mathbf{y}},\widetilde{s}_1-\widetilde{s}_2,\widetilde{\mathbf{y}}_1-\widetilde{\mathbf{y}}_2)\varphi(\widetilde{s}_1,\widetilde{\mathbf{y}}_1)\psi(\widetilde{s}_2,\widetilde{\mathbf{y}}_2)\phi(\bar{s},\bar{\mathbf{y}},\mathbf{y})d\bar{s}d\bar{\mathbf{y}}d\mathbf{y}d\widetilde{s}_1 d\widetilde{s}_2 d\widetilde{\mathbf{y}}_1 d\widetilde{\mathbf{y}}_2,$$

where $\mathbf{C}^{ref}$ is defined by (54). This concludes the proof of Proposition 6.1.

8.2 Proof of Proposition 6.2

This section consists in proving

$$\lim_{\varepsilon\to 0}\mathbb{E}\big[\mathcal{C}^{\varepsilon,ref}(\phi,\varphi,\psi)^2\big] = \mathcal{C}^{ref}(\phi,\varphi,\psi)^2,$$

with $\mathcal{C}^{ref}(\bar{s},\bar{\mathbf{y}},\mathbf{y},\widetilde{s}_1,\widetilde{\mathbf{y}}_1,\widetilde{s}_2,\widetilde{\mathbf{y}}_2) = \mathbf{C}^{ref}(\bar{s},\bar{\mathbf{y}},\widetilde{s}_1-\widetilde{s}_2,\widetilde{\mathbf{y}}_1-\widetilde{\mathbf{y}}_2)$, yielding for any $\eta > 0$

$$\lim_{\varepsilon\to 0}\mathbb{P}\big(\big|\mathcal{C}^{\varepsilon,ref}(\phi,\varphi,\psi) - \mathcal{C}^{ref}(\phi,\varphi,\psi)\big| > \eta\big) = 0,$$

that is the convergence in probability, thanks to the Chebyshev inequality. The proof of the convergence of the second order moment follows closely the one of Proposition 6.1, so that only the key arguments are discussed.

At the leading order in ε, the speckle profile reads

$$S^{\varepsilon,ref}(\bar{s},\bar{\mathbf{y}},\mathbf{y},\widetilde{s},\widetilde{\mathbf{y}}) \simeq \frac{\mathcal{R}}{2(2\pi)^5\varepsilon^{2\gamma}} \iiiint e^{-i\omega\bar{s}/\varepsilon^{2\gamma-1}} e^{-i\omega\widetilde{s}} e^{i\omega\mathbf{q}\cdot\bar{\mathbf{y}}/\varepsilon^{\gamma-1/2}} e^{i\omega\mathbf{q}\cdot\mathbf{y}} e^{i\varepsilon^{\gamma-1/2}\omega\mathbf{q}\cdot\widetilde{\mathbf{y}}} \times e^{i\omega(\mathbf{q}'-\mathbf{q})\cdot(\mathbf{x}'-\mathbf{x}_{int})/\sqrt{\varepsilon}} e^{2i\omega\lambda_0 V(\mathbf{x}'/\varepsilon^\gamma)} \times \hat{\mathcal{U}}_0(\omega,\mathbf{q},z_{int})\hat{\mathcal{U}}_0(\omega,\mathbf{q}',z_{int})\hat{\Psi}(\omega,\mathbf{q}')\omega^4 d\omega d\mathbf{x}' d\mathbf{q}' d\mathbf{q}, \tag{75}$$

so that

$$\begin{aligned}\mathcal{C}^{\varepsilon,ref}(\phi,\varphi,\psi) :=& \frac{\mathcal{R}^2}{4(2\pi)^{10}\varepsilon^{4\gamma}} \int\cdots\int e^{-i(\omega_1-\omega_2)\bar{s}/\varepsilon^{2\gamma-1}} e^{-i(\omega_1\widetilde{s}_1-\omega_2\widetilde{s}_2)} \\ &\times e^{i(\omega_1\mathbf{q}_1-\omega_2\mathbf{q}_2)\cdot\bar{\mathbf{y}}/\varepsilon^{\gamma-1/2}} e^{i(\omega_1\mathbf{q}_1-\omega_2\mathbf{q}_2)\cdot\mathbf{y}} e^{i\varepsilon^{\gamma-1/2}(\omega_1\mathbf{q}_1\cdot\widetilde{\mathbf{y}}_1-\omega_2\mathbf{q}_2\cdot\widetilde{\mathbf{y}}_2)} \\ &\times e^{i\omega_1(\mathbf{q}_1'-\mathbf{q}_1)\cdot(\mathbf{x}_1'-\mathbf{x}_{int})/\sqrt{\varepsilon}} e^{-i\omega_2(\mathbf{q}_2'-\mathbf{q}_2)\cdot(\mathbf{x}_2'-\mathbf{x}_{int})/\sqrt{\varepsilon}} \\ &\times e^{2i\lambda_0(\omega_1 V(\mathbf{x}_1'/\varepsilon^\gamma)-\omega_2 V(\mathbf{x}_2'/\varepsilon^\gamma))} \\ &\times \hat{\mathcal{U}}_0(\omega_1,\mathbf{q}_1,z_{int})\hat{\mathcal{U}}_0(\omega_1,\mathbf{q}_1',z_{int})\overline{\hat{\mathcal{U}}_0(\omega_2,\mathbf{q}_2,z_{int})\hat{\mathcal{U}}_0(\omega_2,\mathbf{q}_2',z_{int})} \\ &\times \hat{\Psi}(\omega_1,\mathbf{q}_1')\overline{\hat{\Psi}(\omega_2,\mathbf{q}_2')}\phi(\bar{s},\bar{\mathbf{y}},\mathbf{y})\varphi(\widetilde{s}_1,\widetilde{\mathbf{y}}_1)\psi(\widetilde{s}_2,\widetilde{\mathbf{y}}_2) \\ &\times \omega_1^4\omega_2^4 d\omega_1 d\omega_2 d\bar{s} d\widetilde{s}_1 d\widetilde{s}_2 d\mathbf{x}_1' d\mathbf{q}_1' d\mathbf{q}_1 d\mathbf{x}_2' d\mathbf{q}_2' d\mathbf{q}_2 d\bar{\mathbf{y}} d\mathbf{y} d\widetilde{\mathbf{y}}_1 d\widetilde{\mathbf{y}}_2.\end{aligned}$$

Taking the expectation of $\mathcal{C}^{\varepsilon,ref}(\phi,\varphi,\psi)^2$ yields the term

$$E_\varepsilon := \mathbb{E}\Big[e^{2i\lambda_0\sum_{j=1}^2 \omega_{1,j}V(\mathbf{x}_{1,j}'/\varepsilon^\gamma)-\omega_{2,j}V(\mathbf{x}_{2,j}'/\varepsilon^\gamma)}\Big].$$

Making the changes of variables

$$\mathbf{x}_{1,j}' \to \mathbf{x}_{int}+\mathbf{r}_j'+\varepsilon^\gamma\mathbf{y}_j'/2 \qquad \text{and} \qquad \mathbf{x}_{2,j}' \to \mathbf{x}_{int}+\mathbf{r}_j'-\varepsilon^\gamma\mathbf{y}_j'/2, \qquad j=1,2,$$

the term E_ε can be recast as

$$\begin{aligned}E_\varepsilon &= \mathbb{E}\Big[e^{2i\lambda_0\sum_{j=1}^2 \omega_{1,j}V((\mathbf{x}_{int}+\mathbf{r}_j')/\varepsilon^\gamma+\mathbf{y}_j'/2)-\omega_{2,j}V((\mathbf{x}_{int}+\mathbf{r}_j')/\varepsilon^\gamma-\mathbf{y}_j'/2)}\Big] \\ &= \mathbb{E}\Big[e^{2i\lambda_0(\omega_{1,1}V(\mathbf{r}_1'/\varepsilon^\gamma+\mathbf{y}_1'/2)-\omega_{2,1}V(\mathbf{r}_1'/\varepsilon^\gamma-\mathbf{y}_1'/2))}e^{2i\lambda_0(\omega_{1,2}V(\mathbf{r}_2'/\varepsilon^\gamma+\mathbf{y}_2'/2)-\omega_{2,2}V(\mathbf{r}_2'/\varepsilon^\gamma-\mathbf{y}_2'/2))}\Big] \\ &\underset{\varepsilon\to0}{\simeq} \mathbb{E}\Big[e^{2i\lambda_0(\omega_{1,1}V(\mathbf{r}_1'/\varepsilon^\gamma+\mathbf{y}_1'/2)-\omega_{2,1}V(\mathbf{r}_1'/\varepsilon^\gamma-\mathbf{y}_1'/2))}\Big]\mathbb{E}\Big[e^{2i\lambda_0(\omega_{1,2}V(\mathbf{r}_2'/\varepsilon^\gamma+\mathbf{y}_2'/2)-\omega_{2,2}V(\mathbf{r}_2'/\varepsilon^\gamma-\mathbf{y}_2'/2))}\Big]\end{aligned}$$

using the stationarity of V as well as Lemma 1.1. With the latter relation, using the same changes of variable as in the proof of Proposition 6.1, for each j, yields

$$\lim_{\varepsilon\to0}\mathbb{E}\big[\mathcal{C}^{\varepsilon,ref}(\phi,\varphi,\psi)^2\big] = \mathcal{C}^{ref}(\phi,\varphi,\psi)^2,$$

which concludes the proof of Proposition 6.2.

9 Proof of Theorem 6.1

The proof we propose follows the ideas of [12, Sect. 9.3.4]. Applying a test function $\phi\in\mathcal{S}(\mathbb{R}\times\mathbb{R}^2\times\mathbb{R}\times\mathbb{R}^2,\mathbb{C})$ to (60) gives

$$\begin{aligned}J^\varepsilon(\phi) &:= \big\langle\hat{\mathcal{S}}_{\mathbf{y}}^{\varepsilon,ref},\phi\big\rangle_{\mathcal{S}',\mathcal{S}} \\ &\simeq \frac{\mathcal{R}}{2(2\pi)^2\varepsilon^{7(\gamma-1/2)+1}} \int\cdots\int e^{-i\omega\bar{s}/\varepsilon^{2\gamma-1}} e^{i\omega\mathbf{p}\cdot\bar{\mathbf{y}}/\varepsilon^{2\gamma-1}} e^{i\omega\mathbf{p}\cdot\mathbf{y}/\varepsilon^{\gamma-1/2}} e^{i\omega(\mathbf{q}'-\mathbf{p}/\varepsilon^{\gamma-1/2})\cdot(\mathbf{x}'-\mathbf{x}_{int})/\sqrt{\varepsilon}} e^{2i\omega\lambda_0 V(\mathbf{x}'/\varepsilon^\gamma)} \\ &\qquad\times \hat{\mathcal{U}}_0(\omega,\mathbf{p}/\varepsilon^{\gamma-1/2},z_{int})\hat{\mathcal{U}}_0(\omega,\mathbf{q}',z_{int})\hat{\Psi}(\omega,\mathbf{q}')\varphi^{1/2}\Big(2\frac{\bar{s}-s_{\mathbf{p}}^{ref}}{\varepsilon^{2(\gamma-1/2)}},2\frac{\bar{\mathbf{y}}-\mathbf{y}_p^{ref}}{\varepsilon^{2(\gamma-1/2)}}\Big)\overline{\phi(\bar{s},\bar{\mathbf{y}},\omega,\mathbf{p})} \\ &\qquad\times \omega^2 d\omega d\bar{s} d\mathbf{x}' d\mathbf{q}' d\bar{\mathbf{y}} d\mathbf{p}.\end{aligned}$$

Using the stationarity of V, without loss of generality, one can assume for simplicity

$$\mathbf{x}_{int} = 0.$$

The following proof is based on evaluating the limit of moments of $J^\varepsilon(\phi)$. This approach allows to characterize the limiting distribution with a bounded second order moment providing the tightness. The key point, when evaluating the moment is to pair two different $\mathbf{x}'$'s to cancel the rapid phase in $\mathbf{x}'$, and use the mixing property of Lemma 1.1. In what follows, the $\mathbf{x}'$'s are paired after ordering their associated ω's. To this end, we denote

$$J^\varepsilon_\pm := \int_0^\infty \mathcal{J}^\varepsilon(\pm\omega)d\omega,$$

with

$$\begin{aligned}\mathcal{J}^\varepsilon(\omega) :=& \frac{\mathcal{R}}{2(2\pi)^2\varepsilon^{7(\gamma-1/2)+1}}\int\cdots\int e^{-i\omega\bar{s}/\varepsilon^{2\gamma-1}}e^{i\omega\mathbf{p}\cdot\bar{\mathbf{y}}/\varepsilon^{2\gamma-1}}e^{i\omega\mathbf{p}\cdot\mathbf{y}/\varepsilon^{\gamma-1/2}}e^{i\omega(\mathbf{q}'-\mathbf{p}/\varepsilon^{\gamma-1/2})\cdot\mathbf{x}'/\sqrt{\varepsilon}}e^{2i\omega\lambda_0 V(\mathbf{x}'/\varepsilon^\gamma)}\\ &\times\hat{\mathcal{U}}_0(\omega,\mathbf{p}/\varepsilon^{\gamma-1/2},z_{int})\hat{\mathcal{U}}_0(\omega,\mathbf{q}',z_{int})\hat{\Psi}(\omega,\mathbf{q}')\varphi^{1/2}\Big(2\frac{\bar{s}-s^{ref}_{\mathbf{p}}}{\varepsilon^{2(\gamma-1/2)}},2\frac{\bar{\mathbf{y}}-\mathbf{y}^{ref}_p}{\varepsilon^{2(\gamma-1/2)}}\Big)\\ &\times\overline{\phi(\bar{s},\bar{\mathbf{y}},\omega,\mathbf{p})}\omega^2 d\bar{s}d\mathbf{x}'d\mathbf{q}'d\mathbf{p}d\bar{\mathbf{y}}. \end{aligned}\tag{76}$$

Even moments. Considering the even moments in a first time, and decomposing the integral w.r.t. ω in $J^\varepsilon(\phi)$ over $(0,\infty)$ and $(-\infty,0)$ yields

$$\mathbb{E}\big[J^\varepsilon(\phi)^{2n}\big] = \sum_{l=0}^{2n}\binom{2n}{l}M_\varepsilon(l,2n-l),$$

where

$$M_\varepsilon(l,2n-l) := \mathbb{E}\big[(J^\varepsilon_+)^l(J^\varepsilon_-)^{2n-l}\big],\tag{77}$$

after making the change of variable $\omega\to-\omega$ for the part corresponding to the integral over $(-\infty,0)$ in ω.

The case $l=n$. The moment $M_\varepsilon(n,n)$, representing the only nontrivial contribution at the limit $\varepsilon\to0$, can be expressed as

$$\begin{aligned}M_\varepsilon(n,n) &= \int_0^\infty\cdots\int_0^\infty\mathbb{E}\Big[\prod_{j=1}^n\mathcal{J}^\varepsilon(\omega_{1,j})\mathcal{J}^\varepsilon(-\omega_{2,j})\Big]d\omega_{1,j}d\omega_{2,j}\\ &= n!^2\int_{\{0<\omega_{1,1}<\cdots<\omega_{1,n}\}}\int_{\{0<\omega_{2,1}<\cdots<\omega_{2,n}\}}\mathbb{E}\Big[\prod_{j=1}^n\mathcal{J}^\varepsilon(\omega_{1,j})\mathcal{J}^\varepsilon(-\omega_{2,j})\Big]d\omega_{1,j}d\omega_{2,j},\end{aligned}$$

where the second line is obtained by symmetry w.r.t. the ω-variables. The ω's are then paired through the ordering by making the change of variables

$$\omega_{1,j}\to\omega_j+\varepsilon^{2\gamma-1}h_j/2\qquad\text{and}\qquad\omega_{2,j}\to\omega_j-\varepsilon^{2\gamma-1}h_j/2,$$

which yields

$$\begin{aligned}M_\varepsilon(n,n) &= \varepsilon^{n(2\gamma-1)}n!^2\int_{\{0<\omega_1<\cdots<\omega_n\}}\int_{H^\varepsilon_n}\mathbb{E}\Big[\prod_{j=1}^n\mathcal{J}^\varepsilon(\omega_j+\varepsilon^{2\gamma-1}h_j/2)\mathcal{J}^\varepsilon(-\omega_j+\varepsilon^{2\gamma-1}h_j/2)\Big]d\omega_j dh_j\\ &= \frac{n!^2\mathcal{R}^{2n}}{4^n(2\pi)^{4n}\varepsilon^{n(12(\gamma-1/2)+2)}}\\ &\qquad\times\int_{\{0<\omega_1<\cdots<\omega_n\}}\int_{H^\varepsilon_n}\int\cdots\int\mathbb{E}\Big[\prod_{j=1}^n M^j_\varepsilon\Big]\prod_{j=1}^n\prod_{l=1,2}d\omega_j dh_j d\bar{s}_{l,j}d\mathbf{x}'_{l,j}d\mathbf{q}'_{l,j}d\mathbf{p}_{l,j}d\bar{\mathbf{y}}_{l,j}.\end{aligned}\tag{78}$$

Here, we have

$$
\begin{aligned}
M_\varepsilon^j := {} & e^{-i\omega_j(\bar s_{1,j}-\bar s_{2,j})/\varepsilon^{2\gamma-1}} e^{-ih_j(\bar s_{1,j}+\bar s_{2,j})/2} \\
& \times e^{i((\omega_j+\varepsilon^{2\gamma-1}h_j/2)\mathbf{p}_{1,j}\cdot(\bar{\mathbf{y}}_{1,j}+\varepsilon^{\gamma-1/2}\mathbf{y})-(\omega_j-\varepsilon^{2\gamma-1}h_j/2)\mathbf{p}_{2,j}\cdot(\bar{\mathbf{y}}_{2,j}+\varepsilon^{\gamma-1/2}\mathbf{y})/\varepsilon^{2\gamma-1}} \\
& \times e^{i((\omega_j+\varepsilon^{2\gamma-1}h_j/2)\mathbf{q}'_{1,j}\cdot(\bar{\mathbf{y}}_{1,j}+\varepsilon^{\gamma-1/2}\mathbf{y})-(\omega_j-\varepsilon^{2\gamma-1}h_j/2)\mathbf{q}'_{2,j}\cdot(\bar{\mathbf{y}}_{2,j}+\varepsilon^{\gamma-1/2}\mathbf{y})/\varepsilon^{\gamma-1/2}} \\
& \times e^{-i((\omega_j+\varepsilon^{2\gamma-1}h_j/2)\mathbf{p}_{1,j}\cdot\mathbf{x}'_{1,j}-(\omega_j-\varepsilon^{2\gamma-1}h_j/2)\mathbf{p}_{2,j}\cdot\mathbf{x}'_{2,j})/\varepsilon^{\gamma}} \\
& \times e^{2i\lambda_0((\omega_j+\varepsilon^{2\gamma-1}h_j/2)V(\mathbf{x}'_{1,j}/\varepsilon^\gamma)-(\omega_j-\varepsilon^{2\gamma-1}h_j/2)V(\mathbf{x}'_{2,j}/\varepsilon^\gamma))} \\
& \times \hat{\mathcal{U}}_0(\omega_j+\varepsilon^{2\gamma-1}h_j/2,\mathbf{p}_{1,j}/\varepsilon^{\gamma-1/2}+\mathbf{q}'_{1,j},z_{int})\overline{\hat{\mathcal{U}}_0(\omega_j-\varepsilon^{2\gamma-1}h_j/2,\mathbf{p}_{2,j}/\varepsilon^{\gamma-1/2}+\mathbf{q}'_{2,j},z_{int})} \\
& \times \hat{\mathcal{U}}_0(\omega_j+\varepsilon^{2\gamma-1}h_j/2,\mathbf{q}'_{1,j},z_{int})\overline{\hat{\mathcal{U}}_0(\omega_j-\varepsilon^{2\gamma-1}h_j/2,\mathbf{q}'_{2,j},z_{int})} \\
& \times \hat\Psi(\omega_j+\varepsilon^{2\gamma-1}h_j/2,\mathbf{q}'_{1,j})\overline{\hat\Psi(\omega_j-\varepsilon^{2\gamma-1}h_j/2,\mathbf{q}'_{2,j})} \\
& \times \varphi^{1/2}\Big(2\frac{\bar s_{1,j}-s^{ref}_{\mathbf{p}_{1,j}}}{\varepsilon^{2(\gamma-1/2)}},2\frac{\bar{\mathbf{y}}_{1,j}-\mathbf{y}^{ref}_{\mathbf{p}_{1,j}}}{\varepsilon^{2(\gamma-1/2)}}\Big)\varphi^{1/2}\Big(2\frac{\bar s_{2,j}-s^{ref}_{\mathbf{p}_{2,j}}}{\varepsilon^{2(\gamma-1/2)}},2\frac{\bar{\mathbf{y}}_{2,j}-\mathbf{y}^{ref}_{\mathbf{p}_{2,j}}}{\varepsilon^{2(\gamma-1/2)}}\Big) \\
& \times \overline{\phi(\bar s_{1,j},\bar{\mathbf{y}}_{1,j},\mathbf{y},\omega_j+\varepsilon^{2\gamma-1}h_j/2,\mathbf{p}_{1,j}+\varepsilon^{\gamma-1/2}\mathbf{q}'_{1,j})} \\
& \times \overline{\phi(\bar s_{2,j},\bar{\mathbf{y}}_{2,j},\mathbf{y},-\omega_j+\varepsilon^{2\gamma-1}h_j/2,\mathbf{p}_{2,j}+\varepsilon^{\gamma-1/2}\mathbf{q}'_{2,j})} \\
& \times (\omega_j+\varepsilon^{2\gamma-1}h_j/2)^2(\omega_j-\varepsilon^{2\gamma-1}h_j/2)^2
\end{aligned}
$$

after the change of variables

$$\mathbf{p}_{1,j}\to\varepsilon^{\gamma-1/2}\mathbf{q}'_{1,j}+\mathbf{p}_{1,j}\qquad\text{and}\qquad\mathbf{p}_{2,j}\to\varepsilon^{\gamma-1/2}\mathbf{q}'_{2,j}+\mathbf{p}_{2,j},$$

and where the integration domain for the h_j's is given by

$$H_n^\varepsilon=\Big\{(h_1,\dots,h_n):\quad h_j\in\Big(2\frac{\omega_j-\omega_{j+1}}{\varepsilon^{2\gamma-1}}+h_{j+1},2\frac{\omega_j-\omega_{j-1}}{\varepsilon^{2\gamma-1}}+h_{j-1}\Big),\qquad j\in\{1,\dots,n\}\Big\}.$$

In H_n^ε, the convention $\omega_{n+1}=\infty$, $h_{n+1}=\omega_0=h_0=0$ has been used. Note that in the limit $\varepsilon\to0$, the domain H_n^ε becomes $\mathbb{R}^n$. Making the changes of variables

$$\mathbf{x}'_{1,j}\to\mathbf{r}'_j+\varepsilon^\gamma\mathbf{y}'_j/2\qquad\text{and}\qquad\mathbf{x}'_{2,j}\to\mathbf{r}'_j-\varepsilon^\gamma\mathbf{y}'_j/2,$$

and taking the expectation to M_ε^j provides the term

$$
\begin{aligned}
\mathbb{E}\Big[\prod_{j=1}^n e^{2i\lambda_0((\omega_j+\varepsilon^\gamma h_j/2)V(\mathbf{r}_j/\varepsilon^\gamma+\mathbf{y}'_j/2)-(\omega_j-\varepsilon^\gamma h_j/2)V(\mathbf{r}_j/\varepsilon^\gamma-\mathbf{y}'_j/2))}\Big] &\simeq \prod_{j=1}^n\mathbb{E}\big[e^{2i\omega_j\lambda_0(V(\mathbf{r}_j/\varepsilon^\gamma+\mathbf{y}'_j/2)-V(\mathbf{r}_j/\varepsilon^\gamma-\mathbf{y}'_j/2))}\big] \\
&\simeq \prod_{j=1}^n\mathbb{E}\big[e^{2i\omega_j\lambda_0(V(\mathbf{y}'_j/2)-V(-\mathbf{y}'_j/2))}\big] \\
&\simeq \prod_{j=1}^n\mathbb{E}\big[e^{2i\omega_j\lambda_0(V(\mathbf{y}'_j)-V(0))}\big]
\end{aligned}
$$

as $\varepsilon\to0$, where the stationarity of V is used at the second and last relations, as well as Lemma 1.1 to obtain the first relation. One can observe that the latter relation does not depend on the $\mathbf{r}_j$'s, so that the resulting terms $e^{i((\omega_j+\varepsilon^{2\gamma-1}h_j/2)\mathbf{p}_{1,j}-(\omega_j-\varepsilon^{2\gamma-1}h_j/2)\mathbf{p}_{2,j})\cdot\mathbf{r}'_j/e^\gamma}$ provide

$$(2\pi)^{2n}\varepsilon^{2n\gamma}\prod_{j=1}^n\delta((\omega_j+\varepsilon^{2\gamma-1}h_j/2)\mathbf{p}_{1,j}-(\omega_j-\varepsilon^{2\gamma-1}h_j/2)\mathbf{p}_{2,j}),$$

and leading to variables $\mathbf{p}_j$ for simplification. At the leading order, we then have

$$\begin{aligned}\mathbb{E}\Big[\prod_{j=1}^n M_\varepsilon^j\Big] \simeq \prod_{j=1}^n & e^{-i\omega_j(\bar s_{1,j}-\bar s_{2,j})/\varepsilon^{2\gamma-1}} e^{-ih_j((\bar s_{1,j}+\bar s_{2,j})/2-s^{ref}_{\mathbf{p}_j^0})} e^{ih_j\mathbf{p}_j\cdot(\bar{\mathbf{y}}_{1,j}-\bar{\mathbf{y}}_{2,j})/2} e^{i\omega_j\mathbf{p}_j\cdot(\bar{\mathbf{y}}_{1,j}-\bar{\mathbf{y}}_{2,j})/\varepsilon^{2\gamma-1}} \\ & \times e^{i\omega_j(\mathbf{q}'_{1,j}\cdot(\bar{\mathbf{y}}_{1,j}-\mathbf{y}^{ref}_{\mathbf{p}_j^0})-\mathbf{q}'_{2,j}\cdot(\bar{\mathbf{y}}_{2,j}-\mathbf{y}^{ref}_{\mathbf{p}_j^0}))/\varepsilon^{\gamma-1/2}} e^{i\omega_j(\mathbf{q}'_{1,j}-\mathbf{q}'_{2,j})\cdot\mathbf{y}} \\ & \times \mathbb{E}\big[e^{2i\omega_j\lambda_0(V(\mathbf{y}'_j)-V(0))}\big] e^{-i\omega_j\mathbf{y}'_j\cdot\mathbf{p}_j} \\ & \times \hat{\mathcal{U}}_0(\omega_j,\mathbf{q}'_{1,j},2z_{int})\overline{\hat{\mathcal{U}}_0(\omega_j,\mathbf{q}'_{2,j},2z_{int})}\hat\Psi(\omega_j,\mathbf{q}'_{1,j})\overline{\hat\Psi(\omega_j,\mathbf{q}'_{2,j})} \\ & \times \varphi^{1/2}\Big(2\frac{\bar s_{1,j}-s^{ref}_{\mathbf{p}_j^0}}{\varepsilon^{2\gamma-1}},2\frac{\bar{\mathbf{y}}_{1,j}-\mathbf{y}^{ref}_{\mathbf{p}_j^0}}{\varepsilon^{2(\gamma-1/2)}}\Big)\varphi^{1/2}\Big(2\frac{\bar s_{2,j}-s^{ref}_{\mathbf{p}_j^0}}{\varepsilon^{2\gamma-1}},2\frac{\bar{\mathbf{y}}_{2,j}-\mathbf{y}^{ref}_{\mathbf{p}_j^0}}{\varepsilon^{2(\gamma-1/2)}}\Big) \\ & \times \overline{\phi(\bar s_{1,j},\bar{\mathbf{y}}_{1,j},\omega_j,\mathbf{p}_j)\phi(\bar s_{2,j},\bar{\mathbf{y}}_{2,j},-\omega_j,\mathbf{p}_j)}\omega_j^2.\end{aligned}$$

Making now the changes of variables

$$\bar s_{1,j}\to s^{ref}_{\mathbf{p}_j^0}+\bar s_j+\varepsilon^{2\gamma-1}\widetilde s_j/2 \qquad \bar s_{2,j}\to s^{ref}_{\mathbf{p}_j^0}+\bar s_j-\varepsilon^{2\gamma-1}\widetilde s_j/2,$$

the resulting term $e^{-ih_j(\bar s_j-s^{ref}_{\mathbf{p}_j^0})}$ yields

$$2\pi\delta(\bar s_j),$$

and with the changes of variables

$$\bar{\mathbf{y}}_{1,j}\to\mathbf{y}^{ref}_{\mathbf{p}_j^0}+\bar{\mathbf{y}}_j+\varepsilon^{2(\gamma-1/2)}\widetilde{\mathbf{y}}_j/2, \qquad \bar{\mathbf{y}}_{2,j}\to\mathbf{y}^{ref}_{\mathbf{p}_j^0}+\bar{\mathbf{y}}_j-\varepsilon^{2(\gamma-1/2)}\widetilde{\mathbf{y}}_j/2$$

together with

$$\mathbf{q}'_{1,j}\to\mathbf{q}_j+\varepsilon^{\gamma-1/2}\mathbf{r}_j/2, \qquad \mathbf{q}'_{2,j}\to\mathbf{q}_j-\varepsilon^{\gamma-1/2}\mathbf{r}_j/2,$$

the resulting term $e^{i\omega_j\mathbf{r}_j\cdot\bar{\mathbf{y}}_j}$ yields

$$(2\pi)^2\delta(\bar{\mathbf{y}}_j)/\omega_j^2.$$

As a result, we obtain

$$\begin{aligned}\lim_{\varepsilon\to0}M_\varepsilon(n,n)=\frac{(2\pi)^n n!^2\mathcal{R}^{2n}}{4^n}\int_{\{0<\omega_1<\cdots<\omega_n\}}\int\cdots\int\prod_{j=1}^n & e^{-i\omega_j\widetilde s_j}e^{i\omega_j\mathbf{p}_j\cdot\widetilde{\mathbf{y}}_j} \\ & \times\mathbb{E}\big[e^{2i\omega_j\lambda_0(V(\mathbf{y}'_j)-V(0))}\big]e^{-i\omega_j\mathbf{y}'_j\cdot\mathbf{p}_j} \\ & \times|\hat\Psi(\omega_j,\mathbf{q}_j)|^2\varphi^{1/2}(\widetilde s_j,\widetilde{\mathbf{y}}_j)\varphi^{1/2}(-\widetilde s_j,-\widetilde{\mathbf{y}}_j) \\ & \times\overline{\phi(s^{ref}_{\mathbf{p}_j^0},\mathbf{y}^{ref}_{\mathbf{p}_j^0},\omega_j,\mathbf{p}_j)\phi(s^{ref}_{\mathbf{p}_j^0},\mathbf{y}^{ref}_{\mathbf{p}_j^0},-\omega_j,\mathbf{p}_j)} \\ & \times d\omega_j d\widetilde s_j d\widetilde{\mathbf{y}}_j d\mathbf{q}_j d\mathbf{y}'_j d\mathbf{p}_j,\end{aligned}$$

and by symmetry of the ω_j's

$$\lim_{\varepsilon\to0}M_\varepsilon(n,n)=\frac{n!}{2^n}\Big(\frac{\mathcal{R}^2}{2}\int_0^\infty\mathcal{J}^0(\omega)d\omega\Big)^n.$$

Finally, using the stationarity of V, but also that φ is an odd function, we have

$$\begin{aligned}\sigma^2_{ref}:=\frac{\mathcal{R}^2}{2}\int_0^\infty\mathcal{J}^0(\omega)d\omega=\frac{\mathcal{R}^2}{4}\int\mathcal{J}^0(\omega)d\omega=\frac{(2\pi)^3\mathcal{R}^2}{4}\int\hat\varphi(\omega,\mathbf{p})\mathcal{A}(2\lambda_0,\omega,\mathbf{p})|\hat\Psi|_2^2(\omega) \\ \times\overline{\phi(s^{ref}_{\mathbf{p}},\mathbf{y}^{ref}_{\mathbf{p}},\omega,\mathbf{p})\phi(s^{ref}_{\mathbf{p}},\mathbf{y}^{ref}_{\mathbf{p}},-\omega,\mathbf{p})}d\omega d\mathbf{p},\end{aligned} \tag{79}$$

where $|\hat\Psi|_2^2$ is given by (56), and $\mathcal{A}$ by (55).

The case $l\neq n$. In this situation, we necessarily have

$$\lim_{\varepsilon\to0}M_\varepsilon(l,2n-l)=0,$$

for any $l\neq n$, where $M_\varepsilon(l,2n-l)$ is defined by (77) and

$$M_\varepsilon(l,2n-l)=\int_0^\infty\cdots\int_0^\infty\mathbb{E}\Big[\prod_{j=1}^l\mathcal{J}^\varepsilon(\omega_{1,j})d\omega_{1,j}\prod_{j'=1}^{2n-l}\mathcal{J}^\varepsilon(-\omega_{2,j'})d\omega_{2,j'}\Big].$$

The reason lies in the unbalanced number of J^ε_+ and J^ε_-, from which not all the rapid phases $e^{-i\omega_j s^{ref}_{\mathbf{p}_j}/\varepsilon^{2\gamma-1}}$ can be canceled as for $l = n$. In fact, these remaining terms that have not been paired correspond have all positive frequency ω_j which cannot compensate with each other. These remaining rapid phases lead to null limits, and we finally obtain

$$\lim_{\varepsilon\to 0}\mathbb{E}\big[J^\varepsilon(\phi)^{2n}\big] = \frac{n!}{2^n}\sigma_{ref}^{2n} = \mathbb{E}[\langle\hat{\mathcal{S}}^{ref}_{\mathbf{y}},\phi\rangle^n_{\mathcal{S}',\mathcal{S}}]. \tag{80}$$

Odd moments. For any odd moments there is necessarily an unbalance number of J^ε_+ and J^ε_- in $M_\varepsilon(l, 2n+1-l)$ for any $l \in \{0,\dots,2n+1\}$. As for the case of even moment with $l \neq n$, not all the rapid phases can be compensated leading to

$$\lim_{\varepsilon\to 0}\mathbb{E}\big[J^\varepsilon(\phi)^{2n+1}\big] = 0.$$

The case of the expectation (moment of order 1) is given by (61).

Tightness. The tightness is obtain from the ones of the real and imaginary part of $\hat{\mathcal{S}}^{\varepsilon,ref}_{\mathbf{y}}$ applied to a test function $\phi \in \mathcal{S}(\mathbb{R}\times\mathbb{R}^2\times\mathbb{R}\times\mathbb{R}^2)$ that takes real values. These tightness properties are obtain from the converging second order moment of J^ε with test functions

$$\phi_r(s,\mathbf{y},\omega,\mathbf{p}) = \frac{1}{2}(\phi(s,\mathbf{y},\omega,\mathbf{p}) + \phi(s,\mathbf{y},-\omega,\mathbf{p})) \qquad \text{and} \qquad \phi_i(s,\mathbf{y},\omega,\mathbf{p}) = \frac{1}{2i}(\phi(s,\mathbf{y},\omega,\mathbf{p}) - \phi(s,\mathbf{y},-\omega,\mathbf{p}))$$

In fact, for these two test functions we have

$$J^\varepsilon(\phi_r) = \big\langle Re(\hat{\mathcal{S}}^{ref}_{\mathbf{y}}),\phi\big\rangle_{\mathcal{S}',\mathcal{S}} \qquad \text{and} \qquad J^\varepsilon(\phi_i) = \big\langle Im(\hat{\mathcal{S}}^{ref}_{\mathbf{y}}),\phi\big\rangle_{\mathcal{S}',\mathcal{S}}.$$

Covariance formulas (62) **and** (63)**.** These formulas follows from (79) and (80) for $n = 2$, together with the standard polarization formulas

$$J^\varepsilon(\phi)J^\varepsilon(\psi) = \frac{1}{4}\Big((J^\varepsilon(\phi+\psi))^2 - (J^\varepsilon(\phi-\psi))^2\Big),$$

and

$$J^\varepsilon(\phi)\overline{J^\varepsilon(\psi)} = \frac{1}{4i}\Big((J^\varepsilon(\phi+i\overline{\psi_-}))^2 - (J^\varepsilon(\phi-i\overline{\psi_-}))^2\Big),$$

where $\psi_-(\omega) = \psi(-\omega)$. This concludes the proof of Theorem 6.1.

A Proof of the jump conditions and continuity relations

This section is devoted to the justification of the jump condition across the plan $z = 0$ produced by the source term, and the continuity relation of the wave field across the randomly perturbed interface.

To exhibit these relations the solution u to the wave equation (3) is decomposed as

$$u(t,\mathbf{x},z) = u^-(t,\mathbf{x},z)\mathbf{1}_{(-\infty,0)}(z) + u^+(t,\mathbf{x},z)\mathbf{1}_{(0,\infty)}(z), \tag{81}$$

where u^+ satisfies

$$\Delta u^+ - \frac{1}{c^2(\mathbf{x},z)}\partial^2_{tt}u^+ = 0 \qquad (t,\mathbf{x},z) \in \mathbb{R}\times\mathbb{R}^2\times\mathbb{R},$$

and u^- satisfies

$$\Delta u^- - \frac{1}{c_0^2}\partial^2_{tt}u^- = 0 \qquad (t,\mathbf{x},z) \in \mathbb{R}\times\mathbb{R}^2\times\mathbb{R}.$$

A.1 Jump conditions across the plan $z = 0$ of the source location

Injecting the decomposition (81) into (3) gives

$$\begin{aligned}\Psi\Big(\frac{t-\mathbf{k}_0\cdot\mathbf{x}}{T_0},\frac{\mathbf{x}}{r_0}\Big)\delta'(z) = \Delta u - \frac{1}{c^2(\mathbf{x},z)}\partial^2_{tt}u &= \big(\partial_z u^+(t,\mathbf{x},z=0) - \partial_z u^-(t,\mathbf{x},z=0)\big)\delta(z)\\ &\quad + \big(u^+(t,\mathbf{x},z=0) - u^-(t,\mathbf{x},z=0)\big)\delta'(z).\end{aligned}$$

Hence, we obtain the jump conditions

$$\begin{aligned}u(t,\mathbf{x},z=0^+) - u(t,\mathbf{x},z=0^-) &= \Psi\Big(\frac{t-\mathbf{k}_0\cdot\mathbf{x}}{T_0},\frac{\mathbf{x}}{r_0}\Big),\\ \partial_z u(t,\mathbf{x},z=0^+) - \partial_z u(t,\mathbf{x},z=0^-) &= 0.\end{aligned} \tag{82}$$

A.2 Continuity relation across the randomly perturbed interface

The continuity relation at the randomly perturbed interface is obtained for u^+, and then for u, in a similar fashion as in the previous section. The term u^+ is decomposed as

$$u^+(t,\mathbf{x},z) = u_0^+(t,\mathbf{x},z)\mathbf{1}_{(-\infty,0)}(z - z_{int}(\mathbf{x})) + u_1^+(t,\mathbf{x},z)\mathbf{1}_{(0,\infty)}(z - z_{int}(\mathbf{x})), \tag{83}$$

where

$$z_{int}(\mathbf{x}) := z_{int} + \sigma V(\mathbf{x}/l_c),$$

and

$$\Delta u_0^+ - \frac{1}{c_0^2}\partial_{tt}^2 u_0^+ = 0 \qquad (t,\mathbf{x}) \in \mathbb{R}\times\mathbb{R}^2 \qquad \text{for} \qquad z < z_{int}(\mathbf{x}),$$

and u_1^+ satisfies

$$\Delta u_1^+ - \frac{1}{c_1^2}\partial_{tt}^2 u_1^+ = 0 \qquad (t,\mathbf{x}) \in \mathbb{R}\times\mathbb{R}^2 \qquad \text{for} \qquad z > z_{int}(\mathbf{x}).$$

The shifted solution

$$U(t,\mathbf{x},Z) = u^+(t,\mathbf{x},Z + z_{int}(\mathbf{x}))$$

satisfies

$$\Delta_\perp U + \Big(1+\frac{\sigma^2}{l_c^2}|\nabla_\perp V(\mathbf{x}/l_c)|^2\Big)\partial_{ZZ}^2 U - \frac{1}{c^2(\mathbf{x},Z+z_{int}(\mathbf{x}))}\partial_{tt}^2 U - \frac{\sigma}{l_c^2}(\Delta_\perp V(\mathbf{x}/l_c))\partial_Z U - \frac{\sigma}{l_c}\nabla_\perp V(\mathbf{x}/l_c)\cdot\nabla_\perp\partial_Z U = 0. \tag{84}$$

The shifted decomposition (83) then reads

$$U(t,\mathbf{x},Z) = U_0(t,\mathbf{x},Z)\mathbf{1}_{(-\infty,0)}(Z) + U_1(t,\mathbf{x},Z)\mathbf{1}_{(0,\infty)}(Z), \tag{85}$$

with U_0 and U_1 satisfying

$$\Delta_\perp U_j + \Big(1+\frac{\sigma^2}{l_c^2}|\nabla_\perp V(\mathbf{x}/l_c)|^2\Big)\partial_{ZZ}^2 U_j - \frac{1}{c_j^2}\partial_{tt}^2 U_j - \frac{\sigma}{l_c^2}(\Delta_\perp V(\mathbf{x}/l_c))\partial_Z U_j - \frac{\sigma}{l_c}\nabla_\perp V(\mathbf{x}/l_c)\cdot\nabla_\perp\partial_Z U_j = 0,$$

for $j = 0, 1$. Injecting the decomposition (85) into (84) provides

$$\begin{aligned} 0 = \delta(Z)\Big(&\Big(1+\frac{\sigma^2}{l_c^2}|\nabla_\perp V(\mathbf{x}/l_c)|^2\Big)\Big(\partial_Z U_1(Z=0) - \partial_Z U_0(Z=0)\Big) \\ &- \frac{\sigma}{l_c^2}(\Delta_\perp V(\mathbf{x}/l_c))(U_1(Z=0) - U_0(Z=0)) \\ &- \frac{\sigma}{l_c}\nabla_\perp V(\mathbf{x}/l_c)\cdot(\nabla_\perp U_1(Z=0) - \nabla_\perp U_0(Z=0))\Big) \\ + \delta'(Z)&\Big(1+\frac{\sigma^2}{l_c^2}|\nabla_\perp V(\mathbf{x}/l_c)|^2\Big)\Big(U_1(Z=0) - U_0(Z=0)\Big) \end{aligned}$$

The term in δ' provides $U_1(Z=0) = U_0(Z=0)$ and then $\nabla_\perp U_1(Z=0) = \nabla_\perp U_0(Z=0)$, so that the term in δ provide only $\partial_Z U_1(Z=0) = \partial_Z U_0(Z=0)$. Going back to the original variables, we obtain the relations

$$u_0^+(z = z_{int}(\mathbf{x})) = u_1^+(z = z_{int}(\mathbf{x})) \qquad \text{and} \qquad \partial_z u_0^+(z = z_{int}(\mathbf{x})) = \partial_z u_1^+(z = z_{int}(\mathbf{x})),$$

leading to the continuity relations for u

$$u(z = z_{int}(\mathbf{x})^+) = u(z = z_{int}(\mathbf{x})^-) \qquad \text{and} \qquad \partial_z u(z = z_{int}(\mathbf{x})^+) = \partial_z u(z = z_{int}(\mathbf{x})^-).$$

B Proof of Lemma 1.1

The proof of this lemma is obtained by induction on n, but we only focus on the second point. The first one can be obtained following the same lines by considering the functions g_j with only one argument and set $\mathbf{y}_j = 0$.

Writing

$$\begin{aligned} \mathbb{E}[X_1^\eta X_2^\eta] &= \mathbb{E}[X_1^\eta X_2^\eta] - \mathbb{E}[X_1^\eta]\mathbb{E}[X_2^\eta] + \mathbb{E}[X_1^\eta]\mathbb{E}[X_2^\eta] \\ &= Corr(X_1^\eta, X_2^\eta)\sqrt{Var(X_1^\eta)Var(X_2^\eta)} + \mathbb{E}[X_1^\eta]\mathbb{E}[X_2^\eta], \end{aligned}$$

with

$$X_1^\eta := g_{n+1}\Big(V\Big(\frac{\mathbf{x}_{n+1}}{\eta}+\frac{\mathbf{y}_{n+1}}{2}\Big),V\Big(\frac{\mathbf{x}_{n+1}}{\eta}-\frac{\mathbf{y}_{n+1}}{2}\Big)\Big) \qquad \text{and} \qquad X_2^\eta := \prod_{j=1}^{n} g_j\Big(V\Big(\frac{\mathbf{x}_j}{\eta}+\frac{\mathbf{y}_j}{2}\Big),V\Big(\frac{\mathbf{x}_j}{\eta}-\frac{\mathbf{y}_j}{2}\Big)\Big),$$

and assuming the desired property holds true for X_2^η involving n terms, we only have to prove that

$$\lim_{\eta\to 0} Corr(X_1^\eta, X_2^\eta) = 0,$$

since $Var(X_1^\eta)Var(X_2^\eta) \leq \sup_{j,v_1,v_2} |g_j(v_1,v_2)|^{2(n+1)} < \infty$. Now, using (12), we have

$$Corr(X_1^\eta, X_2^\eta) \leq \rho\Big(\min_{\substack{j=1,\dots,n\\ \nu_1,\nu_2=\pm}} \Big|\frac{\mathbf{x}_{n+1}-\mathbf{x}_j}{\eta}+\nu_1\frac{\mathbf{y}_{n+1}}{2}+\nu_2\frac{\mathbf{y}_j}{2}\Big|\Big),$$

with

$$\min_{\substack{j=1,\dots,n\\ \nu_1,\nu_2=\pm}} \Big|\frac{\mathbf{x}_{n+1}-\mathbf{x}_j}{\eta}+\nu_1\frac{\mathbf{y}_{n+1}}{2}+\nu_2\frac{\mathbf{y}_j}{2}\Big| \geq \min_{j=1,\dots,n} \frac{|\mathbf{x}_{n+1}-\mathbf{x}_j|}{\eta} - \frac{|\mathbf{y}_{n+1}|}{2} - \max_{j=1,\dots,n}\frac{|\mathbf{y}_j|}{2} \underset{\eta\to 0}{\longrightarrow} \infty,$$

as all the $\mathbf{x}_j$'s are distinct. Finally, using (11) and (13), we obtain

$$\lim_{\eta\to 0} Corr(X_1^\eta, X_2^\eta) = 0,$$

so that

$$\begin{aligned}\lim_{\eta\to 0}\mathbb{E}\Big[\prod_{j=1}^{n+1} g_j\Big(V\Big(\frac{\mathbf{x}_j}{\eta}+\frac{\mathbf{y}_j}{2}\Big),V\Big(\frac{\mathbf{x}_j}{\eta}-\frac{\mathbf{y}_j}{2}\Big)\Big)\Big] &= \lim_{\eta\to 0}\prod_{j=1}^{n+1}\mathbb{E}\Big[g_j\Big(V\Big(\frac{\mathbf{x}_j}{\eta}+\frac{\mathbf{y}_j}{2}\Big),V\Big(\frac{\mathbf{x}_j}{\eta}-\frac{\mathbf{y}_j}{2}\Big)\Big)\Big]\\ &= \prod_{j=1}^{n+1}\mathbb{E}\Big[g_j\Big(V\Big(\frac{\mathbf{y}_j}{2}\Big),V\Big(-\frac{\mathbf{y}_j}{2}\Big)\Big)\Big],\end{aligned}$$

where the last line is obtained through the stationarity of V.

References

[1] R. Alonso, L. Borcea, and J. Garnier, *Wave propagation in waveguides with random boundaries*, Commun. Math. Sci., 11 (2012), pp. 233–267.

[2] J.P. Banon, Ø. S. Hetland, and I. Simonsen, *Physics of polarized light scattering from weakly rough dielectric surfaces: Yoneda and brewster scattering phenomena*, Phys. Rev. A , 99 (2019), 023834.

[3] G.Bal, J. B. Keller, G. C. Papanicoalou, and L. Ryzhik, *Transport theory for acoustic waves with reflection and transmission at interfaces*, Wave Motion, 30 (1999), pp. 303–327.

[4] F. G. Bass and I. M. Fuks, *Wave scattering from statistically rough surfaces*, International series in natural philosophy, Elsevier, 2013.

[5] R.C. Bradley, *Equivalent mixing conditions for random fields*, Ann. Probab., 21 (1993), pp. 1921-1926.

[6] H. Contopanagos, B. Dembart, M. Epton, J.J. Ottusch, V. Rokhlin, J.L. Visher, and S.M. Wandzura, *Well-conditioned boundary integral equations for three-dimensional electromagnetic scattering*, IEEE Trans. Antennas Propag., 50 (2002), pp. 1824–1830.

[7] G. Da Prato and J. Zabczyk, *Stochastic Equations in Infinite Dimensions*, Cambridge University Press, 2014.

[8] M. Darmon, V. Dorval and F. Baqué,*Acoustic scattering models from rough surfaces: a brief review and recent advances*, Appl. Sci., 10 (2020), 8305.

[9] D. A. Dawson and G. C. Papanicolaou, *A random wave process*, Appl. Math. Optim., 12 (1984), pp. 97–114.

[10] J. A. DeSanto, *Scattering from a rough interface*, Radio Sci., 16 (1981), pp. 1021–1024.

[11] T.M. Elfouhaily and C.A. Guérin, *A critical survey of approximate scattering wave theories from random rough surfaces*, Waves in Random Media, 14 (2004), pp. R1–R40.

[12] J.P. Fouque, J. Garnier, G. Papanicolaou, and K. Sølna, *Wave Propagation and Time Reversal in Randomly Layered Media*, Springer, New York, 2007.

[13] B. Gallas, A. Maurel, J.J. Marigo, and A. Ourir, *Light scattering by periodic rough surfaces: equivalent jump conditions*, J. Opt. Soc. Am. A, 12 (2017), pp. 2181–2188.

[14] J.V. Garcia-Ramos and J.A. Sánchez-Gil, *Far-field intensity of electromagnetic waves scattered from random self-affine fractal metal surfaces*, Waves in Random Media, 7 (1997), pp. 285–293.

[15] J. Garnier and K. Sølna, *White-noise paraxial approximation for a general random hyperbolic system*, SIAM J. Multiscale Model. Simul., 13 (2015), pp. 1022–1060.

[16] J. Garnier and K. S olna, *Imaging through a scattering medium by speckle intensity correlations over incident angle*, Inverse Probl., 34 (2018), 094003.

[17] J. Garnier and K. Sølna, *Non-invasive imaging through random media*, SIAM J. Appl. Math., 78 (2018), pp. 3296–3315.

[18] C. Gomez, *Wave propagation in underwater acoustic waveguides with rough boundaries*, Commun. Math. Sci., 13 (2015), pp. 2005–205.

[19] , A. Ishimaru, *Wave propagation and scattering in random media*, Vol. 2, Academic press, 1978.

[20] , A. Ishimaru, *Wave propagation and scattering in random media and rough surfaces*, Proceedings of the IEEE, 79 (1991), pp. 1359–1366.

[21] O. Katz, P. Heidmann, M. Fink, and S. Gigan, *Non-invasive single-shot imaging through scattering layers and around corners via speckle correlations*, Nature Photon, 8 (2014), pp. 784–790.

[22] P. Li, H. Wu, and W. Zheng, *Electromagnetic scattering by unbounded rough surfaces*, SIAM J. Math. Anal., 43 (2011), pp. 1205–1231.

[23] A.A. Maradudin, T. Michel, A.R. McGurn, and E.R. Méndez, *Enhanced backscattering of light from a random grating*, Ann. Phys., 203 (1990), pp. 255–307.

[24] A.A. Maradudin, *Light Scattering and Nanoscale Surface Roughness*, Springer, 2007.

[25] J. Nevard and J.B. Keller, *Homogenization of rough boundaries and interfaces*, SIAM J. Appl. Math., 57 (1997), pp. 1660–1686.

[26] J. A. Ogilvy, *Theory of wave scattering from random rough surfaces*, CRC Press, 1991.

[27] J.A. Sánchez-Gil, J.V. García-Ramos, and E.R. Méndez, *Light scattering from self-affine fractal silver surfaces with nanoscale cutoff: far-field and near-field calculations*, J. Opt. Soc. Am., 19 (2002), pp. 901–911.

[28] A. Santenac and J. Daillant, *Statistical aspects of wave scattering at rough surface*, Daillant, J., Gibaud, A. (eds) X-ray and Neutron Reflectivity. Lecture Notes in Physics, vol 770, Springer, Berlin.

[29] F. Sayas O. Bruno, V. Dominguez, *Convergence analysis of a high-order Nystrom integral-equation method for surface scattering problems*, Numer. Math., 124 (2013), pp. 603–645.

[30] C.J.R Sheppard, *Fractal model of light scattering in biological tissue and cells*, Opt. Lett., 32 (2007), pp. 142–144.

[31] F. Shi, M.J.S. Lowe, and R.V. Craster, *Diffusely scattered and transmitted elastic waves by random rough solid-solid interfaces using an elastodynamic kirchhoff approximation*, Phys. Rev. E, 95 (2017), 214305.

[32] I. Simonsen, D. Vandembroucq, and S. Roux, *Wave scattering from self-affine surfaces*, Phys. Rev. E, 61 (2000), pp. 5914–5917.